IN THIS ISSUE

London Journals Press

IMAGE: OBSERVATORY WITH STAR TRAILS ON MOUNTAINS FOR CLEAR SKY

www.journalspress.com

LONDON JOURNAL OF RESEARCH IN SCIENCE: NATURAL AND FORMAL

Print ISSN: 2631-8490
Online ISSN: 2631-8504
DOI: 10.17472/LJRS

Volume 23 | Issue 5 | Compilation 1.0

COMPILED IN UNITED KINGDOM

ENGLISH

London Journal of Research in Science: Natural and Formal

Volume 23 | Issue 5 | Compilation 1.0

PUBLISHER

London Journals Press
1210th, Waterside Dr, Opposite Arlington Building, Theale, Reading
Phone:+444 0118 965 4033 Pin: RG7-4TY United Kingdom

SUBSCRIPTION

Frequency: Quarterly

Print subscription
$280USD for 1 year
$500USD for 2 year
(color copies including taxes and international shipping with TSA approved)

Find more details at https://journalspress.com/journals/subscription

ENVIRONMENT

London Journals Press is intended about protecting the environment. This journal is printed using led free environmental friendly ink and acid-free papers that are 100% recyclable.

London Journals Press Headquaters

1210th, Waterside Dr,
Opposite Arlington
Building, Theale, Reading
Phone:+444 0118 965 4033
Pin: RG7-4TY
United Kingdom

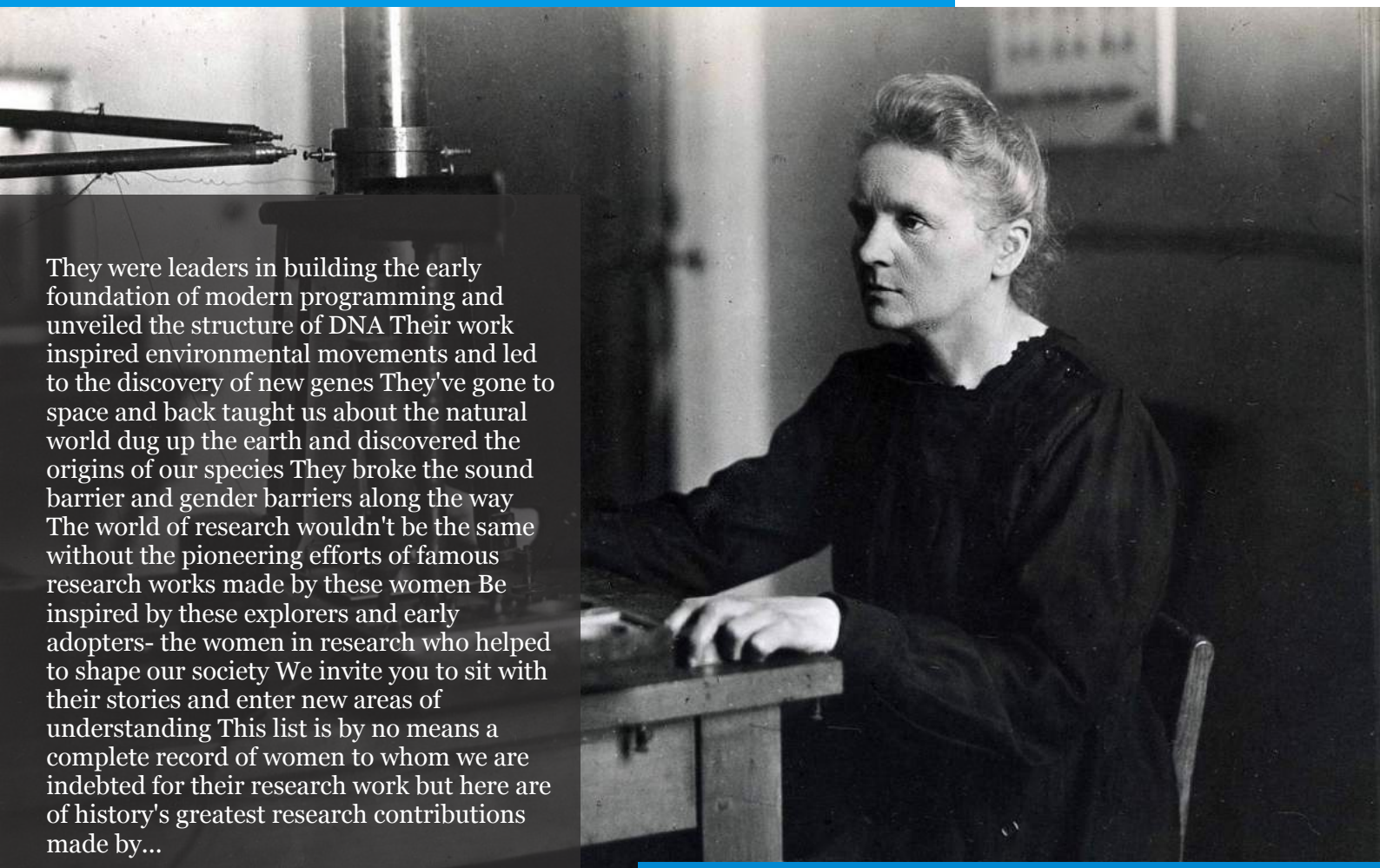

They were leaders in building the early foundation of modern programming and unveiled the structure of DNA Their work inspired environmental movements and led to the discovery of new genes They've gone to space and back taught us about the natural world dug up the earth and discovered the origins of our species They broke the sound barrier and gender barriers along the way The world of research wouldn't be the same without the pioneering efforts of famous research works made by these women Be inspired by these explorers and early adopters- the women in research who helped to shape our society We invite you to sit with their stories and enter new areas of understanding This list is by no means a complete record of women to whom we are indebted for their research work but here are of history's greatest research contributions made by...

Read complete here:
https://goo.gl/1vQ3lS

Women In Research

Computing in the cloud!

Cloud Computing is computing as a Service and not just as a Product Under Cloud Computing...

Read complete here:
https://goo.gl/VvHC72

Writing great research...

Prepare yourself before you start Before you start writing your paper or you start reading other...

Read complete here:
https://goo.gl/np73jP

Journal Content
In this Issue

London Journals Press

Editorial Board

Curated board members

Nicola Mastronardi

Consiglio Nazionaledelle Ricerche,
Ph.D. Applied Mathematics Katholieke
Universiteit Leuven
Belgium

Dr. Indranil Sen Gupta

Ph.D., Mathematics
Texas A & M University
Department of Mathematics
North Dakota State University
North Dakota, USA

Dr. Arvind Chhabra

University of Connecticut Health Center
USA Ph.D., Biotechnology Central
Drug Research Institute

Dr. Vladimir Burtman

Research Scientist
The University of Utah
Geophysics
Frederick Albert Sutton Building
115 S 1460 E Room 383
Salt Lake City, UT 84112, US

Dr. Xianghong Qi

University of Tennessee
Oak Ridge National Laboratory
Center for Molecular Biophysics
Oak Ridge National Laboratory
Knoxville, TN 37922
United States

Dr. Arshak Poghossian

Ph.D. Solid-State Physics
Leningrad Electrotechnical Institute, Russia
Institute of Nano and Biotechnologies
Aachen University of Applied Sciences, Germany

Dr. Bingyun Li

Ph.D. Fellow, IAES
Guest Researcher, NIOSH, CDC, Morgantown, WV
Institute of Nano and Biotechnologies
West Virginia University, US

Dr. Maria Gullo

Ph.D., Food Science, and Technology
University of Catania
Department of Agricultural and Food Sciences
University of Modena and Reggio Emilia, Italy

Dr. A. Heidari

Ph.D., D.Sc
Faculty of Chemistry
California South University (CSU), United States

Dr. Alicia Esther Ares

Ph.D. in Science and Technology,
University of General San Martin, Argentina
State University of Misiones, US

Research papers and articles

Volume 23 | Issue 5 | Compilation 1.0

Nonlinear Analysis as a Calculus

Alexander D. Bruno

ABSTRACT

In the last 60 years, there was formed a universal nonlinear analysis, whose unified algorithms allow to find asymptotic forms and asymptotic expansions of solutions to nonlinear equations and systems of different types: algebraic, ordinary differential (ODE), partial differential (PDE) and systems of mixed-type equations. This calculus contains two main algorithms: (a) Reducing equations to the normal form and (b) Separating truncated equations, and two kinds of transformations of coordinate can be used to simplify the obtained equations: (A) Power and (B) Logarithmic. Here we show that for algebraic equation, single ODE, autonomous system of ODE's, Hamiltonian system, single PDE. Some applications are mentioned as well.

Keywords: NA

Classification: NLM: WC 280

Language: English

London
Journals Press

LJP Copyright ID: 925641
Print ISSN: 2631-8490
Online ISSN: 2631-8504

London Journal of Research in Science: Natural and Formal

Volume 23 | Issue 5 | Compilation 1.0

Nonlinear Analysis as a Calculus

Alexander D. Bruno

ABSTRACT

In the last 60 years, there was formed a universal nonlinear analysis, whose unified algorithms allow to find asymptotic forms and asymptotic expansions of solutions to nonlinear equations and systems of different types: algebraic, ordinary differential (ODE), partial differential (PDE) and systems of mixed-type equations. This calculus contains two main algorithms: (a) Reducing equations to the normal form and (b) Separating truncated equations, and two kinds of transformations of coordinate can be used to simplify the obtained equations: (A) Power and (B) Logarithmic. Here we show that for algebraic equation, single ODE, autonomous system of ODE's, Hamiltonian system, single PDE. Some applications are mentioned as well.

Author: Keldysh Institute of Applied Mathematics of RAS, Moscow, Russia. email: abruno@keldysh.ru

I. INTRODUCTION

There are two universal methods for local study of nonlinear equations and systems of different kinds (algebraic, ordinary and partial differential): **(a)** normal form and **(b)** truncated equations.

(a) Equations with linear parts can be reduced to their normal forms by local changes of coordinates. For algebraic equation, it is Implicit Function Theorem. For systems of ordinary differential equations (ODE), I completed the theory of normal forms, began by Poincaré (1879) [Poincaré, 1928] and Dulac (1912) [Dulac, 1912] for general systems [Bruno, 1964; 1971] and began by Birkhoff (1929) [Birkhoff, 1966] for Hamiltonian systems [Bruno, 1972; 1994].

(b) Equations without linear part: I proposed to study properties of solutions to equations (algebraic, ordinary differential and partial differential) by studying sets of vector power exponents of terms of these equations. Namely, to select more simple ("truncated") equations [Bruno, 1962; 1989; 2000] by means of generalization to polyhedrons the Newton (1678) [Newton, 1964] and the Hadamard (1893) [Hadamard, 1893] polygons.

By means of power transformations [Bruno, 1962; 1989; 2022b] the normal forms and the truncated equations can be strongly simplified and often solved. Solutions to the truncated equations are asymptotically the first approximations of the solutions to the full equations. Continuing that process, we can obtain

London Journal of Research in Science: Natural and Formal

approximations of any precision to solutions of initial equations. Basing on the developed Asymptotic and Local Nonlinear Analysis, I proposed algorithms for solutions of a wide set of singular problems. In particular, for computation of six different types of asymptotic expansions of solutions to ODE [Bruno, 2004; 2018b; Bruno, Goruchkina, 2010], including expansions into trans-series [Bruno, 2019b].

In this article it is shown for a single algebraic equation in Section 2, for a single ordinary differential equation in Section 3, for an autonomous system of ODE's in Section 4, for Hamiltonian system in Subsection 4.5, for a single partial differential equation in Section 5. A survey of some applications is in Section 6.

From that point of view, the usual Classical Analysis is linear one, because it considers only linear approximations of problems near known solutions.

II. SINGLE ALGEBRAIC EQUATION

2.1. The implicit function theorem: Let $X = (x_1, \dots, x_n)$, $Q = (q_1, \dots, q_n)$, then

$$X^Q = x_1^{q_1} \cdots x_n^{q_n}, \quad \|Q\| = q_1 + \cdots + q_n.$$

Theorem 2.1. *Let*

$$f(X, \varepsilon, T) = \Sigma a_{Q,r}(T) X^Q \varepsilon^r, \tag{2.1}$$

where $0 \leqslant Q \in \mathbb{Z}^n$, $0 \leqslant r \in \mathbb{Z}$, *the sum is finite and* $a_{Q,r}(T)$ *are some functions of* $T = (t_1, \dots, t_m)$, *besides* $a_{00}(T) \equiv 0$, $a_{01}(T) \not\equiv 0$. *Then the solution to the equation* $f(X, \varepsilon, T) = 0$ *has the form*

$$\varepsilon = \Sigma b_R(T) X^R \stackrel{\text{def}}{=} b(T, X),$$

where $0 \leqslant R \in \mathbb{Z}^n$, $0 < \|R\|$, *the coefficients* $b_R(T)$ *are functions on* T *that are polynomials from* $a_{Q,r}(T)$ *with* $\|Q\| + r \leqslant \|R\|$ *divided by* $a_{01}^{2\|R\|-1}$. *The expansion* $b(T, X)$ *is unique. Let*

$$g(X, \delta, T) = f(X, \delta + b(T, X), T), \tag{2.2}$$

then $g(X, 0, T) \equiv 0$.

This is a generalization of Theorem 1.1 of [Bruno, 2000, Ch. II] on the implicit function and simultaneously a theorem on reducing the algebraic equation (2.1) to its normal form (2.2) when the linear part $a_{01}(T) \not\equiv 0$ is nondegenerate. In it, we must exclude the values of T near the zeros of the function $a_{01}(T)$.

London Journal of Research in Science: Natural and Formal

Let $X = (x_1, \ldots, x_n) \in \mathbb{R}^n$ or $\mathbb{C}^n$, and $f(X)$ be a polynomial. A point $X = X^0$, $f(X^0) = 0$ is called *simple* if the vector $(\partial f/\partial x_1, \ldots, \partial f/\partial x_n)$ in it is non-zero. Otherwise, the point $X = X^0$ is called *singular* or *critical*. By shifting $X = X^0 + Y$ we move the point X^0 to the origin $Y = 0$. If at this point the derivative $\partial f/\partial x_n \neq 0$, then near X^0 all solutions to the equation $f(X) = 0$ have the form $y_n = \Sigma b_{q_1,\ldots q_{n-1}} y_1^{q_1} \cdots y_{n-1}^{q_{n-1}}$, that is, lie in $(n-1)$-dimensional space.

2.2. Newton's polyhedron: Let the point $X^0 = 0$ be singular. Write the polynomial in the form

$$f(X) = \Sigma a_Q X^Q,$$

where $a_Q = \text{const} \in \mathbb{R}$, or $\mathbb{C}$. Let $\mathbf{S}(f) = \{Q : a_Q \neq 0\}$.

The set $\mathbf{S}$ is called the *support* of the polynomial $f(X)$. Let it consist of points $Q_1, \ldots, Q_k$. The convex hull of the support $\mathbf{S}(f)$ is the set

$$\Gamma(f) = \left\{ Q = \sum_{j=1}^{k} \mu_j Q_j, \mu_j \geqslant 0, \sum_{j=1}^{k} \mu_j = 1 \right\}, \tag{2.3}$$

which is called *Newton's polyhedron*.

Its boundary $\partial\Gamma(f)$ consists of generalized faces $\Gamma_j^{(d)}$, where d is its dimension of $0 \leqslant d \leqslant n-1$ and j is the number.

Each (generalized) face $\Gamma_j^{(d)}$ corresponds to its:

- *boundary subset*

$$\mathbf{S}_j^{(d)} = \mathbf{S} \cap \Gamma_j^{(d)},$$

- *truncated polynomial*

$$\hat{f}_j^{(d)}(X) = \Sigma a_Q X^Q \text{ over } Q \in \mathbf{S}_j^{(d)},$$

- and *normal cone*

$$\mathbf{U}_j^{(d)} = \left\{ P : \langle P, Q' \rangle = \langle P, Q'' \rangle > \langle P, Q''' \rangle, Q', Q'' \in \mathbf{S}_j^{(d)}, Q''' \in \mathbf{S} \backslash \mathbf{S}_j^{(d)} \right\}, \tag{2.4}$$

where $P = (p_1, \ldots, p_n) \in \mathbb{R}_*^n$, the space $\mathbb{R}_*^n$ is conjugate (dual) to the space $\mathbb{R}^n$ and $\langle P, Q \rangle = p_1 q_1 + \ldots + p_n q_n$ is the scalar product.

At $X \to 0$ solutions to the full equation $f(X) = 0$ tend to non-trivial solutions of those truncated equations $\hat{f}_j^{(d)}(X) = 0$ whose normal cone $\mathbf{U}_j^{(d)}$ intersects with the negative orthant $P \leqslant 0$ in $\mathbb{R}_*^n$.

Remark 1. If in the sum (2.1) all Q belong to a forward cone C:

$$\langle Q, K_i \rangle > c_i, \quad i = 1, \ldots, m,$$

then in the solution (2.2) of Theorem 2.1 all R belong to the same cone C: $\langle Q, K_i \rangle > c_i$, $i = 1, \ldots, m$, [Bruno, 1989, Part I, Chapter 1, § 3].

2.3. Power transformations [Bruno, 1962; 2000:] Let $\ln X \stackrel{\text{def}}{=} (\ln x_1, \ldots, \ln x_n)$. The linear transformation of the logarithms of the coordinates

$$(\ln y_1, \ldots, \ln y_n) \stackrel{\text{def}}{=} \ln Y = (\ln X)\alpha, \tag{2.5}$$

where α is a nondegenerate square n-matrix, is called *power transformation*.

By the power transformation (2.5), the monomial X^Q tranforms into the monomial Y^R, where $R = Q\,(\alpha^*)^{-1}$ and the asterisk indicates a transposition.

A matrix α is called *unimodular* if all its elements are integers and $\det \alpha = \pm 1$. For an unimodular matrix α, its inverse α^{-1} and transpose α^* are also unimodular.

Theorem 2.2. *For the face $\Gamma_j^{(d)}$ there exists a power transformation (2.5) with the unimodular matrix α which reduces the truncated sum $\hat{f}_j^{(d)}(X)$ to the sum from d coordinates, that is, $\hat{f}_j^{(d)}(X) = Y^S \hat{g}_j^{(d)}(Y)$, where $\hat{g}_j^{(d)}(Y) = \hat{g}_j^{(d)}(y_1, \ldots, y_d)$ is a polynomial. Here $S \in \mathbb{Z}^n$. The additional coordinates $y_{d+1}, \ldots, y_n$ are local (small).*

The article [Bruno, Azimov, 2023] specifies an algorithm for computing the unimodular matrix α of Theorem 2.2.

2.4. Parametric expansion of solutions: Let $\Gamma_j^{(d)}$ be a face of the Newton polyhedron $\Gamma(f)$. Let the full equation $f(X) = 0$ is changed into the equation $g(Y) = 0$ after the power transformation of Theorem 2.2. Thus $\hat{g}_j^{(d)}(y_1, \ldots, y_d) = g(y_1, \ldots, y_d, 0, \ldots, 0)$.

Let the polynomial $\hat{g}_j$ be the product of several irreducible polynomials

$$\hat{g}_j^{(d)} = \prod_{k=1}^{m} h_k^{l_k}(y_1, \ldots, y_d), \tag{2.6}$$

where $0 < l_k \in \mathbb{Z}$. Let the polynomial h_k be one of them. Three cases are possible:

Case 1. The equation $h_k = 0$ has a polynomial solution $y_d = \varphi(y_1, \ldots, y_{d-1})$. Then in the full polynomial $g(Y)$ let us substitute the coordinates

$$y_d = \varphi + z_d,$$

for the resulting polynomial $h(y_1, \ldots, y_{d-1}, z_d, y_{d+1} \ldots, y_n)$ again construct the Newton polyhedron, separate the truncated polynomials, etc. Such calculations were made in [Bruno, Batkhin, 2012] and were shown in [Bruno, 2000, Introduction].

Case 2. The equation $h_k = 0$ has no polynomial solution, but has a parametrization of solutions

$$y_j = \varphi_j(T), j = 1, \ldots, d, \quad T = (t_1, \ldots, t_{d-1}).$$

Then in the full polynomial g Y (we)substitute the coordinates

$$y_j = \varphi_i(T) + \beta_j \varepsilon, j = 1, \ldots, d, \tag{2.7}$$

where $\beta_j = \text{const}$, $\Sigma\,|\beta_j| \neq 0$, and from the full polynomial $g(Y)$ we get the polynomial

$$h = \Sigma a_{Q'',r}(T) {Y''}^{Q''} \varepsilon^r, \tag{2.8}$$

where $Y'' = (y_{d+1}, \ldots, y_n)$, $0 \leqslant Q'' = (q_{d+1}, \ldots, q_n) \in \mathbb{Z}^{n-d}$, $0 \leqslant r \in \mathbb{Z}$. Thus $a_{00}(T) \equiv 0$, $a_{01}(T) = \sum\limits_{j=1}^{d} \beta_j \partial \hat{g}_j^{(d)} / \partial y_j(T)$.

If in the expansion (5.7) $l_k = 1$, then $a_{01} \not\equiv 0$. By Theorem 2.1, all solutions to the equation $h = 0$ have the form

$$\varepsilon = \Sigma b_{Q''}(T) {Y''}^{Q''},$$

London Journal of Research in Science: Natural and Formal

i.e., according to (2.7) the solutions to the equation $g = 0$ have the form

$$y_j = \varphi_j(T) + \beta_j \Sigma b_{Q''}(T) Y''^{Q''}, j = 1, \ldots, d.$$

Such calculations were proposed in [Bruno, 2018a].

If in (5.7) $l_k > 1$, then in (2.8) $a_{01}(T) \equiv 0$ and for the polynomial (2.8) from Y'', ε we construct a Newton polyhedron by support $\mathbf{S}(h) = \{Q'', r : a_{Q'',r}(T) \not\equiv 0\}$, separate the truncations and so on.

Case 3. The equation $h_k = 0$ has neither a polynomial solution nor a parametric one. Then, using Hadamard's polyhedron [Bruno, 2018a; 2019a], one can compute a piece-wise approximate parametric solution to the equation $h_k = 0$ and look for an approximate parametric expansion.

Similarly, one can study the position of an algebraic manifold in infinity.

III. SINGLE ODE [BRUNO, 2004]

3.1. Setting of the problem: Here we consider an ordinary differential equation of the form

$$f\left(x, y, y', \ldots, y^{(n)}\right) = 0, \tag{3.1}$$

where x is independent variable, y is the dependent variable, $y' = dy/dx$ and f is a polynomial of its arguments. Near $x^0 = 0$ or ∞ we look for solutions of equation (3.1) in the form of asymptotic series

$$y = \sum_{k=1}^{\infty} b_k x^{s_k}, \tag{3.2}$$

where b_k are functions of $\log x$ and $\omega s_k > \omega s_{k+1}$ with

$$\omega = \begin{cases} -1, & \text{if } x^0 = 0, \\ 1, & \text{if } x^0 = \infty. \end{cases} \tag{3.3}$$

We set $X = (x, y)$. By a differential monomial $a(x, y)$ we mean the product of an ordinary monomial

$$c x^{r_1} y^{r_2} \stackrel{\text{def}}{=} c X^R, \tag{3.4}$$

is called a *differential sum*. In equation (3.1) polynomial f is the differential sum.

London Journal of Research in Science: Natural and Formal

To every differential monomial $a\left(X\right)$ one assigns its (vector) *exponent* $Q(a) = (q_1, q_2) \in \mathbb{R}^2$ by the following rules. For a monomial of the form (3.4) let

$$Q\left(cX^R\right) = R,$$

that is, $Q\left(cx^{r_1}y^{r_2}\right) = (r_1, r_2)$; for a derivative of the form (3.5) let

$$Q\left(d^l y/dx^l\right) = (-l, 1).$$

When differential monomials are multiplied, their exponents are summed as vectors:

$$Q\left(a_1 a_2\right) = Q\left(a_1\right) + Q\left(a_2\right).$$

The set $\mathbf{S}(f)$ of exponents $Q\left(a_i\right)$ of all the differential monomials $a_2(X)$ in a differential sum of the form (3.6) is called the *support* of the sum $f\left(X\right)$. Obviously, $\mathbf{S}(f) \in \mathbb{R}^2$. The closure $\Gamma(f)$ of the convex hull of the support $\mathbf{S}(f)$ is referred to as the *polygon of the sum* $f(X)$. The boundary $\partial\Gamma(f)$ of the polygon $\Gamma(f)$ consists of vertices $\Gamma_j^{(0)}$ and edges $\Gamma_j^{(1)}$. These objects are called (generalized) *faces* $\Gamma_j^{(d)}$, where the superscript indicates the dimension of the face and the subscript is the number of the face. Corresponding to any face $\Gamma_j^{(d)}$ are the related *boundary subset* $\mathbf{S}_j^{(d)} = \mathbf{S}(f) \cap \Gamma_j^{(d)}$ of the set $\mathbf{S}$ and the *truncated sum*

$$\hat{f}_j^{(d)}(X) = \sum a_i(X) \quad \text{over} \quad Q\left(a_i\right) \in \mathbf{S}_j^{(d)}. \tag{3.7}$$

Let $\mathbb{R}_*^2$ be the plane conjugate to the plane $\mathbb{R}^2$ so that the inner (scalar) product

$$\langle P, Q\rangle \stackrel{\text{def}}{=} p_1 q_1 + p_2 q_2$$

is defined for any $P = (p_1, p_2) \in \mathbb{R}_*^2$ and $Q = (q_1, q_2) \in \mathbb{R}^2$. Corresponding to any face $\Gamma_j^{(d)}$ are its *normal cone*,

$$\mathbf{U}_j^{(d)} = \left\{ P : \begin{array}{ll} \langle P, Q\rangle = \langle P, Q'\rangle, & Q, Q' \in \mathbf{S}_j^{(d)} \\ \langle P, Q\rangle > \langle P, Q''\rangle, & Q'' \in \mathbf{S}(f) \backslash \mathbf{S}_j^{(d)} \end{array} \right\}$$

and the truncated sum (3.7).

All these constructions are applicable to equation (3.1), where f is a differential sum.

Let $x \to 0$ or $x \to \infty$ and suppose that a solution of the equation (3.1) has the form

$$y = c_r x^r + o\left(|x|^{r+\varepsilon}\right), \tag{3.8}$$

where c_r is a coefficient, $c_r = \text{const} \in \mathbb{C}$, $c_r \neq 0$, the exponents r and ε are in $\mathbb{R}$, and $\varepsilon\omega < 0$. Then we say that the expression

$$y = c_r x^r, \quad c_r \neq 0 \tag{3.9}$$

gives the *power-law asymptotic form* of the solution (3.8).

Thus, corresponding to any face $\Gamma_j^{(d)}$ are the normal cone $\mathbf{U}_j^{(d)}$ in $\mathbb{R}^2_*$ and the truncated equation

$$\hat{f}_j^{(d)}(X) = 0. \tag{3.10}$$

Theorem 3.1 ([Bruno, 2000, Chap. VI, Theorem 1.1])**.** *If the equation* (3.1) *has a solution of the form* (3.8) *and if* $\omega(1,p) \in \mathrm{U}_j^{(d)}$*, then the truncation* (3.9) *of the solution* (3.8) *is a solution of the truncated equation* (3.7), (3.10)*.*

Therefore, to find all truncated solutions (3.9) of the equation (3.1), one must calculate the support $\mathbf{S}(f)$, the polygon $\Gamma(f)$, all its faces $\Gamma_j^{(d)}$, the outward normals N_j to the edges $\Gamma_j^{(1)}$, the normal cones $\mathbf{U}_j^{(1)}$ of the edges, and the normal cones $\mathbf{U}_j^{(0)}$ of the vertices. For each truncated equation (3.7), (3.10) one must then find all its solutions of the form (3.9) such that the vector $(1; r)$ belongs to $\mathbf{U}_j^{(d)}$, and single out the solutions of this kind for which one of the vectors $\pm(1, r)$ belongs to the normal cone $\mathbf{U}_j^{(d)}$. If $d = 0$, then one of the vectors $\pm(1, r)$ belongs to $\mathbf{U}_j^{(d)}$. If $d = 1$, then this property always holds. Here the value of ω is also determined.

3.2. Solution of the truncated equation: Here we consider separately two cases: a vertex $\Gamma_j^{(0)}$ and an edge $\Gamma_j^{(1)}$. Corresponding to a vertex $\Gamma_j^{(0)} = \{Q\}$ is a truncated equation (3.10) with one-point support Q and with $d = 0$. We set $g(X) \stackrel{\text{def}}{=} X^{-Q} \hat{f}_j^{(0)}(X)$. Then the solution (3.7), (3.10) satisfies the equation

$$g(X) = 0$$

Substituting $y = cx^r$ into $g(X)$, we see that $g\left(x, cx^r\right)$ does not depend on x, c and is a polynomial in r, that is,

$$g\left(x, cx^r\right) \equiv \chi(r),$$

where $\chi(r)$ is the *characteristic polynomial* of the differential sum $\hat{f}_j^{(0)}(X)$. Hence, in a solution (3.9) of the equation (3.10) the exponent r is a root of the characteristic equation

$$\chi(r) \stackrel{\text{def}}{=} g\left(x, x^r\right) = 0, \tag{3.11}$$

and the coefficient c_r is arbitrary. Among the roots r_i of the equation (3.11), one must single out only those for which one of the vectors $\omega(1, r)$, where $\omega = \pm 1$, belongs to the normal cone $\mathbf{U}_j^{(0)}$ of the vertex $\Gamma_j^{(0)}$. In this case the value of ω uniquely determined. The corresponding expressions of the sum with an arbitrary constant c_r are candidates for the role of truncated solutions of the equation (3.1). Moreover, by (3.3), if $\omega = -1$, then $x \to 0$, and if $\omega = 1$, then $x \to \infty$.

Complex roots r to characteristic equation (3.11) may bring to *exotic expansions* of solutions (3.2), where coefficients b_k are power series in $x^{\alpha i}$ with real $\alpha \in \mathbb{R}$ and $i^2 = -1$.

Corresponding to an edge $\Gamma_j^{(1)}$ is a truncated equation (3.10) with $d = 1$ whose normal cone $\mathbf{U}_j^{(1)}$ is a ray $\{\lambda N_j, \lambda > 0\}$. If $\omega(1, r) \in \mathbf{U}_j^{(1)}$, this condition uniquely determines the exponent r of the truncated solution (3.9) and the value $\omega = \pm 1$ in (3.3). To find the coefficient c_r, one must substitute the expression (3.9) into the truncated equation (3.10). After cancelling a factor which is a power of x, we obtain an algebraic *defining equation* for the coefficient c_r,

$$\tilde{\tilde{f}}\left(c_r\right) \stackrel{\text{def}}{=} x^{-s} \hat{f}_j^{(1)}\left(x, c_r x^r\right) = 0$$

Corresponding to every root $c_r = c_r^{(i)} \neq 0$ of this equation is an expression of the form (3.9) which is a candidate for the role of a truncated solution of the equation (3.1). Moreover, by (3.3), if in the normal cone $\mathbf{U}_j^{(1)}$ one has $p_1 < 0$, then $x \to 0$, and if $p_1 > 0$, then $x \to \infty$.

Thus, every truncated equation (3.10) has several suitable solutions of the form (3.9). Let us combine these solutions into families that are continuous with

respect to ω, r, c_r, and the parameters of the equation (3.1) and denote these families by $\mathcal{F}_i^{(d)}k$, where $k = 1, 2 \ldots$.

If in the truncated equation (3.10), we make the *power transformation*

$$y = x^P z$$

and the *logarithmic transformation*

$$\xi = \log x,$$

then we obtain ODE

$$\varphi(\xi, z) = 0, \tag{3.12}$$

where φ is a differential sum, i. e. it has the form (3.1). If the equation (3.12) has a solution in the form

$$z = \sum_{j=1}^{\infty} c_j \xi^{r_j}, \quad r_j > r_{j+1},$$

then in the expansion (3.2) coefficients b_k are functions from $\log x$. If $b_1 = \text{const}$, then it is the *power-logarithmic expansion*, where other b_k are polynomials in $\log x$. If b_1 depends of $\log x$, then all b_k are power series in $\log x$ and the expansion (3.2) is *complicated*.

3.3. Computation of solution to equation (3.1) as expansion (3.2)

From the polygon Γ of the initial equation (3.1) we take a vertex or an edge $\Gamma_j^{(d)}$. Then we found a power solution $y = b_1 x^{P_1}$ of the truncated equation $\hat{f}_j^{(d)}(X) = 0$, as it was described above, put

$$y = b_1 x^{P_1} + z$$

and obtain new equation

$$g(x, z) = 0.$$

We construct the polygon ${}_1\Gamma$ for the new equation, take a vertex or an edge ${}_1\Gamma_k^{(e)}$, solve the truncated equation

$$\hat{g}_k^{(e)}(x, z) = 0,$$

and obtain the second term $b_2 x^{P_2}$ of expansion (3.2) and so on.

London Journal of Research in Science: Natural and Formal

We construct the polygon ${}_1\Gamma$ for the new equation, take a vertex or an edge ${}_1\Gamma_k^{(e)}$, solve the truncated equation

$$\hat{g}_k^{(e)}(x,z)=0,$$

and obtain the second term $b_2x^{P_2}$ of expansion (3.2) and so on.

In [Bruno, 2004] there are some properties, that simplify computation.

Thus, we can obtain the 4 types of expansions (3.2) of solutions to equation (3.1):

1. *Power*, when all $b_k=\text{const}$ [Ibid.];
2. *Power-logarithmic*, when $b_1=\text{const}$ and other b_k are polynomial in $\log x$ [Ibid.];
3. *Complicated*, when all b_k are power series in $\log x$ [Bruno, 2006; 2018b];
4. *Exotic*, when all b_k are power series in $x^{i\alpha}$ [Bruno, 2007].

Except expansions (3.2) of solutions $y(x)$ of equation (3.1), there are *exponential expansions*

$$y=\sum_{k=1}^{\infty}b_k(x)\exp\left[k\varphi(x)\right],$$

where $b_k(x)$ and $\varphi(x)$ are power series in x [Bruno, 2012a,b].

Also there are solutions in the form of transseries [Bruno, 2019b].

These results were applied to 6 Painlevè equations [Bruno, 2015; 2018b,c; Bruno, Goruchkina, 2010].

Written as differential sums they are:

Equation P_1**:** $$f(x,y)\stackrel{\text{def}}{=}-y''+3y^2+x=0.$$

Equation P_2**:** $$f(x,y)\stackrel{\text{def}}{=}-y''+2y^3+xy+a=0.$$

Equation P_3**:** $$f(x,y)\stackrel{\text{def}}{=}-xyy''+xy'^2-yy'+ay^3+by+cxy^4+dx=0.$$

Equation P_4**:** $$f(x,y)\stackrel{\text{def}}{=}-2yy''+y'^2+3y^4+8xy^3+4(x^2-a)y^2+2b=0.$$

London Journal of Research in Science: Natural and Formal

Equation P_5:

$$f(z,w) \stackrel{\text{def}}{=} -z^2w(w-1)w'' + z^2\left(\frac{3}{2}w - \frac{1}{2}\right)(w')^2 - zw(w-1)w' + \\ + (w-1)^3(\alpha w^2 + \beta) + \gamma z w^2(w-1) + \delta z^2 w^2(w+1) = 0.$$

Equation P_6:

$$f(x,y) \stackrel{\text{def}}{=} 2y''x^2(x-1)^2y(y-1)(y-x) - (y')^2[\, x^2(x-1)^2(y-1)(y-x) + \\ + x^2(x-1)^2y(y-x) + x^2(x-1)^2y(y-1)\,] + \\ + 2y'[\, x(x-1)^2y(y-1)(y-x) + x^2(x-1)y(y-1)(y-x) + \\ + x^2(x-1)^2y(y-1)\,] - [\, 2\alpha y^2(y-1)^2(y-x)^2 + 2\beta x(y-1)^2(y-x)^2 + \\ + 2\gamma(x-1)y^2(y-x)^2 + 2\delta x(x-1)y^2(y-1)^2\,] = 0.$$

Here a, b, c, d and $\alpha, \beta, \gamma, \delta$ are complex parameters. If all they are nonzero, then polygons for these equations are shown in Figures 1, 2, 3.

Figure 1: Supports and polygons for equations P_1 (left), P_2 (right).

3.4. Normal form: Roots $r_j \stackrel{\text{def}}{=} \lambda_j$ of the equation (3.11) are called as *eigenvalues of the differential sum* $\hat{f}_j^{(0)}(X)$, corresponding to the vertex. If the differential sum $\hat{f}_j^{(0)}(X)$ has order l, then the characteristic equation (3.11) has l roots, $0 \le l \le n$.

Theorem 3.2. *Let*

1) $f(X)$ *be a polynomial in* $x, y, \dots, y^{(n)}$;
2) *its polygon* $\Gamma(f)$ *have a vertex* $\Gamma_1^{(0)} = (v, 1)$ *at the left side of its boundary* $\partial\Gamma$;

London Journal of Research in Science: Natural and Formal

3) truncated differential sum $\hat{f}_1^{(0)}(X)$ *have eigenvalues* $\lambda_1, \ldots, \lambda_l$, $0 \le l \le n$;
4) the most left point of the support $\mathbf{S}(f)$ *in the axis* $q_2 = 0$ *be* $(\alpha, 0)$. *Evidently* $\alpha \in \mathbb{Z}$.

Then there exists such power series $\varphi(x)$ *with integral increasing exponents, that after substitution*

$$y = z + \varphi(x) \tag{3.13}$$

the transformed differential sum

$$g(x, z) = f(x, z + \varphi(x)) \tag{3.14}$$

for

$$z = z' = \cdots = z^{(n)} = 0 \tag{3.15}$$

has only resonant terms $b_m x^m$, *where*

$$m = v + \lambda_k \in \mathbb{Z} \tag{3.16}$$

and $m \ge \alpha$.

So here the eigenvalue λ_k is resonant if $\alpha - v \le \lambda_k \in \mathbb{Z}$.

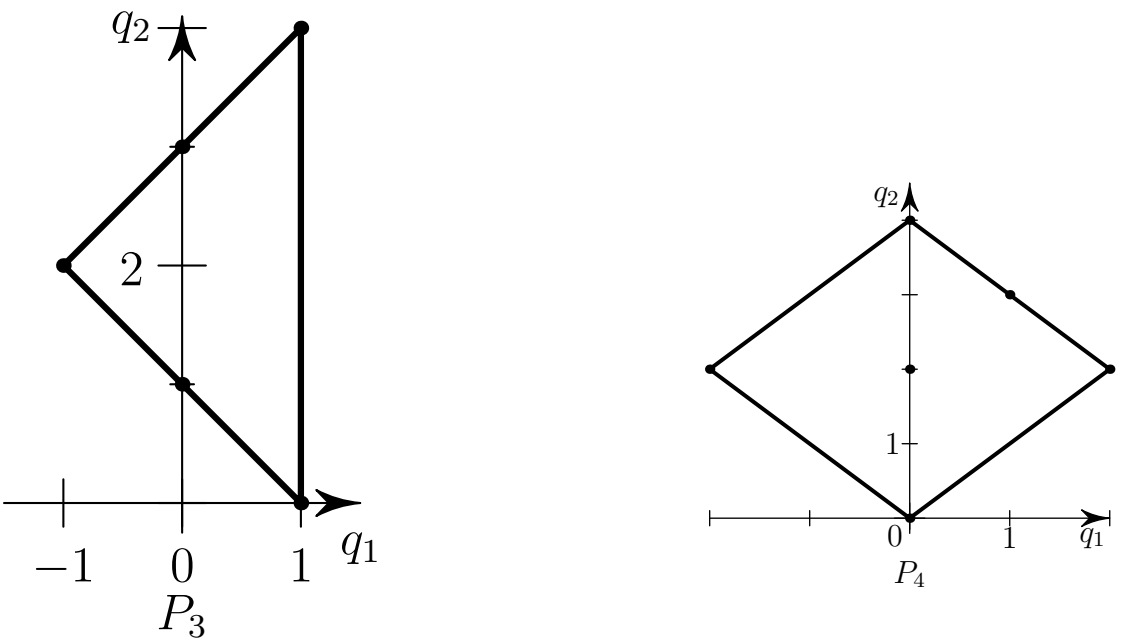

Figure 2: Supports and polygons for equations P_3 (left), P_4 (right).

Theorem 3.3. *Let*

1) $f\left(x, y, y', \ldots, y^{(n)}\right)$ *be a polynomial in* $x, y, y', \ldots, y^{(n)}$*;*

2) its Newton polygon $\Gamma(f)$ *have a vertex* $\Gamma_1^{(0)} = (v, 1)$ *at the right side of its boundary* $\partial\Gamma$*;*

3) truncated differential sum $\hat{f}_j^{(0)}(X)$ *have eigenvalues* $\lambda_1, \ldots, \lambda_l$, $0 \leq l \leq n$*;*

4) the most right point of the support $\mathbf{S}(f)$ *in the axis* $q_2 = 0$ *be* $(\beta, 0)$*. Evidently* $\beta \in \mathbb{Z}$*.*

Then there exists such power series $\varphi(x)$ *with integral decreasing exponents, that after substitution* (3.13)*, the differential sum* (3.14) *for identities* (3.15) *has only resonant terms* $b_m x^m$*, where equality* (3.16) *is true, and* $m \leq \beta$*.*

So here the eigenvalue λ_k is resonant if $\beta - v \geq \lambda_k \in \mathbb{Z}$. Equations $g(x, z) = 0$ for (3.14) in situations of Theorems 3.2 and 3.3 we will call *normal forms.*

Corollary 3.3.1. *If the truncated sum* $\hat{f}_j^{(0)}(X)$ *has no integral eigenvalue* $\lambda_k \geqslant \alpha - v$ *(for Theorem 3.2) or* $\lambda_k \leqslant \beta - v$ *(for Theorem 3.3), then the initial equation* $f(X) = 0$ *has formal solution* $y = \varphi(x)$*. If the truncated sum* $\hat{f}_j^{(0)}(X)$ *contains the derivation* $y^{(n)}$*, then the series* $\varphi(x)$ *converges according to Theorem 3.4 in [Bruno, 2004].*

Remark 2. If the truncated sum $\hat{f}_j^{(0)}(X)$ has integral eigenvalue $\lambda_k \geqslant \alpha - v$ (for Theorem 3.2) or $\lambda_k \leqslant \beta - v$ (for Theorem 3.3), then the initial equation $f(X) = 0$

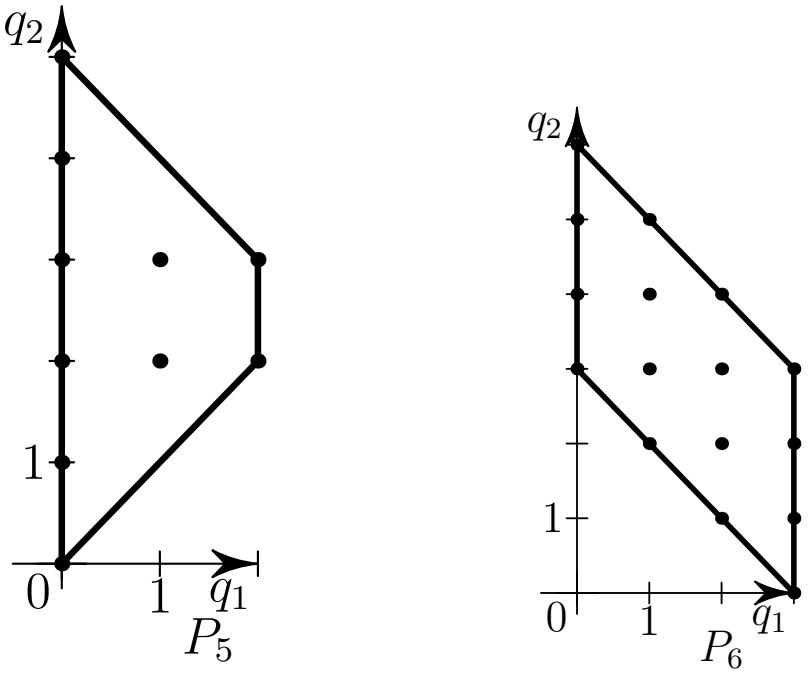

Figure 3: Supports and polygons for equations P_5 (left), P_6 (right).

London Journal of Research in Science: Natural and Formal

3.5. Space Power Geometry: We will consider such a generalization of the power function cx^r which preserves their main properties. The real number

$$p_\omega(\varphi(x)) = \omega \varlimsup_{x^\omega \to \infty} \frac{\log|\varphi(x)|}{\omega \log|x|},$$

where $\arg x = \text{const} \in [0, 2\pi)$, is called the *order* of the function $\varphi(x)$ on the ray when $x \to 0$ or $x \to \infty$. The order $p_\omega(\varphi)$ is not defined on the ray $\arg x = \text{const}$, where the limit point $x = 0$ or $x = \infty$ is a point of accumulation of poles of the function $\varphi(x)$.

In Subsections 3.2–3.4 it was shown that as $x \to 0$ ($\omega = -1$) or as $x \to \infty$ ($\omega = 1$) solutions $y = \varphi(x)$ to the ODE $f(x, y) = 0$, where $f(x, y)$ is a differential sum, can be found by means of algorithms of Plane PG, if

$$p_\omega(\varphi(x)) - l = p_\omega\left(d^l\varphi/dx^l\right), \quad l = 1, \dots, n,$$

where n is the maximal order of derivatives in $f(x, y)$. Here we introduce algorithms, which allow calculate solutions $y = \varphi(x)$ with the property

$$p_\omega(\varphi(x)) + l\gamma_\omega = p_\omega\left(d^l\varphi/dx^l\right), \quad l = 1, \dots, n,$$

where $\gamma_\omega \in \mathbb{R}$, $\omega = \pm 1$.

Lemma 3.3.1. *If*

$$p_\omega(\varphi(x)) = -\gamma_\omega + p_\omega(\varphi'(x)) = -2\gamma_\omega + p_\omega(\varphi''(x)),$$

then $\omega + \omega\gamma_\omega \geqslant 0$.

Note, that in Plane PG we had $\gamma_\omega = -1$, i. e. $\omega + \omega\gamma_\omega = 0$. So, new interesting possibilities correspond to $\omega + \omega\gamma_\omega > 0$.

We consider the ODE

$$f(x,\, y) = \sum_i a_i(x, y) = 0,$$

where $f(x,\, y)$ is a differential sum. To each differential monomial $a_i(x, y)$, we assign its (vector) *power exponent* $\mathbf{Q}(a_i) = (q_1, q_2, q_3) \in \mathbb{R}^3$ by the following rules:

$$\mathbf{Q}\left(cx^{r_1}y^{r_2}\right) = (r_1,\ r_2,\ 0); \quad \mathbf{Q}\left(d^l y/dx^l\right) = (0,\ 1,\ l);$$

power exponent of the product of differential monomials is the sum of power exponents of factors: $\mathbf{Q}(a_1 a_2) = \mathbf{Q}(a_1) + \mathbf{Q}(a_2)$.

The set $\tilde{\mathbf{S}}(f)$ of power exponents $\mathbf{Q}(a_i)$ of all differential monomials $a_i(x, y)$ presented in the differential sum $f(x, y)$ is called the *space support of the sum* $f(x, y)$. Obviously, $\tilde{\mathbf{S}}(f) \subset \mathbb{R}^3$. The convex hull $\mathbf{\Gamma}(f)$ of the support $\tilde{\mathbf{S}}(f)$ is called the *polyhedron of the sum* $f(x, y)$. The boundary $\partial\mathbf{\Gamma}(f)$ of the polyhedron $\mathbf{\Gamma}(f)$ consists of the vertices $\mathbf{\Gamma}_j^{(0)}$, the edges $\mathbf{\Gamma}_j^{(1)}$ and the faces $\mathbf{\Gamma}_j^{(2)}$. They are called (generalized) *faces* $\mathbf{\Gamma}_j^{(d)}$, where the upper index indicates the dimension of the face, and the lower one is its number. Each face $\mathbf{\Gamma}_j^{(d)}$ corresponds to the *space truncated sum*

$$\check{f}_j^{(d)}(x, y) = \sum a_i(x, y) \text{ over } \mathbf{Q}(a_i) \in \mathbf{\Gamma}_j^{(d)} \cap \tilde{\mathbf{S}}(f).$$

The approach allows to obtain solutions with expansions (3.2), where coefficients $b_k(x)$ are all periodic or all elliptic functions [Bruno, 2012c,d; Bruno, Parusnikova, 2012].

Expansions of solutions to more complicated equations such as hierarchies Painlevé see in [Anoshin, Beketova, (et al.), 2023; Bruno, Kudryashov, 2009].

For Painlevé equations P_1 – P_5 with all parameters nonzero, their polyhedrons are shown in Figures 4, 5, 6, 7, 8 correspondingly.

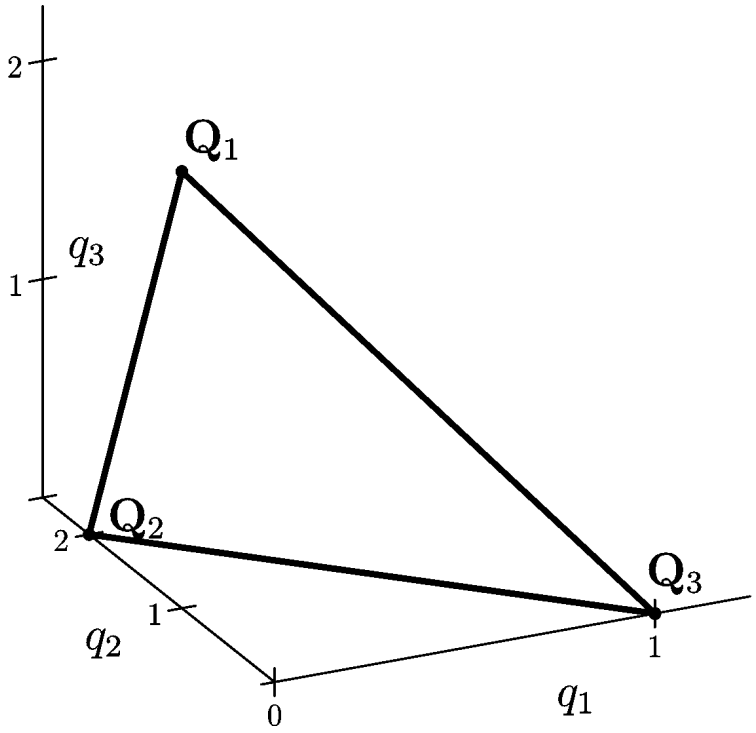

Figure 4: Support and polyhedron for equation P_1.

IV. AUTONOMOUS ODE SYSTEM

Here we consider the system

$$\dot{x}_i = f_i(X), \quad i = 1, \dots, n, \tag{4.1}$$

where $\dot{} = d/dt$, $X = (x_1, \dots, x_n) \in \mathbb{C}^n$ or $\mathbb{R}^n$, all $f_i(X)$ are polynomials from X. A point $X = X^0 = \text{const}$ is called *singular* if all $f_i(X^0) = 0$, $i = 1, \dots, n$.

4.1. Normal form: Let the point $X^0 = 0$ be a singular point. Then the system (4.1) has the linear part

$$\dot{X} = XA,$$

where A is a square n-matrix. Let $\Lambda = (\lambda_1, \dots, \lambda_n)$ be a vector of its eigenvalues.

Theorem 4.1 ([Bruno, 1964; 1971, 1972]). *There exists an invertible formal change of coordinates*

$$x_i = \varphi_i(Y), \quad i = 1, \dots, n,$$

where $\varphi_i(Y)$ are power series from $Y = (y_1, \dots, y_n)$ without free terms, which reduces the system (4.1) to ***normal form***

$$\dot{y}_i = y_i g_i(Y) = y_i \sum g_{iQ} Y^Q, \quad i = 1, \dots, n, \tag{4.2}$$

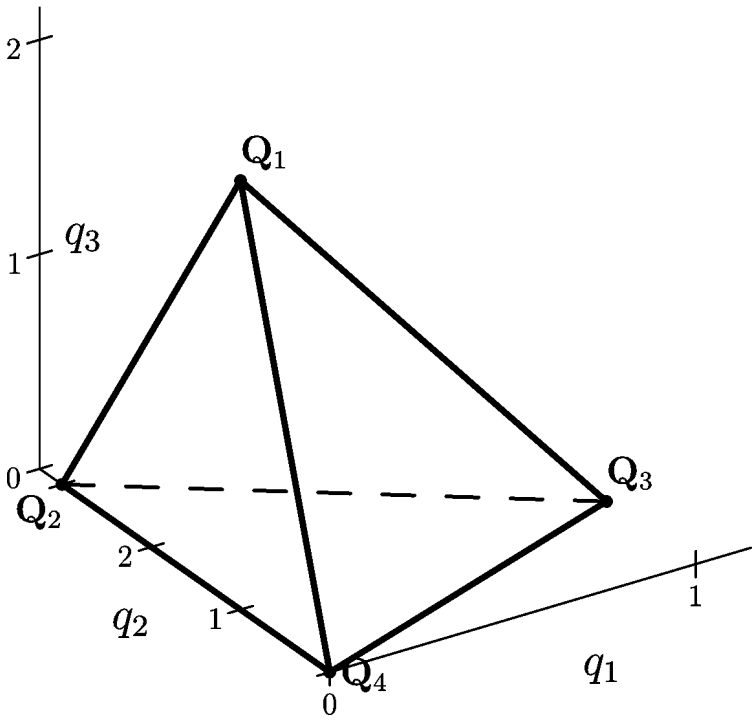

Figure 5: Support and polyhedron for equation P_2.

containing only resonant terms $y_i g_{iQ} Y^Q$, *which have*

$$\langle Q, \Lambda \rangle = 0. \tag{4.3}$$

Here $y_i g_i(Y)$ *are power series on* Y *without free terms.*

Let

$$N_i = \{Q \in \mathbb{Z}^n : q_j \geqslant 0, j \neq i, q_i \geqslant -1\}, i = 1, \ldots, n,$$

and $N = N_1 \cup N_2 \cup \cdots \cup N_n$. Then the number k of linearly independent $Q \in N$ satisfying the equation (4.3) is called *multiplicity of resonance.*

Theorem 4.2. *Let* k *be the multiplicity of resonance of the system* (4.1). *Then there exists a power transformation*

$$\ln Z = (\ln Y)\, \alpha$$

with unimodular matrix α *which reduces the normal form* (4.2), (4.3) *to the system*

$$(\ln \dot{z}_i) = h_i(y_1, \ldots, y_k), \quad i = 1, \ldots, n,$$

in which the first k *coordinates form a closed subsystem without a linear part, and the remaining* $n - k$ *coordinates are expressed via them by means of integrals.*

Thus, if $\Lambda \neq 0$, then the original system (4.1) of order n can be reduced to a system of order k, but without the linear part.

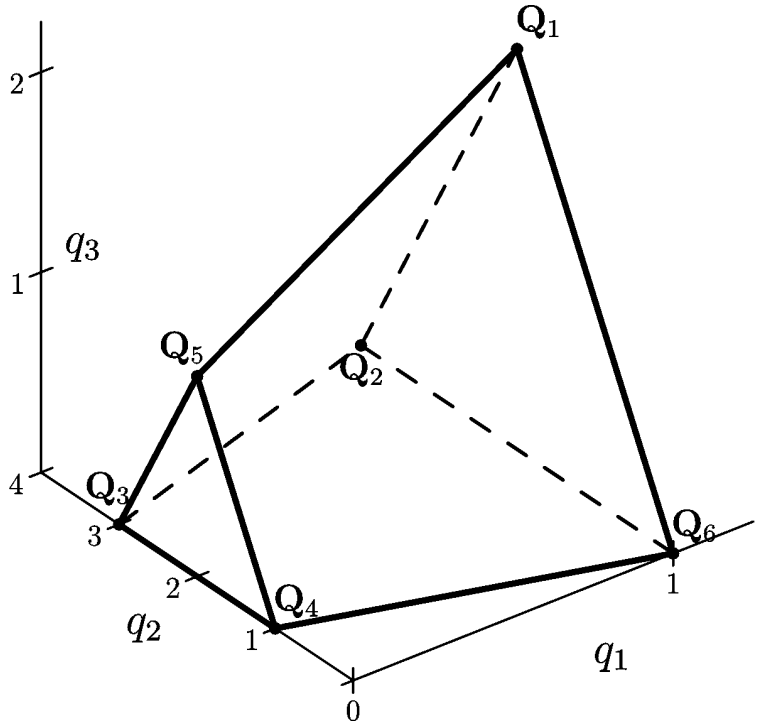

Figure 6: Support and polyhedron for equation P_3.

London Journal of Research in Science: Natural and Formal

4.2: Newton's polyhedron [Bruno, 1962; 2000]. Let's write the system (4.1) as

$$(\ln \dot{x}_i) = \sum a_{iQ} X^Q, \quad i = 1, \dots, n, \tag{4.4}$$

and put $A_Q = (a_{1Q}, \dots, a_{nQ})$.

The set

$$\mathbf{S} = \{Q : A_Q \neq 0\}$$

is called the *support* of the system (4.4). Its convex hull Γ (2.3) is its *Newton's polyhedron*. Its boundary $\partial\Gamma$ consists of generalized faces $\Gamma_j^{(d)}$ of dimensions d, $0 \leqslant d \leqslant n-1$, and with numbers j.

Each generalized face $\Gamma_j^{(d)}$ corresponds to:

- *boundary subset* $\mathbf{S}_j^{(d)} = \Gamma_j^{(d)} \cap \mathbf{S}$,
- *truncated system*

$$(\ln \dot{X}) = \hat{A}_j^{(d)}(X) = \sum A_Q X^Q \text{ over } Q \in \mathbf{S}_j^{(d)}, \tag{4.5}$$

- *normal cone* $\mathbf{U}_j^{(d)} \subset \mathbb{R}_*^n$ (2.4) and
- *tangent cone* $T_j^{(d)}$.

According to [Bruno, 2000, Chapt. 1, §2] let $d > 0$ and $\widetilde{Q}$ be the interior point of a face $\Gamma_j^{(d)}$, that is, $\widetilde{Q}$ does not lie in a face of smaller dimension. If $d = 0$, then

London Journal of Research in Science: Natural and Formal

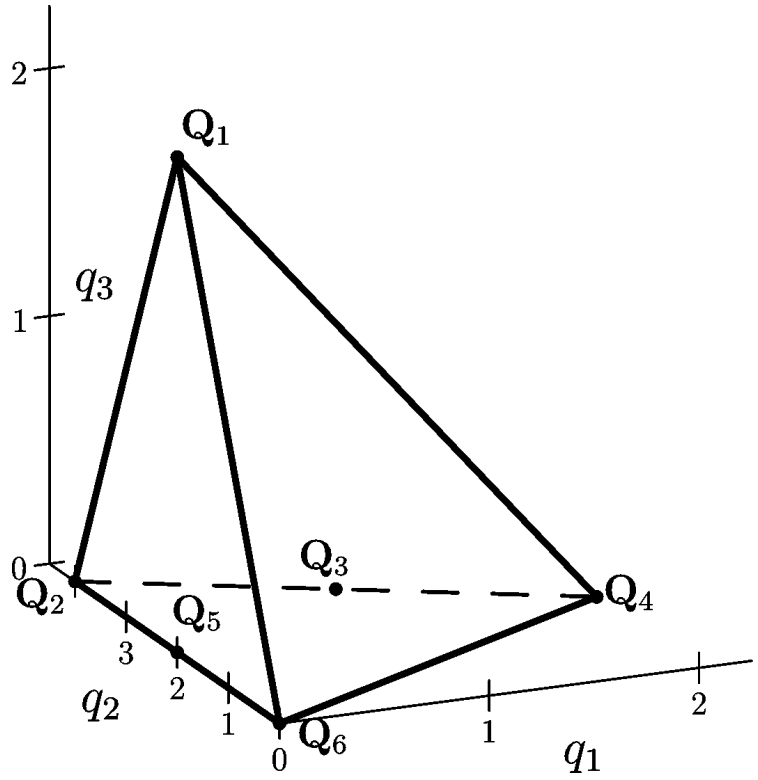

Figure 7: Support and polyhedron for equation P_4.

$\widetilde{Q} = \Gamma_j^{(0)}$. The conic hull of the set $\mathbf{S} - \widetilde{Q}$

$$T_j^{(d)} = \left\{ Q = \mu_1 \left(Q_1 - \widetilde{Q} \right) + \cdots + \mu_k \left(Q_k - \widetilde{Q} \right), \mu_1, \ldots, \mu_k \geqslant 0, Q_1, \ldots, Q_k \in \mathbf{S} \right\}$$

is called the *tangent cone* of the face $\Gamma_j^{(d)}$, $0 \leqslant d \leqslant n-1$, $T_j^{(d)} \subset \mathbb{R}^n$.

Theorem 4.3. *For each generalized face $\Gamma_j^{(d)}$, there exists power transformation*

$$\ln Y = (\ln X)\, \alpha$$

with the unimodular matrix α and change of time

$$d\tau = X^R dt,$$

$R \in \mathbb{Z}^n$, which reduce the system (4.4) to the form

$$d(\ln Y)/d\tau = B(Y), \tag{4.6}$$

where the system

$$d(\ln Y)/d\tau = \hat{B}_j^{(d)}(Y) \equiv \hat{B}_j^{(d)}(y_1, \ldots, y_d) = B(y_1, \ldots, y_d, 0, \ldots, 0), \tag{4.7}$$

corresponds to the truncated system (4.5).

London Journal of Research in Science: Natural and Formal

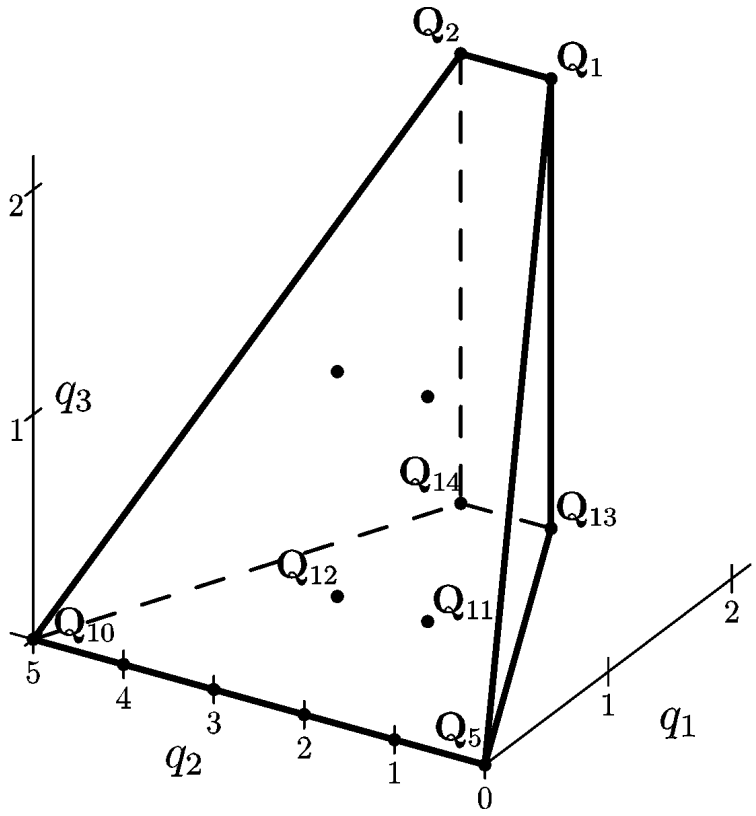

Figure 8: Support and polyhedron for equation P_5.

If the face $\Gamma_j^{(d)}$ had normal and tangent cones $\mathbf{U}_j^{(d)}$ and $T_j^{(d)}$, then the truncated system (4.7) has normal and tangent cones $\widetilde{\mathbf{U}}_j^{(d)}$ and $\widetilde{T}_j^{(d)}$, which are obtained from $\mathbf{U}_j^{(d)}$ and $T_j^{(d)}$ by conjugate linear transformations.

4.3. Generalized normal form [Bruno, 2022b]: Let the point

$$y_1^0, \dots, y_d^0 \neq 0 \tag{4.8}$$

be singular for the truncated system (4.7). Near the point (4.8), the local coordinates are

$$\begin{aligned} z_i &= y_i - y_i^0, \quad i = 1, \dots, d, \\ z_j &= y_j, \quad j = d+1, \dots, n. \end{aligned}$$

Let at the point $Z = (z_1, \dots, z_n) = 0$ the eigenvalues of the matrix of the linear part of the system (4.7) are $\widetilde{\Lambda} = \left(\tilde{\lambda}_1, \dots, \tilde{\lambda}_n\right)$, where $\tilde{\lambda}_1, \dots, \tilde{\lambda}_d$ are the eigenvalues of the subsystem of the first d equations.

Theorem 4.4. *There exists an invertible formal change of coordinates*

$$z_i = \varphi_i(W), \quad i = 1, \dots, n,$$

where $W = (w_1, \dots, w_n)$ *which reduces the system* (4.6) *to the generalized normal form*

$$\dot{w}_i = w_i c_i(W) = w_i \sum c_{iQ} W^Q, \quad i = 1, \dots, n, \tag{4.9}$$

where

$$\left\langle Q, \widetilde{\Lambda} \right\rangle = 0 \text{ and } Q \in \widetilde{T}_j^{(d)} \cap \mathbb{Z}^n. \tag{4.10}$$

Here $\varphi_i = w_i \sum \varphi_{iQ} W^Q$, $i = 1, \dots, n$, *where* $Q \in \widetilde{T}_j^{(d)} \cap \mathbb{Z}^n$.

The system (4.9), (4.10) is reduced to a system of lower order by the power transformation of Theorem 4.2 .

4.4. Analysis of singularities: Let $X = X^0$ be a singular point of the system tem (4.1). Two cases are possible:

Case 1. $\Lambda \neq 0$, then by Theorem 4.1 we reduce the system to a normal form, then by Theorem 4.2 we reduce the normal form to a subsystem of order $k < n$ without linear part and obtain the problem of studying its singular points.

Case 2. $\Lambda = 0$, then we compute the Newton polyhedron and separate truncated systems in which the normal cone $\mathbf{U}_j^{(d)}$ intersects the negative orthant of $P \leqslant 0$. Each of them is reduced to the form (4.6), (4.7) by the transformation of Theorem 4.3. For each singular point (4.8), we apply Theorem 4.4 and obtain a subsystem of smaller order.

Continuing this branching process, after a finite number of resolution of singularities we come to an explicitly solvable system from which we can understand the nature of solutions of the original system.

But Theorem 4.3 can be applied to the original system (4.1), i.e. to each of the generalized faces $\Gamma_j^{(d)}$ of its Newton polyhedron Γ. Then to each singular point (4.8) we apply Theorems 4.4, 4.2 and reduce the order of the system. Here also through a finite number of steps of the singularity resolution we come to an explicitly solvable system. This allows us to study the singularities of the original system in infinity. This is the basis of the integrability criterion in [Bruno, Enderal, 2009; Bruno, Enderal, Romanovski, 2017].

The normal form can be computed in the neighborhood of a periodic solution or invariant torus [Bruno, 1972, II, §11], [Bruno, 2022a].

See [Bruno, Batkhin, 2023] for similar computations for a system of partial differential equations.

4.5. Hamiltonian system: It has the form

$$\dot{x}_i = \partial H/\partial y_i, \quad \dot{y}_i = -\partial H/\partial x_i, \quad i = 1, \dots, m, \tag{4.11}$$

and is defined by one Hamiltonian function $H(\mathbf{x}, \mathbf{y})$, where $\mathbf{x} = (x_1, \dots, x_n)$, $\mathbf{y} = (y_1, \dots, y_m)$. Here the normal form of the system (4.11) corresponds to the normal form of one Hamiltonian function. See details in [Bruno, Batkhin, 2021].

V. ONE PARTIAL DIFFERENTIAL EQUATION

5.1. Support [Bruno, 2000 Ch. 6-8]: Let $X = (x_1, \dots, x_n) \in \mathbb{C}^n$ or $\mathbb{R}^n$ be independent variables and $y \in \mathbb{C}$ or $\mathbb{R}$ be a dependent one. Consider $Z = (z_1, \dots, z_n, z_{n+1}) = (x_1, \dots, x_n, y)$.

Differential monomial $a(Z)$ is called a product of an ordinary monomial

$$cZ^R = cz_1^{r_1} \cdots z_{n+1}^{r_{n+1}},$$

where $c = \text{const}$, and a finite number of derivatives of the following form

$$\frac{\partial^l y}{\partial x_1^{l_1} \cdots \partial^{l_n} x_n} \stackrel{\text{def}}{=} \frac{\partial^l y}{\partial X^L}, \ 0 \leqslant l_j \in \mathbb{Z}, \sum_{j=1}^{n} l_j = l, \ L = (l_1, \dots, l_n)\,.$$

Vector *power exponent* $Q(a) \in \mathbb{R}^{n+1}$ corresponds to the differential monomial $a(Z)$, it is constructed according to the following rules:

$$Q(c) = 0, \text{ if } c \neq 0, \quad Q\left(Z^R\right) = R, \quad Q\left(\partial^l y_j/\partial X^L\right) = (-L, 1).$$

The product of monomials corresponds to the sum of their vector power exponents:

$$Q(ab) = Q(a) + Q(b).$$

Differential sum is the sum of differential monomials

$$f(Z) = \sum a_k(Z). \tag{5.1}$$

If $f(Z)$ has no similar terms, then the set $\mathbf{S}(f) = \{Q(a_k)\}$ is called *support* of the sum (5.1).

5.2. Resonant monomials: Let the support $\mathbf{S}(f)$ of the differential sum (5.1) consists of one point $E_{n+1} = (0, \dots, 0, 1)$. Then the substitution

$$y = cX^P, \quad P = (p_1, \dots, p_n) \in \mathbb{R}^n \tag{5.2}$$

in the differential sum $f(Z)$ gives the monomial

$$c\omega_P(P)X^P$$

where $\omega_P(P)$ is a *polynomial* of P which coefficients depend on P.

Monomial (5.2) will be called *resonant* for $f(Z)$ if for it

$$\omega_P(P) = 0.$$

Let μ_k be the maximal order of the derivative over x_k in $f(Z)$, $k = 1, \dots, n$. If in $P = (p_1, \dots, p_n)$

$$p_k \geqslant \mu_k, \quad k = 1, \dots, n, \tag{5.3}$$

then

$$f(Z) = c\chi(P)X^P,$$

where $\chi(P)$ is the characteristic polynomial of the sum of $f(Z)$ and its coefficients do not depend on P. But if the inequalities (5.3) are not satisfied, then $\omega_P(P) \neq \chi(P)$.

Example. Let $n = 2$, $f(Z) = x_1\dfrac{\partial y}{\partial x_1} + x_2^2\dfrac{\partial^2 y}{\partial x_2^2}$.

If $P = (1, 1)$, then $f(x_1, x_2, cx_1x_2) = cx_1x_2$.
If $P = (1, 2)$, then $f(x_1, x_2, cx_1x_2^2) = c\left(x_1x_2^2 + x_1 \cdot x_2^2 \cdot 2\right) = c \cdot 3x_1x_2^2$.

Generally here for $p_1 \geqslant 1$, $p_2 \geqslant 2$ we have $f(x_1, x_2, cx_1x_2) = c[p_1 + p_2(p_2 - 1)]x_1^{p_1}x_2^{p_2}$ and $\chi(P) = p_1 + p_2(p_2 - 1)$.

5.3. Normal form: For a differential sum $f(Z)$ we denote by $f_k(Z)$ the sum of all differential monomials of $f(Z)$ which have $n+1$ coordinate q_{n+1} of vector power exponents $Q = (q_1, \dots, q_n, q_{n+1})$ equal to k: $q_{n+1} = k$. Denote $\mathbb{Z}_+^n = \{P : 0 \leqslant P \in \mathbb{Z}^n\}$.

Consider the PDE

$$f(Z) = 0. \tag{5.4}$$

Theorem 5.1. *Let*

$$f(Z) = \sum_{k=0}^{\infty} f_k(Z),$$

where all $\mathbf{S}(f_k) \subset \mathbb{Z}_+^n \times \{q_{n+1} = k\}$. *Suppose*

1. $f_0(Z) = \varphi(X)$ *is a power series from* X *without a free term,*
2. $f_1(Z) = a(Z)+b(Z)$, *where* $\mathbf{S}(a) = E_{n+1} = (0, \dots, 0, 1)$, $\mathbf{S}(b) \subset \left(\mathbb{Z}_+^{n+1} \backslash 0\right) \times \{q_{n+1} = 1\}$.

Then there exists a substitution $y = \zeta + \ \ (X)$, *where* $\ \ (X)$ *is a power series from* X *without a free term, which transforms the equation* (5.4) *to the normal form*

$$g(X, \zeta) = 0, \tag{5.5}$$

where $g_0(X) = \sum c_P X^P$ *is a power series without a free term,* $P \in \mathbb{Z}_+^n$ *containing only resonant monomials* $c_P X^P$ *for sum* $a(Z)$.

Corollary 5.1.1. *If the sum* $a\,(P)$ *has no resonance monomials* cX^P *with* $P \in \mathbb{Z}_+^n$, $P \neq 0$, *then* $g_0(X) \equiv 0$ *and*

$$y = \ \psi(X)$$

is the formal solution to the equation (5.4).

If in equation (5.4) differential sum does not contain derivatives, then

$$a(Z) = \text{const} \cdot z_{n+1} = \text{const} \cdot y.$$

Hence $a(Z)$ has no resonant monomials and in the normal form (5.5) the series $g_)(X) \equiv 0$. So Theorem 5.1 gives the Implicit Function Theorem 2.1 without T.

If in Equation (5.4) $n = 1$, then Theorem 5.1 gives Theorem 3.2.

5.4. Polyhedron and truncated equations: Closure of a convex hull

$$\mathbf{\Gamma}(f) = \left\{ Q = \sum \lambda_j Q_j, Q_j \in \mathbf{S}, \lambda_j \geqslant 0, \sum \lambda_j = 1 \right\}$$

of the support $\mathbf{S}(f)$ is called the *polyhedron of sum* $f(Z)$. The boundary $\partial\mathbf{\Gamma}$ of the polyhedron $\mathbf{\Gamma}(f)$ consists of generalized faces $\mathbf{\Gamma}_j^{(d)}$, where $d = \dim \mathbf{\Gamma}_j^{(d)}$. Each face $\mathbf{\Gamma}_j^{(d)}$ corresponds to *normal cone*

$$\mathbf{U}_j^{(d)} = \left\{ P \in \mathbb{R}_*^{n+1} : \langle P, Q' \rangle = \langle P, Q' \rangle > \langle P, Q' \rangle, \text{ where } Q, Q' \in \mathbf{\Gamma}_j^{(d)}, Q' \in \mathbf{\Gamma} \backslash \mathbf{\Gamma}_j^{(d)} \right\},$$

where the space $\mathbb{R}^{n+1}_*$ is conjugate to the space $\mathbb{R}^{n+1}$, $\langle\cdot,\cdot\rangle$ is the scalar product, and *truncated sum*

$$\hat{f}_j^{(d)}(Z) = \sum a_k(Z) \text{by } Q(a_k) \in \mathbf{\Gamma}_j^{(d)} \bigcap \mathbf{S}.$$

Consider the equation

$$f(Z) = 0, \tag{5.6}$$

where f is the differential sum. In the solution of equation (5.6)

$$y = \varphi(X), \tag{5.7}$$

where φ is a series on the powers of x_k and their logarithms, the series φ corresponds to its support, polyhedron, normal cones $\mathbf{u}_i$ and truncations. The logarithm $\ln x_i$ has a zero power exponent on x_i. The truncated solution $y = \hat{\varphi}$ corresponds to the normal cone

$$\mathbf{u} \subset \mathbb{R}^{n+1}_*.$$

Theorem 5.2. *If the normal cone* $\mathbf{u}$ *intersects with the normal cone* (5.2)*, then the truncation* $y = \hat{\varphi}(X)$ *of the solution* (5.3) *satisfies the truncated equation*

$$\hat{f}_j^{(d)}(Z) = 0. \tag{5.8}$$

5.5. Power transformations: To simplify the truncated equation (5.8), it is convenient to use a power transformation. Let α be a square real nondegenerate block matrix of dimension $n+1$ of the form

$$\alpha = \begin{pmatrix} \alpha_{11} & \alpha_{12} \\ 0 & \alpha_{22} \end{pmatrix},$$

where α_{11} and α_{22} are square matrices of dimensions n and 1, respectively. We denote $\ln Z = (\ln z_1, \ldots, \ln z_{n+1})$, and by the asterisk * we denote transposition.

Variable change.

$$\ln W = (\ln Z)\, \alpha \tag{5.9}$$

is called *the power transformation.*

Theorem 5.3 ([Bruno, 2000])**.** *The power transformation* (5.5) *reduces a differential monomial* $a(Z)$ *with a power exponent* $Q(a)$ *into a differential sum* $b(W)$ *with a power exponent* $Q(b)$*:*

$$R = Q(b) = Q(a)\alpha^{-1*}.$$

Corollary 5.3.1. *The power transformation* (5.9) *reduces the differential sum* (2.1) *with support* $\mathbf{S}(f)$ *to the differential sum* $g(W)$ *with support* $\mathbf{S}(g) = \mathbf{S}(f)\alpha^{-1*}$, *i.e.*

$$\mathbf{S}(f) = \mathbf{S}(g)\alpha^{*}$$

Theorem 5.4. *For the truncated equation*

$$\hat{f}_j^{(d)}(Z) = 0$$

there is a power transformation (5.9) *and monomial* Z^T *that translates the equation above into the equation*

$$g(W) = Z^T \hat{f}_j(Z) = 0,$$

where $g(W)$ *is a differential sum whose support has* $n + 1 - d$ *zero coordinates.*

5.6. Logarithmic transformation: Let z_j be one of the coordinates x_k or y. *Transformation*

$$\zeta_j = \ln z_j$$

is called *logarithmic.*

Theorem 5.5. *Let* $f(Z)$ *be a differential sum such that all its monomials have a* j*th component* q_j *of the vector exponent of degree* $Q = (q_1, \ldots, q_{m+n})$ *equal to zero, then the logarithmic transformation* (5.1) *reduces the differential sum* $f(Z)$ *into a differential sum from* $z_1, \ldots, \zeta_j, \ldots, z_n$.

5.7. Calculating asymptotic forms of solutions: A truncated equation $\hat{f}_j^{(n)}(Z) = 0$ is taken. If it cannot be solved, then a power transformation of the Theorem 5.4 and then a logarithmic transformation of the Theorem 5.5 should be performed. Then a simpler equation is obtained. In case it is not solvable again, the above procedure is repeated until we get a solvable equation. Having its solutions, we can return to the original coordinates by doing inverse coordinate transformations. So the solutions written in original coordinates are the asymptotic forms of solutions to the original equation (5.2).

In [Bruno, Batkhin, 2023] method of selecting truncated equations was applied to systems of PDE.

Traditional approach to PDE see in [Oleinik, Samokhin, 1999; Polyanin, Zhurov, 2021].

VI. APPLICATIONS

Here we provide a list of some applications in complicated problems of **(c)** Mathematics, **(d)** Mechanics, **(e)** Celestial Mechanics and **(f)** Hydromechanics.

(c) *In Mathematics*: together with my students I found all asymptotic expansions of five types of solutions to the six Painlevé equations (1906) [Bruno, 2018c; Bruno, Goruchkina, 2010] and also gave very effective method of determination of integrability of ODE system [Bruno, Enderal, 2009; Bruno, Enderal, Romanovski, 2017].

(d) *In Mechanics*: I computed with high precision influence of small mutation oscillations on velocity of precession of a gyroscope [Bruno, 1989] and also studied values of parameters of a centrifuge, ensuring stability of its rotation [Batkhin, Bruno, (et al.), 2012].

(e) *In Celestial Mechanics*: together with my students I studied periodic solutions of the Beletsky equation (1956) [Bruno, 2002; Bruno, Varin, 2004], describing motion of satellite around its mass center, moving along an elliptic orbit. I found new families of periodic solutions, which are important for passive orientation of the satellite [Bruno, 1989], including cases with big values of the eccentricity of the orbit, inducing a singularity. Besides, simultaneously with [Hénon, 1997], I found all regular and singular generating families of periodic solutions of the restricted three-body problem and studied bifurcations of generated families. It allowed to explain some singularities of motions of small bodies of the Solar System [Bruno, Varin, 2007]. In particular, I found orbits of periodic flies round planets with close approach to the Earth [Bruno, 1981].

(f) *In Hydromechanics*: I studied small surface waves on a water [Bruno, 2000, Chapter 5], a boundary layer on a needle [Bruno, Shadrina, 2007], where equations of a flow have a singularity, and an one-dimensional model of turbulence bursts [Bruno, Batkhin, 2023].

REFERENCES

Anoshin V. I., Beketova A. D., Parusnikova A., Prokopenko E. D. Convergence of formal solutions to the second term of the fourth Painlevé hierarchy in a neighborhood of origin // Computational Mathematics and Mathematical Physics. — 2023. — Vol. 63, no. 1. — P. 86–95. — "DOI:10:1134// S0965542523010049.

Batkhin A. B., Bruno A. D., Varin V. P. Stability sets of multiparameter Hamil- tonian systems // Journal of Applied Mathematics and Mechanics. — 2012.— Vol. 76, no. 1. — P. 56–92. — DOI: 10.1016/j.jappmathmech.2012.03.006.

London Journal of Research in Science: Natural and Formal

Birkhoff G. D. Dynamical Systems. Vol. 9. — Revised edition. — Providence, Rhode Island : AMS, 1966. — 305 p. — (Colloquim Publications).

Bruno A. D. The asymptotic behavior of solutions of nonlinear systems of differ- ential equations // Soviet Math. Dokl. — 1962. — Vol. 3. — P. 464–467.

Bruno A. D. Normal form of differential equations // Soviet Math. Dokl. — 1964. — Vol. 5. — P. 1105–1108.

Bruno A. D. Analytical form of differential equations (I) // Trans. Moscow Math. Soc. — 1971. — Vol. 25. — P. 131–288.

Bruno A. D. Analytical form of differential equations (II) // Trans. Moscow Math. Soc. — 1972. — Vol. 26. — P. 199–239.

Bruno A. D. On periodic flybys of the Moon // Celestial Mechanics. — 1981. — Vol. 24, no. 3. — P. 255–268. — DOI: 10.1007/BF01229557.

Bruno A. D. Local Methods in Nonlinear Differential Equations. — Berlin, Hei- delberg, New York, London, Paris, Tokyo : Springer–Verlag, 1989.

Bruno A. D. The Restricted 3–body Problem: Plane Periodic Orbits. — Berlin : Walter de Gruyter, 1994.

Bruno A. D. Power Geometry in Algebraic and Differential Equations. — Ams- terdam : Elsevier Science, 2000.

Bruno A. D. Families of periodic solutions to the Beletsky equation // Cosmic Research. — 2002. — Vol. 40, no. 3. — P. 274–295. — DOI: 10.1023/A: 1015981105366.

Bruno A. D. Asymptotics and expansions of solutions to an ordinary differential equation // Russian Mathem. Surveys. — 2004. — Vol. 59, no. 3. — P. 429–480. — DOI: 10.1070/RM2004v059n03ABEH 000736.

Bruno A. D. Complicated expansions of solutions to an ordinary differential equa- tion // Doklady Mathematics. — 2006. — Vol. 73, no. 1. — P. 117–120. — DOI: 10.1134/S1064562406010327.

Bruno A. D. Exotic expansions of solutions to an ordinary differential equation // Doklady Mathematics.—2007.—Vol. 76, no. 2.—P. 729–733.—DOI: 10.1134/S1064562407050237.

Bruno A. D. Exponential expansions of solutions to an ordinary differential equa- tion // Doklady Mathematics. — 2012a. — Vol. 85, no. 2. — P. 259–264. —DOI: 10.1134/S1064562412020287.

Bruno A. D. Power-exponential expansions of solutions to an ordinary differential equation // Doklady Mathematics.—2012b. —Vol. 85,no.3. — P. 336–340. — DOI: 10.1134 S106456241 203009X.

Bruno A. D. Power geometry and elliptic expansions of solutions to the Painlevé equations // International Journal of Differential Equations. — 2015. — Vol. 2015. — P. 340715. — DOI: 10.1155/2015/340715.

Bruno A. D. Algorithms for solving an algebraic equation // Programming and Computer Software. — 2018a. — Vol. 44, no. 6.—P. 533–545. — DOI: 10. 1134/ S0361768819100013.

Bruno A. D. Complicated and exotic expansions of solutions to the Painlevé equations // Formal and Analytic Solutions of Diff. Equations. FASdiff 2017. Vol. 256 / ed. by G. Filipuk, A. Lastra, S. Michalik. — Cham. : Springer, 2018b. — P. 103–145. — DOI: 10.1007/978-3-319-99148-1_7.

Bruno A. D. Power geometry and expansions of solutions to the Painlevé equa- tions // Transnational Journal of Pure and Applied Mathematics. — 2018c. — Vol. 1, no. 1. — P. 43–61.

Bruno A. D. On the parametrization of an algebraic curve // Mathematical Notes.—2019a.—Vol. 106, no. 6.—P. 885–893.—DOI: 10 . 1134 / S0001434619110233.

Bruno A. D. Power-exponential transseries as solutions to ODE // Journal of Mathematical Sciences: Advances and Applications. — 2019b. — Vol. 59.—P. 33–60. — DOI: 10.18642/jmsaa_7100122093.

Bruno A. D. Families of periodic solutions and invariant tori of Hamiltonian systems // Formal and Analytic Solutions of Differential Equations / ed. by G. Filipuk, A. Lastra, S. Michalik. — WORLD SCIENTIFIC (EUROPE), 02/2022a. — ISBN 9781800611351. — DOI: 10.1142/q0335.

Bruno A. D. On the generalized normal form of ODE systems // Qual. Theory Dyn. Syst. — 2022b. — Vol. 21, no. 1. — DOI: 10.1007/s12346-021-00531-4.

Bruno A. D., Azimov A. A. Computation of unimodular matrices of power trans- formations // Programming and Computer Software.—2023.—Vol. 49, no. 1.—P. 32–41.—DOI: 10.1134/S0361768823010036.

Bruno A. D., Batkhin A. B. Resolution of an algebraic singularity by power geometry algorithms // Programming and computer software. — 2012. — Vol. 38, no. 2. — P. 57–72. — DOI: 10.1134/S036176881202003X.

Bruno A. D., Batkhin A. B. Survey of Eight Modern Methods of Hamiltonian Mechanics // Axioms. — 2021. — Vol. 10, no. 4. — ISSN 2075-1680. — DOI: 10.3390/axioms10040293.

Bruno A. D., Batkhin A. B. Asymptotic forms of solutions to system of nonlinear partial differential equations // Universe. — 2023. — Vol. 9, no. 1. — P. 35. — DOI: 10.3390/universe9010035.

Bruno A. D., Enderal V. F. Algorithmic analysis of local integrability // Doklady Mathematics. — 2009. — Vol. 79, no. 1. — P. 48–52. — DOI: 10.1134/ S1064562409010141.

Bruno A. D., Enderal V. F., Romanovski V. G. Computer Algebra in Scientific Computing: Proceedings CASC 2017 //. Vol. 10490 / ed. by V. P. Gerdt, et al. — Berlin Heidelberg : Springer, 2017. — Chap. On new integrals of the Algaba-Gamero-Garcia system. — (Lecture Notes in Computer Science). — DOI: 10.1007/978-3-642-32973-9.

Bruno A. D., Goruchkina I. V. Asymptotic expansions of solutions of the sixth Painlevé equation // Transactions of Moscow Math. Soc.—2010.—Vol. 71.—P. 1–104.—DOI: 10.1090/ S0077- 1554-2010-00186-0.

Bruno A. D., Kudryashov N. A. Expansions of solutions to the equation P12 by algorithms of power geometry // Ukrainian Mathematical Bulletin. — 2009. — Vol. 6, no. 3. — P. 311–337.

Bruno A. D., Shadrina T. V. Axisymmetric boundary layer on a needle // Trans- actions of Moscow Math. Soc. — 2007. — Vol. 68. — P. 201–259. — DOI: 10.1090/S0077-1554-07-00165-3.

Bruno A. D., Varin V. P. Classes of families of generalized periodic solutions to the Beletsky equation // Celestial Mechanics and Dynamical Astronomy. — 2004. — Vol. 88, no. 4. — P. 325–341. — DOI: 10.1023/B:CELE.0000023390. 25801.f9.

Bruno A. D., Varin V. P. Periodic solutions of the restricted three-body problem for small mass ratio // J. Appl. Math. Mech.—2007.—Vol. 71, no. 6. —P. 933–960.—DOI: 10.1016/ j.jappmathmech. 2007.12.012.

Bruno A. D. Chapter 6. Space Power Geometry for one ODE and P1–P4, P6 // Proceedings of the International Conference, Saint Petersburg, Russia, June 17-23, 2011 / ed. by A. D. Bruno, A. B. Batkhin.—Berlin, Boston: De Gruyter, 2012c.—P. 41–52.—ISBN 9783110275667.— DOI: doi:10. 1515/9783 110275667.41.

Bruno A. D. Chapter 8. Regular Asymptotic Expansions of Solutions to One ODE and P1–P5 // Proceedings of the International Conference, Saint Petersburg, Russia, June 17-23, 2011 / ed. by A. D. Bruno, A. B. Batkhin. — Berlin, Boston : De Gruyter, 2012d. — P. 67–82. — ISBN 9783110275667. — DOI:doi:10.1515/9783110275667.67.

Bruno A. D., Parusnikova A. V. Chapter 7. Elliptic and Periodic Asymptotic Forms of Solutions to P5 // Proceedings of the International Conference, Saint Petersburg, Russia, June 17-23, 2011 / ed. by A. D. Bruno, A. B. Batkhin. — Berlin, Boston : De Gruyter, 2012. — P. 53–66.—ISBN 9783110275667. — DOI: doi:10.1515/9783110275667.53.

Dulac H. Solutions d'un système d'équations différentialles dans le voisinage des valeures singulières // Bull. Soc. Math. France. — 1912. — T. 40. — P. 324- 383.

Gontsov R. R., Goryuchkina I. V. Convergence of formal Dulac series satisfying an algebraic ordinary differential equation // Sb. Math.—2019.— Vol. 210, no. 9. — P. 1207–1221. — DOI: 10.1070/SM9064.

Hadamard J. Etude sur les propriétés des fonctions entières et en particulier d'une fonction considérée par Riemann // Journal de mathématiques pures et appliquées 4e série. — 1893. — T. 9. — P. 171-216

Hénon M. Generating Families in the Restricted Three-Body Problem. — Berlin, Heidelber, New York : Springer, 1997. — 278 p. — (Lecture Note in Physics.Monographs ; 52).

Newton I. A treatise of the method of fluxions and infinite series, with its ap- plication to the geometry of curve lines // The Mathematical Works of Isaac Newton. Vol. 1 / ed. by H. Woolf. — New York – London : Johnson Reprint Corp., 1964. — P. 27–137.

Oleinik O. A., Samokhin V. N. Mathematical Models in Boundary Layer The- ory. — New York : Chapman & Hall/CRC, 1999.—528 p.—DOI: 10.1201/ 9780203749364.

Poincaré H. Sur les propriétés des fonctions définities par les équations aux diffé- rence partielles // Oeuvres de Henri Poincaré. T. I. — Paris : Gauthier–Villars, 1928. — P. XLIX-CXXIX.

Polyanin A. D., Zhurov A. I. Separation of Variables and Exact Solutions to Nonlinear PDEs. — New York : Chapman & Hall/CRC, 2021. — 401 p.

This page is intentionally left blank

Genomic Characteristics of Listeria that Caused Invasive Listeriosis During the COVID-19 Pandemic

Olga L. Voronina, Marina S. Kunda, Natalia N. Ryzhova, Ekaterina I. Aksenova, Anzhelika V. Kutuzova, Anna N. Tikulmina, Tatiana I. Karpova, Alina R. Melkumyan, Elena A. Klimova, Olga A. Gruzdeva & Igor S. Tartakovsky

N.F. Gamaleya National Research Center for Epidemiology and Microbiology

ABSTRACT

Invasive listeriosis is relatively rare, but is one of the deadliest food-borne infections, affecting pregnant women, their fetuses and newborn infants, the elderly and immunocompromised people. The aim of this study was to research the impact of the COVID-19 pandemic on invasive listeriosis in the metropolis. Loci and whole-genome sequencing with subsequent bioinformatic analysis were used for the study of clinical and food Listeria monocytogenes isolates revealed in 2018–2022. The results indicate the crucial change in the spectrum of the L. monocytogenes sequence types (ST) causing invasive listeriosis during the COVID-19 pandemic, with slight changes in the ST spectrum of the food isolates. An increase in sensitivity to previously non-human L. monocytogenes genotypes, namely ST8, 21, 37, 391, and 425, was observed. L. monocytogenes of ST20 and 425 carried plasmids with virulence factors (VF), in addition to the 42 VF identified in the genomes with the vip gene exclusion in the genomes of ST7, 8, 21, and 37. Perinatal listeriosis cases were associated with the new hypervirulent L. monocytogenes of ST1, 4, and 219 compiled with old ST6. These data indicate the need for the more stringent control of food products for high-risk group.

Keywords: listeria monocytogenes; food-borne pathogen; invasive listeriosis; MLST; cgMLST; whole-genome sequencing; plasmid; virulence factors; covid-19; epidemic outbreak.

Classification: FOR: 0605

Language: English

London Journals Press

LJP Copyright ID: 925642
Print ISSN: 2631-8490
Online ISSN: 2631-8504

London Journal of Research in Science: Natural and Formal

Volume 23 | Issue 5 | Compilation 1.0

Genomic Characteristics of Listeria that Caused Invasive Listeriosis During the COVID-19 Pandemic

Olga L. Voronina[α], Marina S. Kunda[σ], Natalia N. Ryzhova[ρ], Ekaterina I. Aksenova[ↀ], Anzhelika V. Kutuzova[¥], Anna N. Tikulmina[§], Tatiana I. Karpova[χ], Alina R. Melkumyan[ν], Elena A. Klimova[Θ], Olga A. Gruzdeva[ζ] & Igor S. Tartakovsky[£]

ABSTRACT

Invasive listeriosis is relatively rare, but is one of the deadliest food-borne infections, affecting pregnant women, their fetuses and newborn infants, the elderly and immunocompromised people. The aim of this study was to research the impact of the COVID-19 pandemic on invasive listeriosis in the metropolis. Loci and whole-genome sequencing with subsequent bioinformatic analysis were used for the study of clinical and food Listeria monocytogenes isolates revealed in 2018–2022. The results indicate the crucial change in the spectrum of the L. monocytogenes sequence types (ST) causing invasive listeriosis during the COVID-19 pandemic, with slight changes in the ST spectrum of the food isolates. An increase in sensitivity to previously non-human L. monocytogenes genotypes, namely ST8, 21, 37, 391, and 425, was observed. L. monocytogenes of ST20 and 425 carried plasmids with virulence factors (VF), in addition to the 42 VF identified in the genomes with the vip gene exclusion in the genomes of ST7, 8, 21, and 37. Perinatal listeriosis cases were associated with the new hypervirulent L. monocytogenes of ST1, 4, and 219 compiled with old ST6. These data indicate the need for the more stringent control of food products for high-risk groups.

Keywords: listeria monocytogenes; food-borne pathogen; invasive listeriosis; MLST; cgMLST; whole-genome sequencing; plasmid; virulence factors; covid-19; epidemic outbreak.

Author α σ ρ ↀ ¥§ χ £: N.F. Gamaleya National Research Center for Epidemiology and Microbiology, Ministry of Health, Russia; Gamaleya Str., 18, 123098 Moscow, Russia;
ν: F.I. Inosemtsev City Clinical Hospital, Fortunatovskaya Str., 1 105187 Moscow, Russia;
Θ: A.I. Yevdokimov Moscow State University of Medicine and Dentistry, Ministry of Health, Russia, Department of Infectious Diseases and Epidemiology, Delegatskaya, Str., 20, building 1, 127473 Moscow, Russia;
ζ: Federal State Budgetary Educational Institution of Further Professional Education Russian Medical Academy of Continuous Professional Education, Ministry of Health, Russia; Barrikadnaya Str., 2/1, building 1, 125993 Moscow, Russia.

I. BACKGROUND

Listeria monocytogenes is a saprophyte that is ubiquitously distributed in the environment. With the modern development of the food industry, *L. monocytogenes* has become an actual food-borne pathogen, being psychrophilic and salt-tolerant [1]. Entering the human body through foodstuffs and ready-to eat (RTE) foods, *L. monocytogenes* causes fecal carriage, as was detected in 10% of humans from an independent cohort of 900 healthy asymptomatic donors [2], or listeriosis at high levels of contamination (> 1000 cfu/g) [3]. A more severe form of the disease is invasive listeriosis, which has a high mortality rate (20%–30%) [4]. This form of the disease affects the elderly, the

immunocompromised (patients undergoing treatment for cancer, AIDS and organ transplants), pregnant women and their unborn or newborn infants [4, 5]. Defining the age limits of the elderly group, Mook et al. concluded that age >60 years was associated with an increased risk for listeriosis in England and Wales [5]. According to Goulet et al., the age of the high-risk group with no underlying conditions was >65 years in France [6]. Immunosenescence in the elderly is associated with declines in adaptive and innate immunity [7]. Immunocompromised persons have suppressed T-cell-mediated immunity as a consequence of the treatment [5]. The decrease in the number of helper T cells in the second and third trimesters of normal pregnancy is evidence of immunodeficiency in pregnant women [8]. In addition, in pregnancy, in the second and third trimesters, the gastrointestinal (GI) tract undergoes a series of changes, the root cause of which is a decrease in intestinal motility [9]. GI motility plays a key role in mucus renewal. The mucus is the first line of defense against the infiltration of microorganisms [10]. It coats the interior surface of the GI tract, lubricates luminal contents and physically entraps bacteria, sweeping ingested bacteria out of the small bowel into the colon [11]. Decreased GI motility results in the enrichment of the mucus with Proteobacteria and Actinobacteria (in October 2021, the valid names became Pseudomonadota and Actinomycetota [12]), and in the reduction in the health-related bacterial abundances [13]. Alterations in the mucus microbial community result in a decrease in the production of protective factors including short chain fatty acids (SCFAs), in particular, acetate and formate, which have antimicrobial properties against enteric pathogens [11], and butyrate, which has anti-inflammatory effects [13].

Neurological disorders, stress, and antibiotic treatment are also accompanied by a reduction in the mucus-associated gut microbiota layer and mucus secretion [10, 14, 15]. The damage to the GI mucosa could be caused by viral pathogens often having seasonal patterns [16, 17]. Schwartz et al. were the first to analyze the association of invasive listeriosis with the consequences of a viral infection in Philadelphia between 1 December and 1 April 1987, i.e., during the period of the epidemic rise in the incidence of influenza virus in the Northern Hemisphere [17]. The subsequent years of intensive study into the microbial communities in different environmental niches within human bodies demonstrated the effects of viral infections on both the gut and respiratory microbiome. Influenza infection, for instance, has been found to result in significant changes in the gut microbiome, despite the lack of detectable virions in the GI tract [18]. Furthermore, according to Bortel et al. pulmonary infection triggers the production of IL-10 by Ncr1+ cells, which could be a factor that increases the survival of invasive *L. monocytogenes* [19].

At the end of 2019, humanity faced a new virus, SARS-CoV-2, which caused severe respiratory coronavirus disease 2019 (COVID-19), reaching pandemic levels on March 11 2020 [20]. In 2020, Xiao et al. and other researchers provided evidence for the GI infection of SARS-CoV-2 [21,22,23]. A cell receptor for SARS-CoV-2, angiotensin-converting enzyme 2 (ACE2) protein, was demonstrated to be abundantly expressed in the glandular cells of gastric, duodenal, and rectal epithelia, supporting the entry of SARS-CoV-2 into the host cells [21, 23]. Among the hospitalized patients infected with SARS-CoV-2, 53.42% tested positive for SARS-CoV-2 RNA in their stool, and more than 20% of patients with SARS-CoV-2 remained positive for viral RNA in feces even after the test results for viral RNA in the respiratory tract became negative [21]. Furthermore, SARS-CoV-2 infection causes an alteration of intestinal permeability, resulting in enterocyte dysfunction [22]. These data suggest a direct effect of SARS-CoV-2 on the gut microbiota, in addition to in-direct effects via the gut–lung axis [24, 25].

Previously, we showed the impact of respiratory viral infections on the incidence of invasive listeriosis in a metropolis in 2018/2019. *L. monocytogenes* of phylogenetic lineage (PL) II prevailed in the groups of cases that occurred when the epidemic threshold for influenza was crossed during the 2018/2019 season. Listeria pneumonia identified in the senior age group occurred during the season

of autumn acute respiratory viral infections and was primarily caused by *L. monocytogenes* of PLI [26]. It is strains of PL I and II that cause the majority of human illness, despite the fact that the population of *L. monocytogenes* consists of four divergent lineages (I– IV) [27].

The aim of this study was to research the impact of the COVID-19 pandemic on the incidence of invasive listeriosis in the same metropolis, comparing the spectrum of the *Listeria* genotypes that previously caused the disease with the spectrum of the *Listeria* pathogens identified during the COVID-19 pandemic.

II. RESULTS

The monitoring of the clinical and food-borne *L. monocytogenes* isolates started in November 2018 in a large metropolis with a population of 20.4 million (https://mosstat.gks.ru/folder/64634 / (accessed on 24 July 2022)). The COVID-19 pandemic divided our study into two periods: before the pandemic (November 2018–October 2019) and during the pandemic (March 2020–January 2022). Since SARS-CoV-2 was constantly mutating during the pandemic, we characterized the stages of the pandemic by the number of genotypes (pangolineages) circulating at the same time.

1. The analysis of the change in SARS-CoV-2 pangolineages in the Moscow metropolis.

The large amount of data on SARS-CoV-2 sequences related to the Moscow region, presented in the GISAID EpiFlu™ Database (http://gisaid.org / (accessed on 24 July 2022)) including our own data (EPI_ISL_421275, EPI_ISL_1708505, EPI_ISL_1708506, EPI_ISL_1708510 - EPI_ISL_1708519, EPI_ISL_1731043 - EPI_ISL_1731045, EPI_ISL_2322757 - EPI_ISL_2322762, EPI_ISL_2356912, EPI_ISL_2356913, EPI_ISL_3102159, EPI_ISL_9058873, EPI_ISL_9058988 - EPI_ISL_9058990, EPI_ISL_9058992), indicates that the pandemic period included in our observation can be divided into two stages (Figure 1) in accordance with the number of simultaneously circulating pangolineages of SARS-CoV-2. At the first stage, from the beginning of the pandemic until the beginning of June 2021, various pangolineages were circulating: B.1.1 B.1.1.523, B.1.1.397, B.1.1.294, B.1.1.336, the Moscow endemic variants B.1.1.317, B.1.1 .141, and subsequently Alpha B.1.1.7 (VOC, the variants of concern) [28].

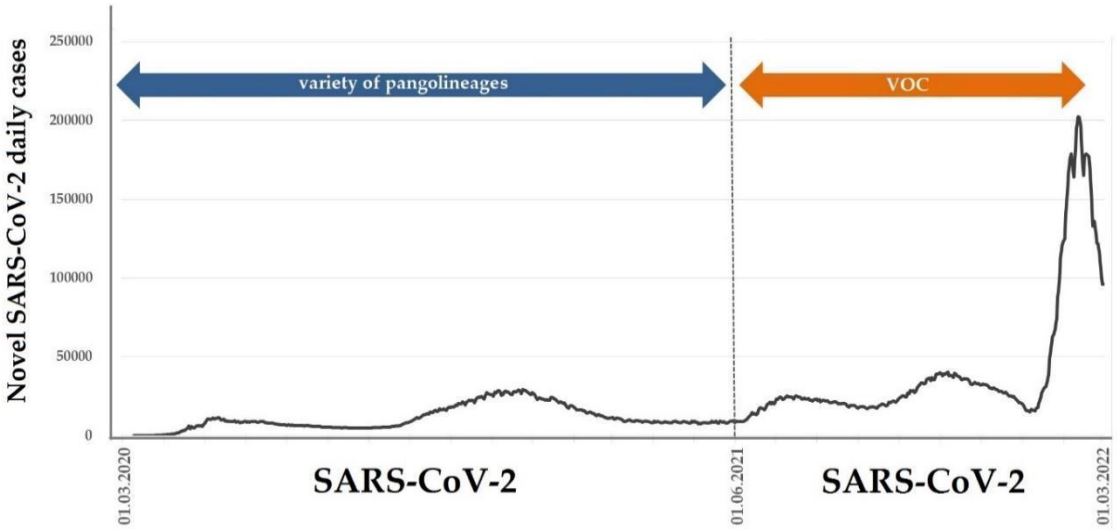

Figure 1: The stages of the COVID-19 pandemic. VOC—the variants of concern

At the second stage, from the beginning of June 2021 to the end of January 2022, VOC dominated in the Moscow region, successively replacing each other. The frequency of Delta (B.1.617.2) strain among the Moscow region samples had been growing since March 2021, and reached 80.0% in June, and 98.0% in early July 2021 [29, 30]. The Omicron strain (B.1.1.529), which appeared on December 3 [29], reached a frequency of 49.2% on January 4 and 90.1% on January 14 (https://www.youtube.com/watch?v=u-_NDK4DCLU / (accessed on 24 July 2022)).

2. Comparison of L. monocytogenes of two periods of time: before the pandemic and during the pandemic.

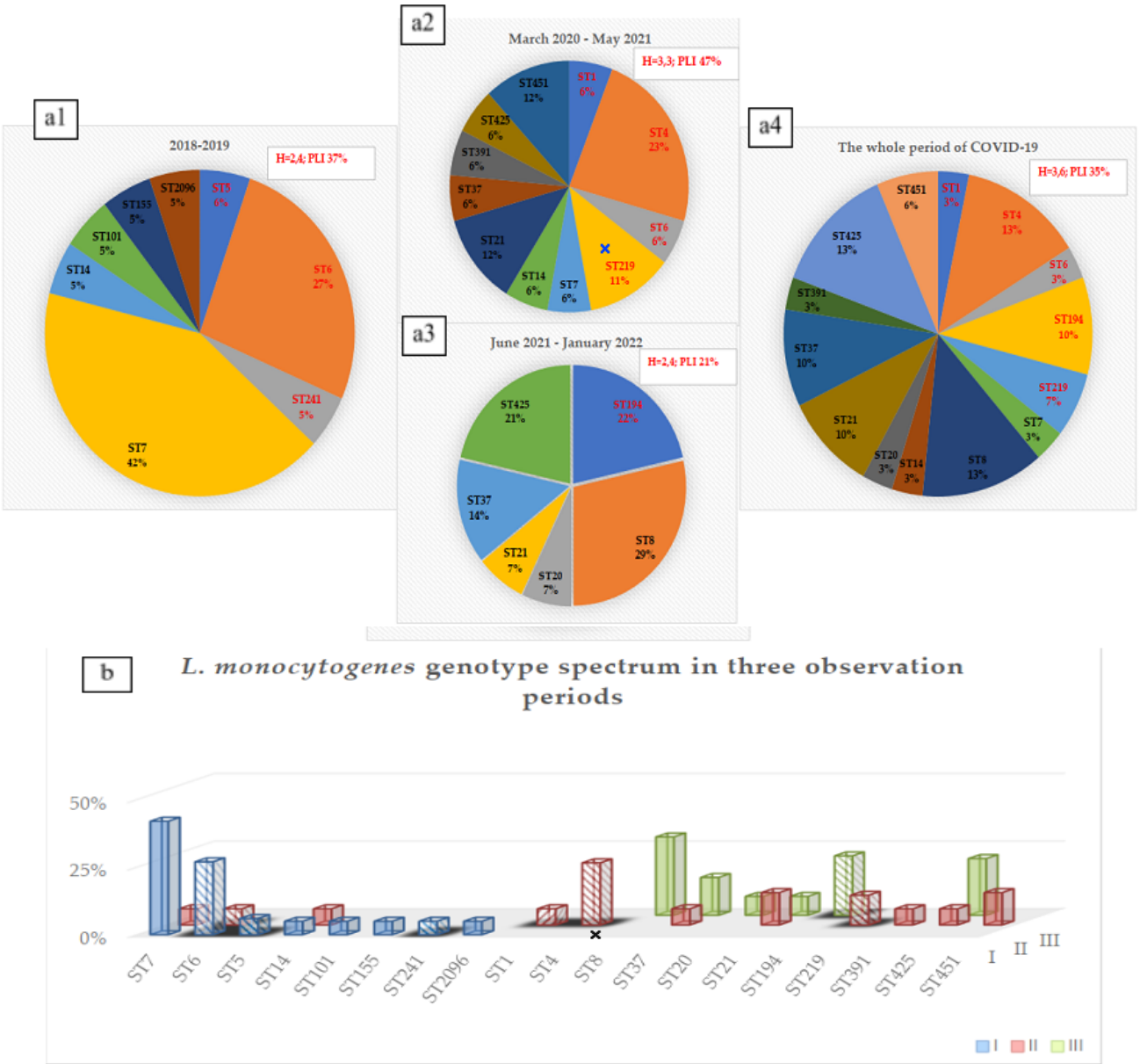

a1) before the COVID-19 pandemic, 2018-2019; a2) during the COVID-19 pandemic, March 2020–May 2021; a3) during the COVID-19 pandemic, June 2021–January 2022; a4) during the COVID-19 pandemic as a whole. b) *L. monocytogenes* genotype spectrum in three observation periods: I—before the COVID-19 pandemic, 2018-2019; II—during the COVID-19 pandemic, March 2020 May 2021; III—during the COVID-19 pandemic, June 2021 - January 2022. The genotypes of the first phylogenetic lineage are highlighted with hatching and shadow. H—the Shannon diversity index; PLI—phylogenetic lineage I; ST—sequence type.

Figure 2: *L. monocytogenes* genotypes identified during the observation periods.

In the period before the pandemic, the autochthonous ST7 of PLII prevailed, while ST6 (PLI) was the second most prevalent (Fig. 2a1, 2b), (Table S1). If ST7 is typical in Russia (with the exception of the Far East Federal District (FD)) for isolates from food and the environment [31,32], then the sources of ST6 have not yet been found. *L. monocytogenes* of this genotype is absent in food from domestic production in the Moscow region [31]. In perinatal listeriosis, only listeria of these two STs were found (Fig. 3a), while in invasive listeriosis in the older age group (meningitis and sepsis), three more STs of PLII and two STs of PLI added diversity (Fig. 4a). In general, during the period before the pandemic, *L. monocytogenes* of STs of PLII prevailed, which is typical for the population of listeria in most of the territories of the Russian Federation. Only in the Far East FD did listeria of PLI predominate both in the environment and among the clinical isolates [33, 34].

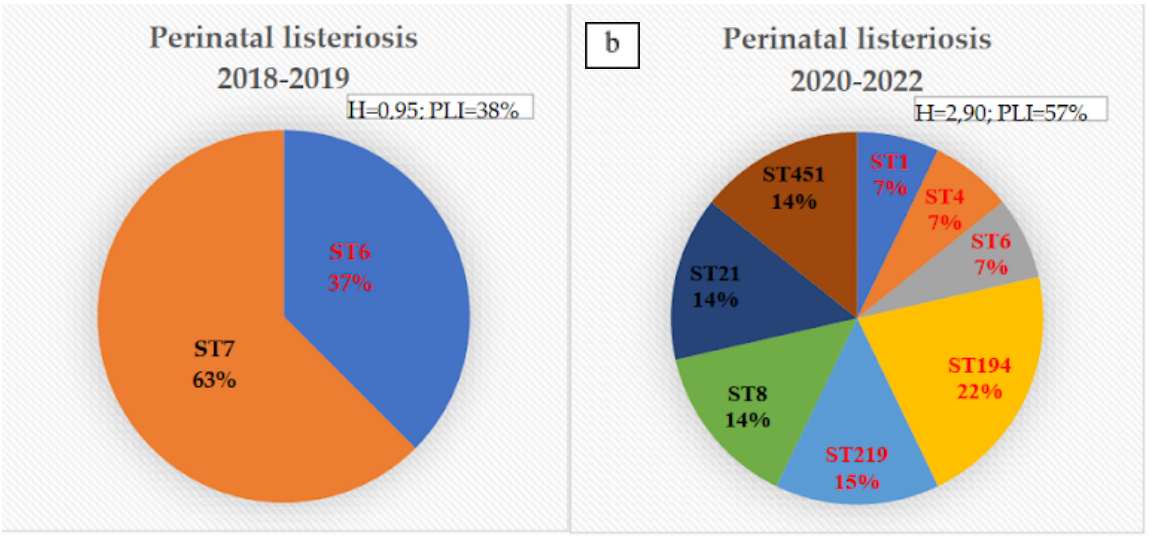

a)—before the COVID-19 pandemic, 2018-2019; b)—during the COVID-19 pandemic.
H—the Shannon diversity index; PLI—phylogenetic lineage I; ST—sequence type

Figure 3: *L. monocytogenes* genotypes causing invasive perinatal listeriosis.

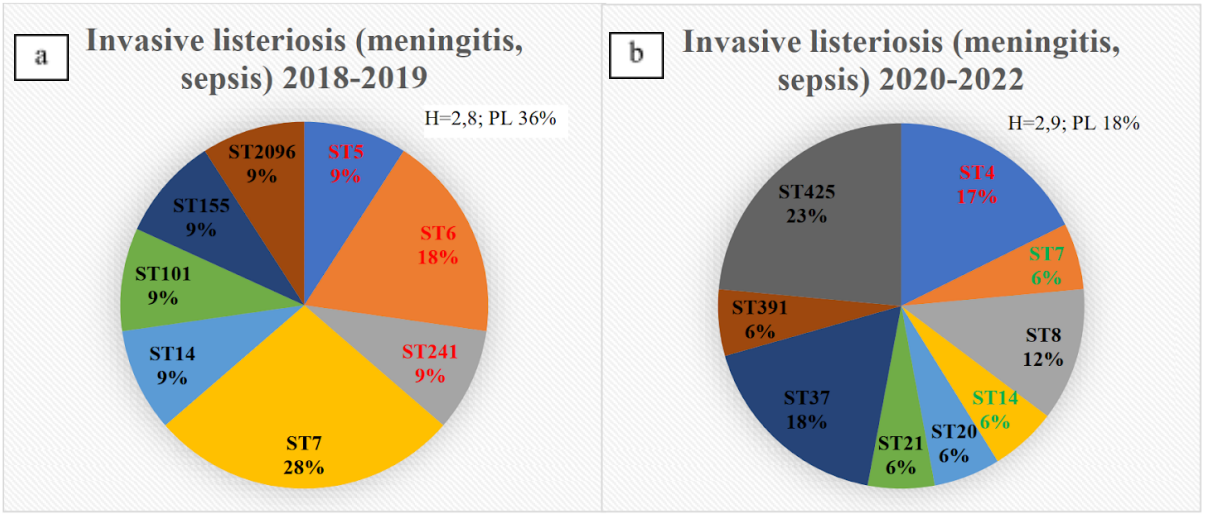

a)—before the COVID-19 pandemic, 2018-2019; b)—during the COVID-19 pandemic.
H—the Shannon diversity index; PLI—phylogenetic lineage I; ST—sequence type

Figure 4: *L. monocytogenes* genotypes causing meningitidis and sepsis.

From the eight genotypes of PLII, only two STs (7 and 14) coincided with those identified in the period before the pandemic (Figure 2b). From the STs that appeared during the pandemic (Figure 2a4), ST451 was attributed only to perinatal listeriosis. ST451 was new in the Central FD in January 2021. In August 2021, the strain with the same ST and internalin profile (IP), including *inlA*, *inlB*, *inlC,* and *inlE*, was isolated from a lightly salted salmon fillet imported from the Faroe Islands. However, in 2016/2017, *L. monocytogenes* ST451 was also isolated in the Northwestern FD in the case of perinatal listeriosis (ID 37701) [35], and from chilled beef of unknown origin (ID 42266) [35]. It should be noted that comparative analysis of the sequences of internalin A demonstrated that isolates of ST451 had the same N187S substitution in the leucine-rich repeat (LRR) 5 domain as the strains of PLI. This is important for internalin A–E–cadherin interaction, which is exploited by *L. monocytogenes* for the invasion of enterocytes and to cross the placental barrier [36].

The two more STs, 21 and 8, were revealed not only in the perinatal listeriosis group (Figure 3b), but in the meningitis and sepsis group too (Figure 4b). Previously, ST21 was not observed in human listeriosis. In 1975, an isolate of this genotype was isolated from a goat in the North Caucasian FD of Russia [32], but it differed from the human isolate by the locus of internalin C in the IP. The *L. monocytogenes* isolates of ST8 were previously found in food (meat, fish, dairy) in Russia, but were absent in clinical cases of listeriosis. The isolates of Clonal Complex (CC) 8 were detected in meat (ST16, ID 42269) [35] and in the environment (ST758) [34], and in cases of meningitis (ST2096) before the COVID-19 pandemic [26]. All isolates of CC8 but one (ST758, IP34), had the same IP53. During the COVID-19 pandemic, *L. monocytogenes* ST8 was revealed in four clinical cases (Figures 3b and 4b), and one of them had a fatal outcome.

The greatest diversity of the PLII genotypes was noted in the older age group (meningitis and sepsis) during the pandemic (Figure 4b), and each of the genotypes was associated with a case of listeriosis with a fatal outcome (Table S1). ST20 was first detected in human listeriosis in the Central FD, but in 2007 an isolate of this genotype was isolated from the crucian carp (*Carassius carassius*) [34]. The IP of clinical and environmental isolates were identical. However, in 2016 *L. monocytogenes* ST20 was isolated in the North-western FD in the case of perinatal listeriosis (ID 42272), later, in 2017, a strain of this ST was isolated from chilled beef of unknown origin (ID 42270), and then, in 2018, it was isolated from wastewater (ID 42274) [35].

L. monocytogenes of ST425 is also new in human listeriosis in Russia but was isolated in the environment (from red deer (*Cervus elaphus*) feces) in 2009 [34]. However, in this case, clinical and environmental isolates differed in the internalin B locus of the IP. A single-nucleotide variant (SNV) in the same position of the *inlB* alleles relative to the most common for the PLII allele 14 (A/T, A/C) leads to the same amino acid substitution (Ile/Leu).

ST37, found in food and food processing environments (FPEs) in 2017 (ID 37695) [35], and in 2019-2021 (ID 49371, 49372, 76388) [31], was isolated for the first time in 2021 in a case of human listeriosis. Note that food and clinical isolates had the same IP.

Finally, ST391 (CC89) was discovered for the first time, but it is a single locus variant (SLV) of ST1547 (CC89) identified in human listeriosis in 1997 [32]. The internalin B locus distinguishes the IP of these genotypes.

Thus, we note a significant role of the PLII STs in the group of diseases “meningitis and septicemia”. Evaluating the *L. monocytogenes* genotypes in the older age group for the entire observation period (Fig. 4b), it should be noted that the proportion of the PLI is low, but the diversity index is high, which is provided by the PLII STs.

3. Comparison of L. monocytogenes of two stages of the COVID-19 pandemic

Comparing the causative agents of invasive listeriosis in the two periods of time, before the pandemic and during the pandemic, we saw a significant difference in the diversity of genotypes, in the representation of phylogenetic lineages, and in the number of deaths (43.8% before the pandemic and 81.2% during the pandemic in the group of the meningitis and septicemia [37]). Noteworthy is the sharp decrease in age in the group with meningitis and septicemia: from 59 to 33 years (Figure 5).

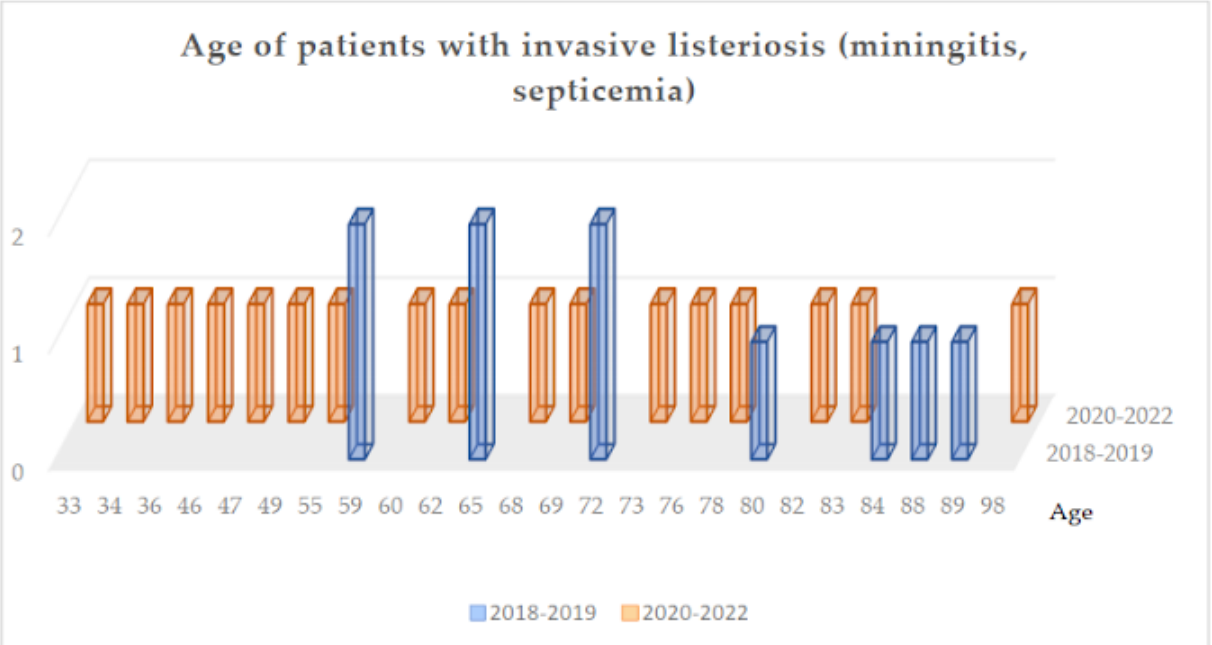

Figure 5: The age of patients with invasive listeriosis manifesting as septicemia and meningitis.

Since the pandemic period can be divided into two stages according to the number of circulating pangolineages, we compared the diversity of the *L. monocytogenes* genotypes between the pandemic stages (Figure 2a2, 2a3). As can be seen from the data in Figure 2a2, the increase in the diversity of the *L. monocytogenes* STs and in the proportion of the PLI genotypes occurred precisely at the first stage of the pandemic. At the second stage of the COVID-19 pandemic (Figure 2a3), the diversity of the *L. monocytogenes* STs was equal to the data for the period before the pandemic, and the proportion of the PLI genotypes was even lower than before the pandemic. However, the list of STs changed dramatically: all genotypes revealed at the second stage of the pandemic are new for clinical cases in the Central FD (Figure 2b).

4. Internalins' diversity in the different phylogenetic lineages

The internalins, as factors of the pathogenicity of listeria, are important for the bacteria–human cells interaction, and listeria adaptation [36]. As a result, we note a large number of IP in the batch of Russian isolates, with the new ones among them in recent times presented in Table 1.

Table 1: New internalin profiles (IP) from this research

CC	ST	inlA	inlB	inlC	inlE	IP	Phylogenetic Lineage
CC21	21	12	14	7	8	56	II
CC11	451	22 (MW538938)	23 (MW538939)	6	6	58	II
CC26	26	7	14	6	6	59	II

CC4	219	23 (MW965279)	8	4	3	60	I
CC89	391	15	14	17	6	61	II
CC90	425	13	24 (MZ486423)	13	8	62	II
CC403	403	9	23	21 (OM240823)	17 (OM240824)	66	II

** IP57 (7; 13, 16, 6) was detected by Ermolaeva S.A. and Psareva E.K. (not published); IP63-65 were published in [85]. For new alleles of the internalin genes, the GenBank Accession Numbers are given in the parentheses.*

Different internalins contribute to the diversity of IP of the clinical isolates in two phylogenetic lineages (Table 2). In the group of the clinical isolates of PLI, the *inlA* locus was the most diverse, according to the H value, and *inlC* was the least diverse locus. At the same time, in PLII, both *inlA* and *inlC* were the most diverse loci. It was the *intC* locus that distinguished isolates of ST21 when comparing the bacteria that caused human and goat listeriosis.

Table 2: Shannon's diversity index for internalin alleles of clinical *L. monocytogenes* isolates

Phylogenetic lineage	Shannon's diversity index (H)			
	inlA	inlB	inlC	inlE
I	2,5	1,8	1,1	1,4
II	3,1	1,4	2,3	1,4

5. Virulence factors

The virulence of *L. monocytogenes* depends on its ability to colonize the gut and disseminate within the host [38]. The key genes and gene products involved in microbial virulence were named as virulence factors (VFs) [39]. A number of well-studied VFs are also known as pathogenicity factors, such as internalins, because virulence and pathogenesis represent two sides of one coin. The former is viewed from the point of view of the microorganism and the latter from its effect on the host [40]. The virulence factor database (VFDB) (http://www.mgc.ac.cn/VFs/ (accessed on 24 July 2022)), which is an extensive collection of VFs from the important bacterial pathogens [41], was used for the VF analysis of *L. monocytogenes*, revealed during the monitoring.

Whole-genome sequencing (WGS) was performed for the isolates of the repeated genotypes and new genotypes for the clinical cases or for the *Listeria* population in Russia. Thus, the cohort of the sequenced isolates included *L. monocytogenes* of 12 STs, four of which belonged to PLI, and eight to PLII (Table S2). As a result, 45 virulence genes related to 12 VF classes were identified (Table 3). The VF classes “Adherence”, “Invasion” and “Regulators” were the most numerous: seven, seven and nine genes, respectively, were revealed in all analyzed genomes. Only one VF of the “Invasion” class which was encoded by the *vip* gene (bold font in Table 3) was absent in the genomes of ST7, 8, 21, and 37. The vip protein (lmo0320) is an LPXTG surface protein, but does not contain LRRs, and thus does not belong to the internalin family [42]. According to Cabanes et al., vip is required for entry into some eukaryotic cells via the endoplasmic reticulum resident chaperone Gp96 [42]. Doumith et al. demonstrated the presence of lmo0320 in seven *L. monocytogenes* strains of the serovar 1/2a isolated in cases of human sporadic or epidemic listeriosis [43].

Table 3: Virulence factors revealed in the sequenced genomes of *L. monocytogenes* isolates.

VFclass	Virulence factors	Related genes	VFclass	Virulence factors	Related genes	VFclass	Virulence factors	Related genes
1. Adherence	D-alanine-polyphosphoribitol ligase	*dltA*	5. Intracellular survival	Lipoate protein ligase A1	*lplA1*	10. Regulation	AgrA/AgrC	*agrA*
	Fibronectin-binding protein	*fbpA*		Oligopeptide-binding protein	*oppA*			*agrC*
	GW autolysin	*ami*		Post-translocation chaperone	*prsA2*		CheA/CheY	*cheA*
	Internalin F	*inlF*		Sugar-uptake system	*hpt*			*cheY*
	Internalin J (LPXTG protein)	*inlJ*	6. Invasion	Autolysin (GW protein)	*aut*		LisR/LisK	*lisK*
	Listeria adhesion protein	*lap*		Cell wall hydrolase	*iap/cwhA*			*lisR*
		lapB		Cell wall teichoic acid glycosylation protein	*gtcA*		Positive regulatory factor	*prfA*
2. Bile resistance	Bile-salt hydrolase	*bsh*		Internalin A (LPXTG protein)	*inlA*		VirR/VirS	*virR*
3. Enzyme	Metalloproteinase	*mpl*		Internalin B (GW protein)	*inlB*			*virS*
	PC-PLC	*plcB*		Internalin P	*inlP*	11. Surface protein anchoring	Lipoprotein diacylglyceryl transferase	*lgt*
	PI-PLC	*plcA*		Lipoprotein promoting entry protein	*lpeA*		Lipoprotein-specific signal peptidase II	*lspA*
	Serine-threonine phosphatase	*stp*		**Virulence protein (LPXTG protein)**	*vip*		Sortase A	*srtA*
4. Immune modulator	InlC	*inlC*	7. Iron uptake	Hemoglobin binding protein	*hbp2*		Sortase B	*srtB*
	InlK	*inlK*	8. Nucleation-promoting factor	ActA	*actA*	12. Toxin	Listeriolysin O	*hly*
	LntA	*lntA*	9. Peptidoglycan modification	OatA	*oatA*			
				PdgA	*pdgA*			

Bold font—virulence factor gene, which is absent in the genomes of ST7, 8, 21, 37

In our cohort, the *vip* gene was absent in the genomes of the isolates (ST7, 8, 21, 37) that caused serious consequences or even the death of patients (Table S1). In the reference genome of *L. monocytogenes* EGD-e (serotype 1/2a), the *vip* gene (lmo0320) is flanked by lmo0319 (phospho-beta-glucosidase) and lmo0321 (a protein of unknown function). The size of the *vip* gene is 1200 bp. In the genomes of ST7, 8, 21, and 37, the intergenic region between the genes encoding phospho-beta-glucosidase and uncharacterized protein is 275 bp. These data suggest the absence of the ORF (open reading frame) for *vip* in the mentioned genomes.

6. Plasmids as source of genes essential for cellular survival

The plasmids can help *L. monocytogenes* in its adaptation to survive both in the environment as well as within the body of humans and other animals, mediating heavy metals, heat resistance and virulence [44, 45]. However, as demonstrated by Lebrun et al., only 13% of strains from humans and animals with listeriosis harbored plasmids [46].

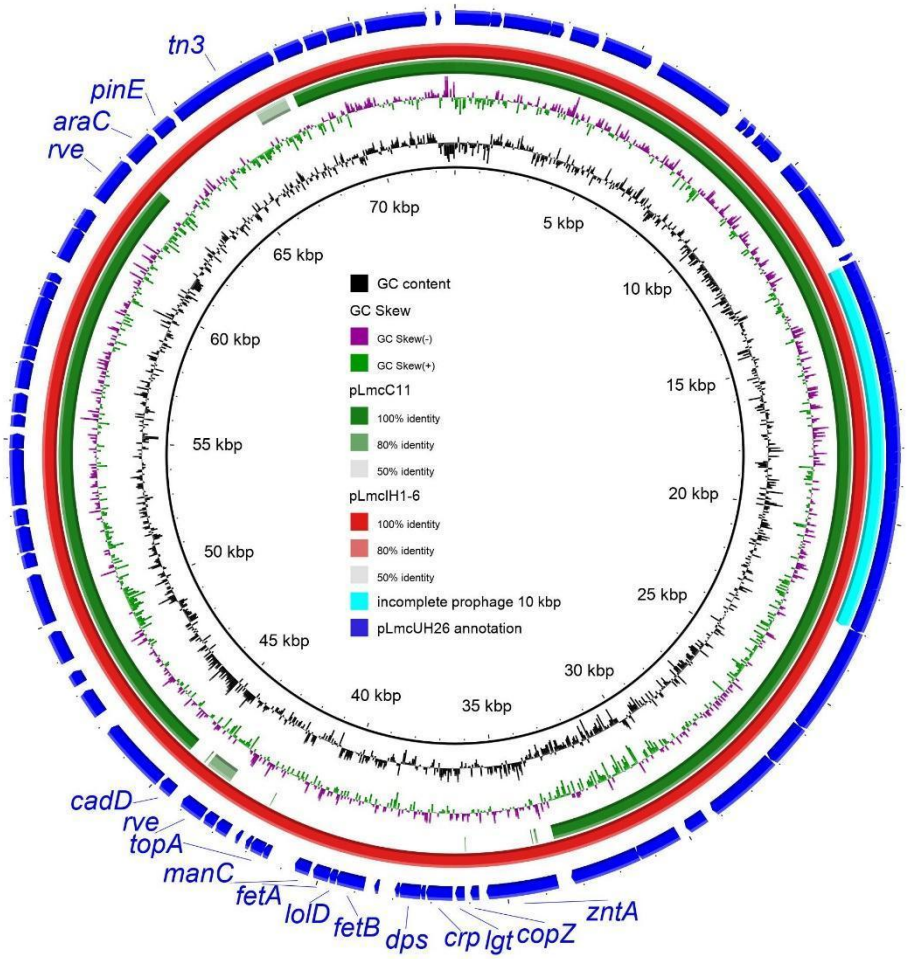

Figure 6: The comparison of *L. monositogenes* and *L. welshimeri* plasmids by using BLAST Ring Image Generator (BRIG) with blast-2.7.1.

The blue ring—pLmcUH26 (*L. monocytogenes* GIMC2079: LmcUH26, ST425); the gene names highlighted in blue refer to the two regions of difference annotated by the RAST; the red ring—pLmcIH1-6 (*L. monocytogenes* GIMC2088:LmcIH1-6, ST20); and the green ring—pLmcC11 (*L. welshimeri* GIMC2049:LmcC11, ST2331). The position of the incomplete prophage is shown by an aqua-colored segment.

In our WGS research, 5 isolates from 35 of the PLI and the PLII bore plasmids: four isolates were ST425, CC90, PLII and one isolate was ST20, CC20, PLII. These plasmids (accession numbers MZ869810, MZ869811, OM867528 - OM867530) were 72,763 bp in length (Table 4). We designate them here as pLm. The plasmids contained the incomplete prophage 10 Kb, a part of the *Listeria* phage A006 (Figure 6). Sixteen ORFs of prophage included the post-segregational killing system, encoded by a co-transcriptional gene pair of Phd antitoxin (prevent host death protein) and Doc (death on curing protein) toxin, which is involved in maintaining the plasmid in host cells [47, 48]. This set of *Listeria* adaptive genes is known also as the *mazEF*-like toxin-antitoxin system, which modulates the growth in the response to specific stress factors [49]. Another pair of genes encoding CadA and CadC proteins constituted the cadmium efflux system. One more interesting gene encoded the CRISPR-associated protein Cas5.

The same incomplete prophage we revealed earlier in a plasmid 57,530 bp in length (Accession Number MZ869809) was from the *L. welshimeri* strain of ST2331 isolated in the meat processing plant (Table 4). We will designate it here as pLw.

The alignment percentage (AP) of the six plasmids was more than 89% and the average nucleotide identity (ANI) was more than 99%. The GC content of identified plasmids was 36%. The number of coding sequences (CDS) varied from 67 in pLw to 86/88 in pLm.

The main region of differences between pLm and pLw was a pathogenicity island including 17 ORFs (Figure 6). First of all, these ORFs encoded proteins for the copper homeostasis, which is particularly acute during infections (copper-translocating ATPase and copper chaperone). The levels of copper fluctuate in the host from high in the gallbladder to low in the liver and spleen [50]. Thus, the plasmid coding the copper homeostasis proteins helps in adapting to these different niches, which is important for a successful infection.

The second group of genes encode the proteins contributing to the regulation of the iron concentration: the complex of the ABC transporters and the permease responsible for the iron export, and the Dps protein (DNA protection during starvation). The Dps, a ferritin-like protein, forms dodecamers that can bind approximately 500 iron molecules [51]. Moreover, Dps has a dual role in protecting the cells against oxidative stress, either by binding directly to DNA, or by sequestering iron, thus avoiding oxidative damage [87], because in the presence of iron, superoxide and hydrogen peroxide can be transformed into the highly reactive hydroxyl radical [52].

One more gene of this region encoded deoxythymidine diphosphates (dTDP)-4-dehydro rhamnose 3,5-epimerase, or cupin RmlC. This protein's synthesis is the precursor of L- rhamnose, which is used by the *L. monocytogenes* serogroup ½ for the modification of the peptidoglycan-attached teichoic acids (wall teichoic acids). Such modification is significant for *L. monocytogenes* virulence [53].

The smaller region deleted in pLmcC11 is represented by three genes encoding transposase, site-specific DNA recombinase and AraC family transcriptional regulator.

The comparison of pLm with the *Listeria* plasmids deposited in GenBank showed high similarity to the pLIS19 (MZ089999), pLIS38 (MZ127847), and pLIS43 (MZ147615) plasmids of *L. innocua* strains, isolated from food and city environments in 2003-2017 in Poland [54] (Table 4). The ANI and AP among these plasmids are more than 99%.

The pLw showed more than 99% similarity to the plasmids of *L. innocua* strains isolated from food [55] and to the plasmids of *L. monocytogenes* strains isolated from food and from clinical sources in different years and different geographical locations [56-59] (Table 4). The *L. monocytogenes* strains belonged to ST3 of PLI and to different STs of PLII. The oldest clinical strain was isolated in 1967 in Germany [58]. The 13 plasmid replicons mentioned above (Table 4) were included in the analysis. The neighbor-joining tree (Figure 7) was built on the basis of the ANI of whole-genome alignment and revealed two closely related groups of plasmid replicons. Group I, which is located at the top of the figure, includes smaller plasmids, which are distributed according to the source of isolation. In group II, in the lower part of the figure, there are larger plasmids, and the most different among them is the plasmid of the strain isolated from the environment.

Table 4: GenBank plasmids with high similarity to those found in the study.

Size	Plasmid name	GenBank ID	Strain	Species	ST	CC	Phylogenetic lineage	Isolation date	Source	Country	Reference
72763 bp	pLmcUH26	MZ869810	GIMC2079:LmcUH26	*L. monocytogenes*	425	90	II	2021	Homo sapiens (blood)	Russia	this research
	pLmcUH27	MZ869811	GIMC2080:LmcUH27	*L. monocytogenes*	425	90	II	2021	Homo sapiens (blood)	Russia	this research
	pLmcH67_6	OM867530	GIMC2090:LmcH67_6	*L. monocytogenes*	425	90	II	2021	Homo sapiens (cerebrospinal fluid)	Russia	this research
	pLmcH67_8	OM867529	GIMC2095:LmcH67_8	*L. monocytogenes*	425	90	II	2021	Homo sapiens (blood)	Russia	this research
	pLmcIH1-6	OM867528	GIMC2088:LmcIH1-6	*L. monocytogenes*	20	20	II	2021	Homo sapiens (cerebrospinal fluid)	Russia	this research
	pLIS19	MZ089999	297/05	*L. innocua*	nd	nd	*L. innocua*	2005	food (ice cream)	Poland	[54]
	pLIS38	MZ127847	10/03	*L. innocua*	nd	nd	*L. innocua*	2003	food (food contact surface swab)	Poland	[54]
	pLIS43	MZ147615	Sr108	*L. innocua*	nd	nd	*L. innocua*	2017	environment (city)	Poland	[54]
57530 bp	pLmcC11	MZ869809	GIMC2049:LmcC11	*L. welshimeri*	2331	2331	Other *Listeria* species	2020	meat processing plant	Russia	this research
	pCFSAN044836	CP045744	CFSAN044836	*L. innocua*	448	448	*L. innocua*	2005	food (minced meat)	Italy	[55]
	pPIR00545	CP025561	PIR00545	*L. monocytogenes*	199	199	II	-	food	Switzerland	[56]
	pR2-502	CP006595.1	R2-502	*L. monocytogenes*	3	3	I	1994	food	USA	[57]
	pLM1-2bUG1	FR667692.1	SLCC2755	*L. monocytogenes*	66	3	I	1967	Homo sapiens	Germany	[58]
	pl2015TE24968	CP015985.1	2015TE24968	*L. monocytogenes*	7	7	II	2015	Homo sapiens (blood)	Italy	[59]
	pAUSMDU00000224_01	CP045973.1	AUSMDU00000224	*L. monocytogenes*	122	9	II	2009	Homo sapiens	Australia	Unpublished

Listeria plasmids have been classified into two groups based on their replication protein RepA sequences [58]. According to this classification, all of the analyzed plasmids belong to the repA_G1-Replication system group, which is the most common group [54]. All of the analyzed plasmids also carried two loci involved in the active partitioning of plasmid molecules (PAR_1 and additional *parA*), and the loci coding Y-family polymerase components (UvrX and YolD) representing

the POL_1 group. A whole conjugative transfer module is absent in the studied plasmids, except for the relaxase component of the mobL_1a type.

Of the functional genes that promote adaptation and are present in all plasmids, mention should be made of a region encoding a glycine betaine ABC transport system substrate-binding protein and an oxidoreductase (NADH peroxidase), and the gene for the ATP-dependent protease ClpL. The first group of the genes may play a role in responses to high osmolarity and oxidative stress, and was shown to be upregulated under high-salt conditions [60]. The ATP-dependent protease ClpL was shown to be involved in the increased heat resistance of *L. monocytogenes* strains [45], and was also found to be upregulated in response to low pH [60].

No other additional genes, such as arsenic resistance loci, fluoride efflux transporters, or antibiotics resistance loci, or virulence factors, have been found in plasmids.

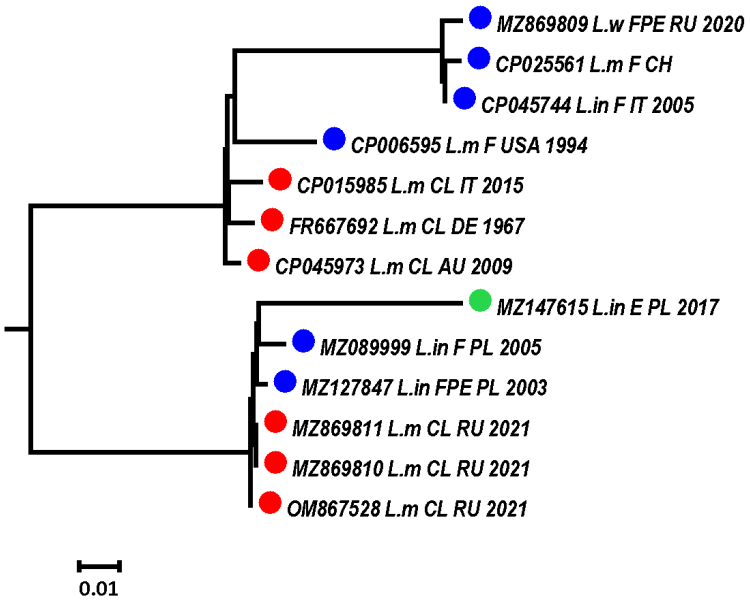

Figure 7: The neighbor-joining tree of the *Listeria* plasmid similarity based on the average nucleotide identity (ANI).

The *Listeria* species are labeled: L.m—*L. monocytogenes*, L.w—*L. welshimeri*, L.in—*L. innocua*. The countries of the isolates' origin are labeled: AU— Australia, CH—Switzerland, DE—Germany, IT—Italy, PL—Poland, RU—Russia, USA—USA. The sources of isolates are indicated as F—food, FPE—food production environment, CL—clinical. The color of the circles means: red—clinical isolate, blue—food isolate, green—environment isolate.

7. *Core genome comparison*

During the monitoring, especially in the pandemic period, we observed repeated genotypes among clinical isolates. To determine the epidemic relationship between isolates of the same genotype, we used the approach of cgMLST genotyping, developed by Moura et al. and having the discriminatory power required for epidemiological surveillance [39]. The criteria for assignment to an epidemic outbreak was seven or fewer allelic mismatches between cgMLST profiles, including 1748 loci.

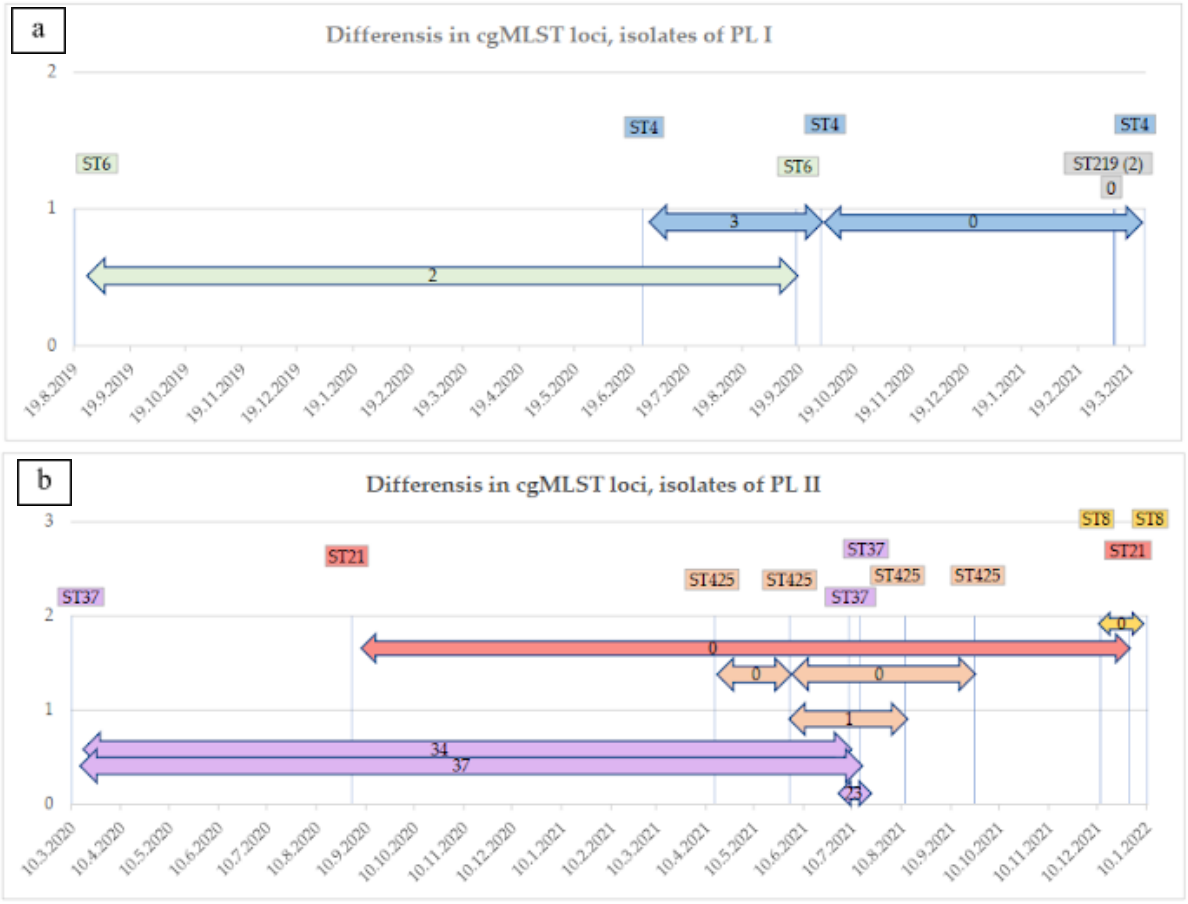

Figure 8: A number of allelic mismatches between cgMLST profiles for isolates of the same ST (sequence type). a)—phylogenetic lineage I (PLI), b)—phylogenetic lineage II (PLII).

The results of the comparison are shown in Figure 8. Among the isolates of PLI (Figure 8a), complete coincidence of the profiles was observed for isolates of ST219 attributed to perinatal listeriosis. Both strains were isolated in March 2021. One strain was isolated from a newborn, and a second strain was from a woman in the seventh week of pregnancy. The second group of isolates of PLI with minimal differences in cgMLST profiles belongs to ST4. The isolate from July 2020 (fatal) differs from the isolate from October 2020 (newborn) and the isolate from March 2021 (fatal) in three loci. The last two isolates have the same cgMLST profiles. The two isolates of ST6 (August 2019 and September 2020, both from newborns) have only two allelic mismatches, but the earlier isolate (March 2019, newborn) differs in 13-15 loci.

In PLII (Figure 8b), the isolates of ST8 (December 2021 (newborn) and January 2022 (meningitis, alive)), and ST21 (September 2021 (pregnant women) and December 2021 (septicemia, fatal)) had the same cgMLST profiles. Attention is drawn to strains of ST425. The four isolates shown in the figure are divided into two pairs according to the places of hospitalization. The isolates from April 2021 (septicemia, fatal) and June 2021 (meningitis, alive) were isolated from COVID-19 patients in one hospital with an interval of one and a half months, and had identical cgMLST profiles. The same profile is seen in the isolate from September 2021 (meningitis, fatal) from the second pair of the patients, which were from another hospital. The second isolate from this pair, from August 2021 (meningitis, alive), has one difference in the cgMLST profile from the three previous isolates of ST425. Thus, the isolates of ST219, 4, and two isolates of ST6 from the PLI, and the isolates of ST21, 8 and 425 from PLII can be attributed to epidemic outbreaks.

However, the isolates of ST37, often revealed during the COVID-19 pandemic in the group with meningitis and sepsis, had more than seven mismatches in the cgMLST profile (Figure 8b). The presented isolates, from March 2020 (meningitis, fatal), July 2021 (meningitis), and July 2021 (meningitis, fatal), were from three different hospitals. The isolates from July 2021 had fewer distinct loci (23) compared to the isolate at the start of the pandemic, March 2020, (34 and 37). As such, the three patients had different sources of the infection.

Previously, we obtained similar results for the isolates of the autochthonous ST7, which also belongs to PLII and was the most common in the pre-COVID-19 period (Figure 2a1) [26]. We compared the following isolates of ST7: the clinical isolates from June 2020 and February 2019 and a food isolate from May 2018. *L. monocytogenes* "February 2019" caused premature birth and pneumonia in a newborn, and listeria "June 2020" caused the death of an elderly patient recovering from COVID-19. The clinical isolates differed in 20 loci of cgMLST profiles, and both had 23 allelic mismatches with the food isolate. As such, three isolates of ST7 had no epidemiological link, but were closely related. The most considerable common mutation of the three isolates was the nine-nucleotide deletion in the MFS transporter gene (lmo2172) sequence, which distinguished this group of isolates from other food isolates and from the clinical *L. monocytogenes* ST7 previously isolated in Russia [26].

8. Possible functional role of mutated genes

The comparison of ST7 clinical isolates revealed 20 distinct loci coding for the proteins required for the metabolism of bacteria parasitizing in the human body. First of all, there were two virulence factors: listeriolysin O (lmo0202) and hexose phosphate transporter (lmo0838). According to the classification of pathways and functional systems using categories of the Clusters of Orthologous Genes (COG) [61], 20 loci can be classified into 12 COG categories (Figure 9); note that a quarter were related to the category "Carbohydrate transport and metabolism".

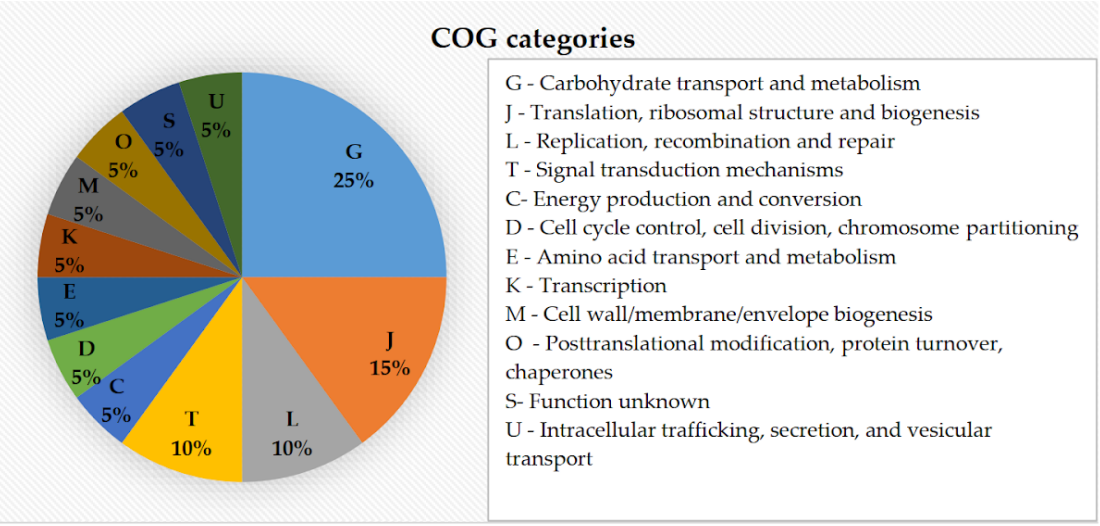

Figure 9: Distribution of genes differing in mismatches between the core genomes of *L. monocytogenes* ST7 according to the Clusters of Orthologous Genes (COG) category.

Four genes belonging to this category were transporters of two types: secondary and ATP-dependent transporters, as follows from the analysis using the TransportDB 2.0 [62]. Secondary active transporters, lmo0831 and lmo0838, have malonate/malate and hexose phosphate as a substrate, respectively, and couple the transport of substrates against their concentration gradients with the

transport of other solutes down their concentration gradients [63]. Two other transporters, lmo0980 and lmo2123 (ATP-dependent), belonged to the ABC family most represented (89.7%) among the transporters of *L. monocytogenes* (http://www.membranetransport.org/ (accessed on 24 July 2022)). If lmo2130 was responsible for the transport of maltose/maltodextrin, then lmo0980 was classified as a multidrug resistance transporter.

The fifth gene of this COG category was glucosamine-fructose-6-phosphate aminotransferase (lmo0727), an important point in the biosynthesis of amino sugar-containing macromolecules. It has been marked by Zhou et al. as the gene encoding the bile-induced protein of *L. monocytogenes* wild-type strain EGD [64].

It is interesting that in the COG category "Translation, ribosomal structure and biogenesis", there were two tRNA synthetases (RS), PheRS (lmo1222) and AlaRS (lmo1504), included in the Class IIc, showing distinctive quaternary features. These enzymes are hetero- and homo-tetramers [64]. Moreover, Phe-RS is indispensable for growth in all organisms [65].

The third gene in this category is lmo2620, encoding 50S ribosomal protein L5. Prokaryotic 5S rRNA interacts with the ribosomal protein L5, forming 5S ribonucleoprotein particles, and enhances protein synthesis by the stabilization of the ribosome structure [66].

In the category "Replication, recombination and repair", the delta subunit of DNA polymerase III (lmo1481) is remarkable. It is present in 5–7-fold excess over the gamma complex, and probably performs the clamp unloading function, sparing the limited number of gamma complex and polymerase III molecules in the cell for other important functions such as processive DNA replication. Additionally, the delta subunit does not require ATP for its activity, so the delta-catalyzed unloading reaction cannot be quenched with hexokinase and glucose as described for the gamma complex and polymerase III [67].

The next gene, lmo1646 (exonuclease SbcD), is part of the heterotetrameric SbcCD complex, which cleaves DNA hairpin structures. SbcC might constantly check the replication fork for misfolded DNA and associate with SbcD only when DNA repair is necessary, so a small amount of protein SbcD is required for the complex activity [68].

In the category "Signal transduction mechanisms", two loci distinguish clinical strains of ST7. Response regulator LiaR (lmo1022) is a component of the LiaFSR system, including membrane-bound inhibitor protein LiaF, sensor histidine kinase and a cognate response regulator. Additionally, LiaR is the less abundant component of this system. The LiaFSR system strongly responds to the presence of a number of cell wall antibiotics, such as bacitracin, daptomycin, nisin, ramoplanin and vancomycin, and is weakly induced by other more unspecific stresses that interfere with envelope integrity, such as alkaline shock and secretion stress [69].

The arginine phosphatase (lmo2540) is the next important protein for bacteria stress response. It modulates the arginine phosphorylation states of regulators such as the stress response regulator CtsR and the global regulator MgrA, particularly in response to oxidative stress [70].

Thus, using the example of the most represented categories of COG, we have shown the importance of genes affected by mutations for the vital activity of *L. monocytogenes* ST7.

Two loci distinguishing isolates of ST6 (August 2019 and September 2020, both from newborns) also belonged to the category "Carbohydrate transport and metabolism": lmo1728—cellobiose phosphorylase, and lmo2761—beta-glucosidase. These enzymes catalyze anaerobic (phosphorolytic) and aerobic (hydrolytic) pathways of the cellobiose catabolism, respectively. The phosphorolytic

pathway requires one less ATP for each molecule of cellobiose to be metabolized by glycolysis, so it performs better than the hydrolytic pathway in terms of product yield in stressful conditions [71].

Three loci distinguishing the isolates of ST4 "October 2020 (newborn)" and "March 2021 (fatal)" from the isolate "July 2020 (fatal)" belonged to the three COG categories: "Transcription" (lmo0520—NagC transcriptional regulator), "General function prediction only" (lmo2049—nucleotidyltransferase), and "Translation, ribosomal structure and biogenesis" (lmo2596—30S ribosomal protein S9). Consider the most impressive locus lmo0520. In *E. coli*, as demonstrated Bréchemier-Baey et al., NagC is the transcriptional repressor of the catabolism of the mucin-derived sugars N-acetylglucosamine, and the activator of the locus of enterocyte effacement, which is critical regulator for the colonization of the intestine by bacteria [72].

9. The genotypes of L. monocytogenes isolated from food

The search for the source of infection that caused the cases of invasive listeriosis prompted us to analyze *L. monocytogenes* isolated from food in the metropolis during the monitoring period (Table S3).

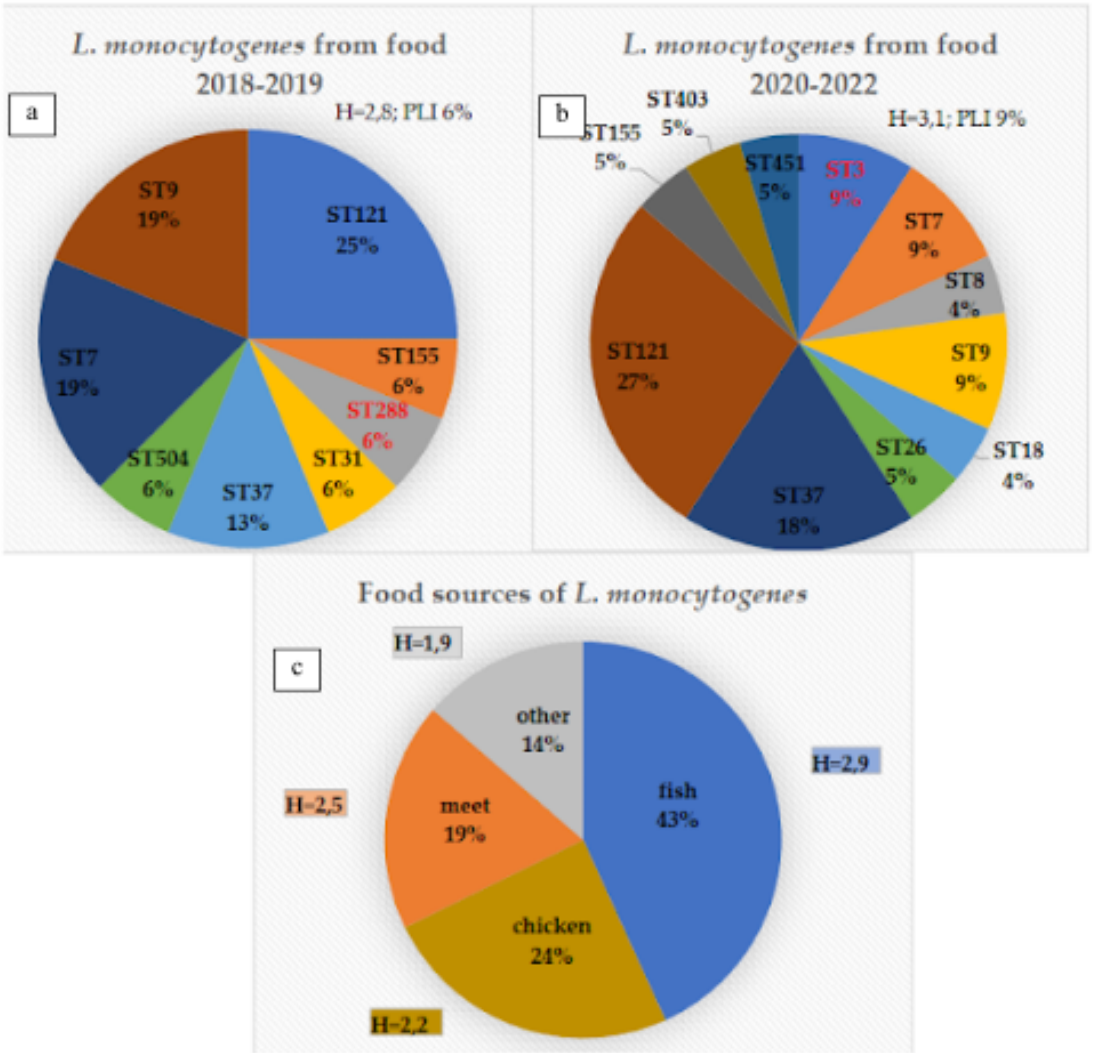

a)—before the COVID-19 pandemic, 2018-2019; b)—during the COVID-19 pandemic; and c—the food sources of the L. monocytogenes isolates. H—the Shannon diversity index; PLI—phylogenetic lineage I; ST—sequence type.

Figure 10: *L. monocytogenes* from food sources.

L. monocytogenes was most commonly isolated from fish, followed by chicken and meat (Figure 10c). All food isolates were subdivided into two groups according to the isolation data: before the pandemic and during the pandemic (Figure 10).

The proportion of genotypes that coincided in the two periods of observation, namely ST7, 9, 37, 121, and 155, was 69% and 68%, respectively. The differing genotypes were more diverse during the COVID-19 period (5ST vs. 3ST), which led to a slight increase in the Shannon diversity index from 2.8 to 3.1 (Figures 10a, 10b). The proportion of PLI increased insignificantly during the pandemic, and ST288 of PLI was replaced by ST3, which had not previously been found in Russia. As such, the genotypes of *L. monocytogenes* infecting foods did not change significantly during the COVID-19 pandemic. In the final list of the genotypes of the clinical isolates of the second stage of the COVID-19 pandemic, only ST8 and ST37 coincide with the list of the food isolates' genotypes.

III. DISCUSSION

Listeriosis is relatively rare, but is one of the deadliest food-borne infections. In Russia in 2020, clinical diagnosis of listeriosis was laboratory-confirmed in 42 patients, and six cases were fatal (https://rospotrebnadzor.ru/ (accessed on 24 July 2022)). In Moscow, 18 cases of listeriosis were registered in 2020, and 21 cases in 2021 (https://77.rospotrebnadzor.ru/ (accessed on 24 July 2022)). The analysis of food included 6883 samples subjected to laboratory control in the departments of Rospotrebnadzor in Moscow in 2020, and 0.6% of samples were positive for *L. monocytogenes* (https://77.rospotrebnadzor.ru/ (accessed on 24 July 2022)). However, persons with recognized underlying diseases such as liver disease, cancer, diabetes and COVID-19 in the case of listeriosis can be counted as having an underlying disease in the clinical report. In perinatal listeriosis, neonatal complications (respiratory failure and heart failure in newborns, cerebral ischemia, etc.) can also be registered as the main diagnosis. Therefore, cases of listeriosis may be underreported in statistics.

Our study included 50 clinical and 37 food *L. monocytogenes* isolates revealed from November 2018 to January 2022 in the metropolis. The obtained results clearly indicate a change in the spectrum of the *Listeria* genotypes causing invasive listeriosis during the COVID-19 pandemic.

L. monocytogenes ST7 (PLII) and ST6 (PLI), which previously typically prevailed among the clinical isolates in the metropolis (Figure 2a1), were changed by the variety of the PLI genotypes (ST1, ST4, ST194, ST219) and the PLII genotypes (ST8, ST20, ST21, ST37, ST391, ST425, ST451) (Figure 2a4). *L. monocytogenes* of ST8 and ST425 were previously found in food and in the environment, but during the pandemic, *L. monocytogenes* of these genotypes were isolated for the first time in cases of human listeriosis in Russia along with ST21, ST37, and ST391. In addition, we observed an increase in the number of fatal cases of invasive listeriosis in the group with meningitis and sepsis (43.8% vs. 81.2%), as well as a sharp decrease in age in this listeriosis group: from 59 to 33 years.

Previously, we showed the impact of respiratory viral infections on the incidence of invasive listeriosis in a metropolis in 2018/2019 [26]. The consequences of SARS-CoV-2 on gastrointestinal tract conditions and sensitivity to food-borne pathogens have yet to be fully characterized. The available evidence suggests that SARS-CoV-2 infection alters the gut barrier, leading to the systemic spread of bacteria, endotoxins, and microbial metabolites [73]. Gut disorders during SARS-CoV-2 infection might also participate in concomitant or secondary bacterial infections, which develop in severely ill COVID-19 patients [73]. According to our observations, infection with SARS-CoV-2 not only contributed to an increase in the incidence of invasive listeriosis even among younger patients, but

also increased the sensitivity to a range of previously non-human *L. monocytogenes* genotypes: ST8, 20, 21, 37, 391, and 425.

Almost all new genotypes of the clinical isolates revealed during the COVID-19 pandemic in the metropolis were previously described in the works of European researchers. The *L. monocytogenes* diversity which related to 1185 cattle abortion cases in Latvia during the period of 2013–2018 included 27 different ST overall [74]. Four of them, ST29, 37, 451 and 7, covered more than half of the *L. monocytogenes* isolates; ST8, 20, 21, 391, and 425 were also detected [74]. Kubicová et al. (Slovakia, 2010 – 2020) described ST451 as the most prevalent in the cohort (15.3%) as a whole, and especially in food (14.8%) and animal isolates (17.5%) [75]. In food, CC11-ST451, followed by CC7, CC14, and CC37, were the most prevalent CCs in the milk sector, and CC9 and CC8 were most prevalent in the meat sector [75]. In the Czech Republic, ST29, 37, and 451 were the most frequent genotypes of *L. monocytogenes*, isolated from vacuum-packed steak tartare in 2013–2016 [76]. In 2019, as non-human isolates, *L. monocytogenes* ST8, ST21, and ST451 were mentioned in the work of researchers from Austria [77]. They found ST21 to be more associated with vegetables, and ST451 with dairy products [77]. Finally, during the COVID-19 pandemic in Italy (September and October 2020), a nosocomial outbreak of listeriosis caused by an ST451 strain of *L. monocytogenes* was recorded [78]. This outbreak involved one immunocompromised patient and three cancer patients hospitalized in different units of the same hospital. The source of contamination was identified in the hospital kitchen, where a meat slicer used to prepare meals tested positive for the same ST of *L. monocytogenes*. This was the first report of an outbreak of listeriosis caused by ST451 in Italy [78].

In our study, the epidemic connections were shown for the PLI isolates (ST219, ST4, ST6), and also for new clinical isolates of ST21, 8 and 425 (PLII), which can be attributed to epidemic outbreaks because of similar cgMLST profiles (0–3 allelic mismatches of cgMLST). The strains of ST425 were isolated from four COVID-19 patients in two hospitals with an interval of 5.0 months. The sources of outbreaks have not been identified.

L. monocytogenes of all genotypes revealed in the clinical cases were analyzed for the presence of 42 VFs. All VFs but one (*vip*) were observed in all of the analyzed isolates. The vip involved in cell invasion [42] was absent in the isolates of ST7, 8, 21, and 37, which were associated with clinical cases (perinatal listeriosis, septicemia, meningitis), including fatal ones. We found confirmation of our results in the works of a number of researchers. The lack of the *vip* gene in FPE *L. monocytogenes* isolates of ST8 and ST37 was noted by Alvarez-Molina et al. from Spain [79]. In the research into the isolates obtained from cattle abortion cases by Šteingolde et al. (Latvia), the list of *vip*-missing genotypes was expanded and additionally included ST29, 120, 226, 391, 403, 573 (PL II) and even ST 2, 4, and 6 (PL I) [74]. Thus, the thesis about the obligatory presence of the *vip* gene in the genomes of isolates of the PLI and PLII [42, 43] needs to be revised.

In addition to the main 42 virulence factors, Maury et al. noted the following features of the PLI isolates with high clinical frequency (CC1, CC2, CC4, and CC6), which were named as hypervirulent: 1) the over-representation of genes involved in replication, recombination, and repair, which may indicate a higher exposure to genotoxic conditions; and 2) the over-representation of genes involved in cell wall and membrane biogenesis, which may reflect the selection of genes involved in interactions with the host [80]. In our investigation, the cases of perinatal listeriosis were associated with hypervirulent *L. monocytogenes* of ST6 during the pre-COVID-19 period. *Listeria* belonging to the additional genotypes of CC1 (ST1) and CC4 (ST4 and ST219) caused the perinatal listeriosis during the COVID-19 pandemic. According to Charlier et al., *L. monocytogenes* of CC1, CC2, CC4, are overrepresented in maternal–neonatal (MN) infections in France, with more than two-thirds of cases

being due to one of these CCs. [81]. Among them, CC4 is the most associated with MN infections, with 20% of CC4 isolates being of MN origin [81].

The plasmids can become an additional source of virulence factors. The presence of plasmid replicons in the clinical *L. monocytogenes* isolates is not a frequent phenomenon [46]. In our study, the plasmids were found in five isolates: four isolates of ST425 and one of ST20. All of them were new in clinical cases. More often, the discussion of *Listeria* plasmids takes place in the context of the ability of *Listeria* spp. to colonize various environments, especially the FPE, with a focus on the genes that provide resistance to sanitizers [82], heavy metals [58] or elevated temperatures [45]. However, according to Chmielowska et al., there is evidence that the presence of some cadAC resistance cassettes in *Listeria* can influence other phenotypic traits, such as virulence and biofilm formation, which suggests that these heavy metal resistance determinants may have additional functions [54]. Other genes encoding the proteins contributing to copper homeostasis, the regulation of iron concentration, the modification of wall teichoic acids and even in-creased heat resistance may facilitate the increase in virulence and the spread and survival of *Listeria* in the human body. Thus, on the one hand, if, during the COVID-19 period, invasive listeriosis is caused by listeria of genotypes previously typical of food isolates, in addition to containing plasmids, then we can confirm that SARS-CoV-2 has a serious damaging effect on the defense system of the gastrointestinal tract. On the other hand, *L. monocytogenes* of ST425 (of one epidemic cluster, according to cgMLST analysis) caused disease not only in people in the older age category, but also in younger people (36 and 47 years old); therefore, isolates of this genotype can hardly be classified as hypovirulent, and their virulence factors, including those introduced by plasmids, are subject to further study.

IV. CONCLUSIONS

The COVID-19 pandemic has had a significant impact on the health of the human population, promoting bacterial infections in weakened organisms. Listeriosis, as one of the deadliest foodborne infections, completely changed the portrait of those *L. monocytogenes* genotypes that caused invasive listeriosis both in the perinatal group and in the group with meningitis and sepsis, according to monitoring in a metropolis with a population of 20.4 million. The rejuvenation of listeriosis and increase in mortality in the group with meningitis and sepsis, the emergence of new genotypes of PLII, previously classified as food and hypovirulent, and new genotypes of *L. monocytogenes* of PLI in the perinatal group indicate the need for the even more stringent control of food products for the high-risk groups regarding invasive listeriosis.

V. MATERIALS AND METHODS

5.1 Bacterial isolates

Fifty clinical *L. monocytogenes* isolates (19 isolates from the first time period: November 2018–October 2019; 31 isolates from the second time period: March 2020–January 2022) were obtained from microbiological laboratories of the Moscow laboratory diagnostic centers. All *L. monocytogenes* were isolated from the samples of the patients with invasive listeriosis: perinatal listeriosis—44%, meningitis and listeria septicemia—56%. Isolates were submitted in the Bacterial Isolate Genome Sequence Database for *L. monocytogenes* (BIGSdb-Lm) (https://bigsdb.pasteur.fr/listeria/ (accessed on 24 July 2022)), ID: 42973-42983, 45724-45730, 49373-49375, 75929, 75931, 75932, 76308-76311, 76389, 77384-77386, 78377, 78378, 78657-78660, 78714, 82478-82480, 82484-82486, 82489-82492, 82494 (Table S1).

The *Listeria* isolates from food (ID: 42984-42998, 45731, 49370- 49372, 75930, 75933, 76312, 76385-76388, 78379, 78713, 78715, 78717, 82479, 82481-82483, 82487, 82488, 82493) and food processing environments (ID: 49188-49202, 49206) were used in the comparison groups (Table S2).

5.2 Methods

5.2.1 DNA isolation

For genotyping, listeria isolates were grown on BHI agar overnight at 37 °C. One loopful of cells was suspended in 20 µL of the lysis buffer (0.25% SDS and 0.05 M NaOH), warmed up for 15 min at 95 °C, and 180 µL of the bidistilled water was added. The resulting lysate was stored at temperature 4 °C. For the whole-genome sequencing, listeria isolates grown on BHI agar overnight at 37 °C were suspended in the BHI broth and grown overnight at the same temperature. The cells were centrifuged, and the washed pellet was used for DNA isolation according to the Monarch Kit instructions (New England Biolabs, Ipswich, Massachusetts, USA).

5.2.2 MultiLocus Sequence Typing (MLST) and Multi-Virulent-Locus Sequence Typing (MvLST)

For MLST, we used a combination of primers [83] and [84], laboratory-designed *ldh* primers, and our modification of PCR and sequencing protocols [31]. New alleles and new sequence types (ST) for MLST genes were controlled by the team of curators of the Institut Pasteur MLST system (Paris, France).

The MvLST scheme including four internalin genes (*inlABCE*) chosen earlier by [33] was used with our modification [30]. The alleles of the internalin genes were numbered in the order of the detection, submitted in GenBank and published in [26, 31-33, 85, 86]. For each *L. monocytogenes* isolate, the combination of four detected alleles (in order *inlABCE*) received an internalin profile (IP) number. New alleles and IP from this research are presented in Table 1.

5.2.3 Whole genome sequencing (WGS)

The genomes of the strains with ST6, ST7, ST451, and new ST for the Russian listeria population (ST4, 194, 219), and new ST for clinical listeria isolates (8, 21, 425), were sequenced on the Illumina platform. The Nextera DNA Flex Library Prep (Illumina, San Diego, CA, USA) protocol was used for the library's preparation. Sequencing was performed on MiSeq and NextSeq 500/550 (Illumina, San Diego, CA, USA).

5.2.4 Data analysis

CLC Genomic Workbench v.20.0.4 (QIAGEN, Germantown, MD, USA) and SPAdes v.3.13.0 (St. Petersburg genome assembler, Russia, URL: http://cab.spbu.ru/software/spades/ (accessed on 24 July 2022)) were used for genome assembling. CGView Server (http://stothard.afns.ualberta.ca/cgview_server/ (accessed on 24 July 2022)) was applied for the visualization of assembling results and for the genome comparison [87]. The software Rapid Annotations Subsystems Technology (RAST) and SEED were used for genome annotation [88, 89]. Prophage sequences were revealed with the help of PHASTER (PHAge Search Tool Enhanced Release, https://phaster.ca/ (accessed on 24 July 2022)) [90].

WGS data are available in GenBank: Bio Project PRJNA605697. Previously published ST7 genomes (GenBank Accession Numbers CP060433- CP060435) were used for the comparison. The plasmid sequences of the strains GIMC 2079:Lmc UH26, GIMC2080:Lmc UH27, GIMC2090:LmcH67_6,

GIMC2095:LmcH67_8 (ST425) and GIMC2088:LmcIH1-6 (ST20) were submitted to GenBank (Accession Numbers MZ869810, MZ869811, OM867528 - OM867530).

The core genome MLST scheme of 1748 loci (cgMLST) was used for *L. monocytogenes* genome characterization [91] on the basis of an open bioinformatics platform (https://bigsdb.pasteur.fr/listeria/(accessed on 24 July 2022)). Alleles which were not characterized by the computational tool due to their difference from the registered sequences were searched by comparing genomic data with alleles of the reference EGD-e strain using BLAST NCBI. The identified sequences of the corresponding alleles of the isolates of the same ST were compared by the number of differences with the closest match. New alleles were considered identical if there were the same substitutions.

The assignment of genes to different Clusters of Orthologous Genes (COG) categories was carried out with NCBI Blastp and the COG database/Conserved Protein Domain Family database [61].

The comparison of the plasmids pLmcIH1-6 and pLmcC11 with the reference pLm-cUH26 was performed by using BLAST Ring Image Generator (BRIG) with blast-2.7.1+ [92].

CLC Genomics Workbench v. 21.0.1 with the Whole Genome Alignment 21.0 plugin was used for plasmid alignment and tree building. The Whole Genome Alignment 21.0 plugin works by identifying seeds (short stretches of nucleotide sequence that are shared between multiple genomes but not present multiple times on the same genome) in the plasmid. This option determines the number of nucleotides required for a seed to be included in the later stages of the alignment. The minimum initial seed length was 15 bp. From the initial extended seed matches, a distance matrix between the input plasmid was calculated. This distance matrix was used for the subsequent pairwise processing, where the most similar plasmid sequences were processed first. Proceeding iteratively on the most similar pair of plasmids, the tool extended and merged seed matches to create longer alignment blocks. The minimum alignment block length was 100 bp.

The Create Average Nucleotide Identity Comparison tool was useful for obtaining a quantitative measure of the similarity between plasmids. This tool took whole-genome alignment as input, and for each pair of plasmids, the regions aligned between the two plasmids were identified. The toll was launched using the following parameters: the minimum similarity fraction—0.8 and the minimum length fraction—0.8. On the basis of Create Average Nucleotide Identity Comparison tool data, the neighbor-joining tree was constructed.

The analysis of virulence factors was performed using the Virulence Factors Database (VFDB, http://www.mgc.ac.cn/VFs/ (accessed on 24 July 2022)) and VF analyzer (http://www.mgc.ac.cn/cgi-bin/ VFs/v5/main.cgi?func=VFanalyzer/ (accessed on 24 July 2022)) [41].

The Shannon diversity index (H) was used to characterize *L. monocytogenes* diversity and was calculated by the formula:

$$H = -\sum_{i=1}^{\%} pi \ln ln\, pi$$

where pi is the proportion of the number of isolates of genotype i (ni) relative to the total number of isolates (N): pi = ni/N.

List of abbreviations

ACE2 - angiotensin-converting enzyme 2
AIDS - acquired immunodeficiency syndrome

ANI - average nucleotide identity
AP - alignment percentage
BIGSdb-Lm - Bacterial Isolate Genome Sequence Database for *L. monocytogenes*
CC - Clonal Complex
CDS - coding sequences
cgMLST - core genome MLST
COG - Clusters of Orthologous Genes
Dps protein - DNA protection during starvation protein
FD - Federal District
GI - gastrointestinal tract
IP - internalin profile
LRR - leucine-rich repeat
MLST -. MultiLocus Sequence Typing
MvLST - Multi-Virulent-Locus Sequence Typing
ORF - open reading frame
PL - phylogenetic lineage
RAST - Rapid Annotations Subsystems Technology
RTE - ready-to eat
SCFAs - short chain fatty acids
SLV - single locus variant
SNV - single-nucleotide variant
ST - sequence types
VF - virulence factors
VOC - variants of concern
WGS - whole genome sequencing

Supplementary Materials: Table S1: The clinical *L. monocytogenes* isolates; Table S2: Virulence factors revealed in *L. monocytogenes* genomes by the VF analyzer; Table S3: The food *L. monocytogenes* isolates.

Declarations

- Ethics approval and consent to participate. The authors of the study conducted only with microorganisms provided by the clinical laboratories. Consent to the study in the clinic was issued by patients during hospitalization.
- Consent for publication. The publication of the research data was approved by the Biomedical Ethics Committee at the Gamaleya National Research Center for Epidemiology and Microbiology, Ministry of Health of the Russian Federation.
- Availability of data and materials. Data of the MLST are available in in the Bacterial Isolate Genome Sequence Database for *L. monocytogenes* (BIGSdb-Lm) (https://bigsdb.pasteur.fr/listeria/) under the IDs indicated in the methods section. WGS data are available in GenBank: Bio Project PRJNA605697, GenBank Accession Numbers: CP060433- CP060435, MZ869810, MZ869811, OM867528 - OM867530, MZ869809
- Competing interests. There are no competing interests to declare.
- Funding. This research received no external funding.
- Authors' contributions. Conceptualization, O.L.V., E.A.K., O.A.G., A.R.M. and I.S.T.; methodology, O.L.V., N.N.R., M.S.K. and E.I.A.; software, N.N.R., M.S.K. and E.I.A; validation, O.L.V., N.N.R., M.S.K. and E.I.A.; formal analysis, A.V.K., A.N.T.; investigation, O.L.V., N.N.R., M.S.K., E.I.A., A.V.K., A.N.T. and T.I.K.; resources, O.L.V., E.A.K., O.A.G., A.R.M. and I.S.T.; data curation, M.S.K., N.N.R., and O.L.V.; writing—original draft preparation, O.L.V., N.N.R., M.S.K.

and E.I.A.; writing—review and editing, O.L.V., N.N.R., M.S.K. and E.I.A.; visualization, M.S.K., N.N.R., and O.L.V.; supervision, O.L.V.; project administration, I.S.T.; funding acquisition, O.L.V., E.A.K., O.A.G., A.R.M. All authors have read and agreed to the published version of the manuscript.

- Acknowledgements. The authors are grateful to the laboratory assistants of the microbiological laboratories of the Moscow laboratory diagnostic centers for providing L. monocytogenes isolates for the study: Burmistrova E.N., Dudnikova S.V., Gambaryan K.U., Mammadova A.M., Nechaeva S.A., Orlova O.E., Pokidysheva A.Y., Prokopaeva M.A., Pronina T.V.

REFERENCES

1. Listeria monocytogenes risk assessment. Appendix 8: Growth of Listeria monocytogenes in foods. FDA. Available online: URL https://www.fda.gov/media/77930/download (accessed on 15.07.2022).
2. Hafner L, Pichon M, Burucoa C, Nusser SHA, Moura A, Garcia-Garcera M, Lecuit M. Listeria monocytogenes faecal carriage is common and depends on the gut microbiota. Nat Commun. 2021; doi: 10.1038/s41467-021-27069-y.
3. RASFF – the Rapid Alert System for Food and Feed. Available online: URL https://ec.europa.eu/food/safety/rasff-food-and-feed-safety-alerts_en (accessed on 15.07.2022).
4. World Health Organization. Listeriosis. Available online: URL www.who.int/newsroom/factsheets/detail/listeriosis (ac-cessed on 15.07.2022).
5. Mook P, O'Brien SJ, Gillespie IA. Concurrent conditions and human listeriosis, England, 1999-2009. Emerg Infect Dis. 2011; doi: 10.3201/eid1701.101174.
6. Goulet V, Hebert M, Hedberg C, Laurent E, Vaillant V, De Valk H, Desenclos JC. Incidence of listeriosis and related mortality among groups at risk of acquiring listeriosis. Clin Infect Dis. 2012; doi: 10.1093/cid/cir902.
7. Fuentes E, Fuentes M, Alarcón M, Palomo I. Immune system dysfunction in the elderly. An Acad Bras Cienc. 2017; doi: 10.1590/0001-3765201720160487.
8. Sridama V, Pacini F, Yang SL, Moawad A, Reilly M, DeGroot LJ. Decreased levels of helper T cells: a possible cause of immunodeficien.cy in pregnancy. N Engl J Med. 1982; doi: 10.1056/NEJM198208053070606.
9. Vanagunas A. Gastrointestinal complications in pregnancy. Glob. libr. women's med. 2008; doi: 10.3843/GLOWM.10172.
10. Herath M, Hosie S, Bornstein JC, Franks AE, Hill-Yardin EL. The Role of the gastrointestinal mucus system in intestinal homeostasis: implications for neurological disorders. Front Cell Infect Microbiol. 2020; doi:10.3389/fcimb.2020.00248.
11. Navaneethan U, Giannella RA. Mechanisms of infectious diarrhea. Nat Clin Pract Gastroenterol Hepatol. 2008; doi: 10.1038/ncpgasthep1264.
12. Oren A, Garrity GM. Valid publication of the names of forty-two phyla of prokaryotes. Int J Syst Evol Microbiol. 2021; doi: 10.1099/ijsem.0.005056.
13. Koren O, Goodrich JK, Cullender TC, Spor A, Laitinen K, Bäckhed HK, Gonzalez A, Werner JJ, Angenent LT, Knight R, Bäckhed F, Isolauri E, Salminen S, Ley RE. Host remodeling of the gut microbiome and metabolic changes during pregnancy. Cell. 2012; doi: 10.1016/j.cell.2012.07.008.
14. He J, Guo H, Zheng W, Yao W. Effects of stress on the mucus-microbial interactions in the gut. Curr Protein Pept Sci. 2019; doi: 10.2174/1389203719666180514152406.
15. Hendrickx AP, Top J, Bayjanov JR, Kemperman H, Rogers MR, Paganelli FL, Bonten MJ, Willems RJ. Antibiotic-driven dysbiosis mediates intraluminal agglutination and alternative segregation of Enterococcus faecium from the intestinal epithelium. mBio. 2015; doi: 10.1128/mBio.01346-15.
16. Schlech WF. Epidemiology and clinical manifestations of Listeria monocytogenes infection. Microbiol Spectr. 2019; doi: 10.1128/microbiolspec.GPP3-0014-2018.

17. Schwartz B, Hexter D, Broome CV, Hightower AW, Hirschhorn RB, Porter JD, Hayes PS, Bibb WF, Lorber B, Faris DG. Investigation of an outbreak of listeriosis: new hypotheses for the etiology of epidemic Listeria monocytogenes infections. J Infect Dis. 1989; doi: 10.1093/infdis/159.4.680.
18. Hanada S, Pirzadeh M, Carver KY, Deng JC. Respiratory viral infection-induced microbiome alterations and secondary bacterial pneumonia. Front Immunol. 2018; doi: 10.3389/fimmu.2018.02640.
19. Bortell N, Aguilera ER, Lenz LL. Pulmonary insults exacerbate susceptibility to oral Listeria monocytogenes infection through the production of IL-10 by NK cells. PLoS Pathog. 2021; doi: 10.1371/journal.ppat.1009531.
20. Origin of SARS-CoV-2. WHO reference number: WHO/2019-nCoV/FAQ/Virus_origin/2020.1.
21. Xiao F, Tang M, Zheng X, Liu Y, Li X, Shan H. Evidence for gastrointestinal infection of SARS-CoV-2. Gastroenterology. 2020; doi: 10.1053/j.gastro.2020.02.055.
22. Villapol S. Gastrointestinal symptoms associated with COVID-19: impact on the gut microbiome. Transl Res. 2020; doi: 10.1016/j.trsl.2020.08.004.
23. Hikmet F, Méar L, Edvinsson A, Micke P, Uhlén M, Lindskog C. The protein expression profile of ACE2 in human tissues. Mol Syst Biol. 2020; doi: 10.15252/msb.20209610.
24. Zhang D, Li S, Wang N, Tan HY, Zhang Z, Feng Y. The cross-talk between gut microbiota and lungs in common lung diseases. Front Microbiol. 2020; doi: 10.3389/fmicb.2020.00301.
25. Enaud R, Prevel R, Ciarlo E, Beaufils F, Wieërs G, Guery B, Delhaes L. The gut-lung axis in health and respiratory diseases: a place for inter-organ and inter-kingdom crosstalks. Front Cell Infect Microbiol. 2020; doi: 10.3389/fcimb.2020.00009.
26. Voronina O, Tartakovsky I, Yuyshchuk N, Ryzhova N, Kunda M, Aksenova E, Kutuzova A, Melkumyan A, Karpova T, Gruzdeva O, et al. Analysis of sporadic cases of invasive listeriosis in a metropolis. J. Microbiol. Epidemiol. Immunobiol. = Zhurnal Mikrobiol. èpidemiologii i Immunobiol. 2020; doi:10.36233/0372-9311-2020-97-6-3.
27. Orsi RH, den Bakker HC, Wiedmann M. Listeria monocytogenes lineages: genomics, evolution, ecology, and phenotypic characteristics. Int J Med Microbiol. 2011; doi: 10.1016/j.ijmm.2010.05.002.
28. Gushchin VA, Dolzhikova IV, Shchetinin AM, Odintsova AS, Siniavin AE, Nikiforova MA, Pochtovyi AA, Shidlovskaya EV, Kuznetsova NA, Burgasova OA, Kolobukhina LV, Iliukhina AA, Kovyrshina AV, Botikov AG, Kuzina AV, Grousova DM, Tukhvatulin AI, Shcheblyakov DV, Zubkova OV, Karpova OV, Voronina OL, Ryzhova NN, Aksenova EI, Kunda MS, Lioznov DA, Danilenko DM, Komissarov AB, Tkachuck AP, Logunov DY, Gintsburg AL. Neutralizing activity of sera from Sputnik V-vaccinated people against variants of concern (VOC: B.1.1.7, B.1.351, P.1, B.1.617.2, B.1.617.3) and Moscow endemic SARS-CoV-2 variants. Vaccines (Basel). 2021; doi: 10.3390/vaccines9070779.
29. Latif AA, Mullen JL, Alkuzweny M, Tsueng G, Cano M, Haag E, Zhou J, Zeller M, Hufbauer E, Matteson N, Wu Ch, Andersen KG, Su AI, Gangavarapu K, Hughes LD.; and the Center for Viral Systems Biology. Moscow City, Russia Variant Report. outbreak.info, (available at https://outbreak.info/location-reports?xmin=2021-02-26&xmax=2021-08-09&loc=RUS_RU-TW9zY293IENpdHk). Accessed 18 July 2022.
30. Klink GV, Safina K, Nabieva E, Shvyrev N, Garushyants S, Alekseeva E, Komissarov AB, Danilenko DM, Pochtovyi AA, Divisenko EV, Vasilchenko LA, Shidlovskaya EV, Kuznetsova NA, Coronavirus Russian Genetics Initiative (CoRGI) Consortium Samoilov AE, Neverov AD, Popova AV, Fedonin GG, CRIE Consortium Akimkin VG, Lioznov D, Gushchin VA, Shchur V, Bazykin GA. The rise and spread of the SARS-CoV-2 AY.122 lineage in Russia. medRxiv [Preprint]. 2021; doi: 10.1101/2021.12.02.21267168.
31. Voronina OL, Kunda MS, Ryzhova NN, Kutuzova AV, Aksenova EI, Karpova TI, Tartakovskij IS, Yushchuk ND, Klimova EA, Karetkina GN, Chemeris OYu, Gruzdeva OA, Melkumyan AR, Orlova

OE, Burmistrova EN. Listeriosis: genotyping as a key for identification a possible source of infection. Clinical Microbiology and Antimicrobial Chemotherapy. 2019; doi: 10.36488/cmac.2019.4.261273.
32. Psareva EK, Egorova IY, Liskova EA, Razheva IV, Gladkova NA, Sokolova EV, Potemkin EA, Zhurilov PA, Mikhaleva TV, Blokhin AA, Chalenko YM, Kolbasov DV, Ermolaeva SA. Retrospective study of Listeria monocytogenes isolated in the territory of inner Eurasia from 1947 to 1999. Pathogens. 2019; https://doi.org/10.3390/pathogens8040184
33. Adgamov R, Zaytseva E, Thiberge JM, Brisse S, Ermolaeva S. Genetically related Listeria monocytogenes strains isolated from lethal human cases and wild animals. In: Genetic Diversity in Microorganisms, Caliskan M. ed., 2012. Chapter 9. ISBN: 978¬953¬51¬0064¬5.
34. Voronina OL, Kunda MS, Ryzhova NN, Aksenova EI, Semenov AN, Kurnaeva MA, Ananyina YuV, Lunin VG, Gintsburg AL. Regularities of the ubiquitous polyhostal microorganisms selection by the example of three taxa. Molecular Biology. 2015; doi: 10.1134/S0026893315030176
35. Astashkin EI, Alekseeva EA, Borzenkov VN, Kislichkina AA, Mukhina TN, Platonov ME, Svetoch EA, Shepelin AP, Fursova NK. Molecular-genetic characteristics of polyresistant Listeria monocytogenes strains and identification of new sequence types. Mol. Genet. Microbiol. Virol. 2021; https://doi.org/10.3103/S0891416821040029
36. Bierne H, Sabet C, Personnic N, Cossart P. Internalins: a complex family of leucine-rich repeat-containing proteins in Listeria monocytogenes. Microbes Infect. 2007; doi: 10.1016/j.micinf.2007.05.003.
37. Klimova EA, Voronina OL, Karetkina GN, Posukhovsky EA, Ryzhova NN, Kunda MS, Aksenova EI, Kutuzova AV, Karpova TI, Tartakovsky IS, Pokidysheva AYu, Pronina TV, Melkumyan AR, Orlova OE, Burmistrova EN, Syrochev AA, Smetanina SV, Yushchuk ND. Listeriosis and the COVID-19 pandemic. Infectious Diseases: News, Opinions, Training. 2022; doi: https://doi.org/10.33029/2305-3496-2022-11-1-102-112.
38. Disson O, Moura A, Lecuit M. Making sense of the biodiversity and virulence of Listeria monocytogenes. Trends Microbiol. 2021; doi: 10.1016/j.tim.2021.01.008.
39. Maury MM, Tsai YH, Charlier C, Touchon M, Chenal-Francisque V, Leclercq A, Criscuolo A, Gaultier C, Roussel S, Brisabois A, Disson O, Rocha EPC, Brisse S, Lecuit M. Uncovering Listeria monocytogenes hypervirulence by harnessing its biodiversity. Nat Genet. 2016; doi: 10.1038/ng.3501.
40. Weiss RA. Virulence and pathogenesis. Trends Microbiol. 2002; doi: 10.1016/s0966-842x(02)02391-0.
41. Chen L, Yang J, Yu J, Yao Z, Sun L, Shen Y, Jin Q. VFDB: a reference database for bacterial virulence factors. Nucleic Acids Res. 2005; doi: 10.1093/nar/gki008.
42. Cabanes D, Sousa S, Cebriá A, Lecuit M, García-del Portillo F, Cossart P. Gp96 is a receptor for a novel Listeria monocytogenes virulence factor, Vip, a surface protein. EMBO J. 2005; doi: 10.1038/sj.emboj.7600750.
43. Doumith M, Cazalet C, Simoes N, Frangeul L, Jacquet C, Kunst F, Martin P, Cossart P, Glaser P, Buchrieser C. New aspects regarding evolution and virulence of Listeria monocytogenes revealed by comparative genomics and DNA arrays. Infection and immunity. 2004; https://doi.org/10.1128/IAI.72.2.1072-1083.2004
44. Parsons C, Lee S, Kathariou S. Heavy metal resistance determinants of the foodborne pathogen Listeria monocytogenes. Genes (Basel). 2018; doi: 10.3390/genes10010011.
45. Pöntinen A, Aalto-Araneda M, Lindström M, Korkeala H. Heat resistance mediated by pLM58 plasmid-borne ClpL in Listeria monocytogenes. mSphere. 2017; doi: 10.1128/mSphere.00364-17.
46. Lebrun M, Loulergue J, Chaslus-Dancla E, Audurier A. Plasmids in Listeria monocytogenes in relation to cadmium resistance. Appl Environ Microbiol. 1992; doi: 10.1128/aem.58.9.3183-3186.1992.

47. Lehnherr H, Maguin E, Jafri S, Yarmolinsky MB. Plasmid addiction genes of bacteriophage P1: doc, which causes cell death on curing of prophage, and phd, which prevents host death when prophage is retained. J Mol Biol. 1993; doi: 10.1006/jmbi.1993.1521.
48. Li YJ, Liu Y, Zhang Z, Chen XJ, Gong Y, Li YZ. A Post-segregational killing mechanism for maintaining plasmid PMF1 in its Myxococcus fulvus host. Front Cell Infect Microbiol. 2018; doi: 10.3389/fcimb.2018.00274.
49. Curtis TD, Takeuchi I, Gram L, Knudsen GM. The influence of the toxin/antitoxin mazEF on growth and survival of Listeria monocytogenes under stress. Toxins (Basel). 2017; doi: 10.3390/toxins9010031.
50. Jesse HE, Roberts IS, Cavet JS. Metal ion homeostasis in Listeria monocytogenes and importance in host-pathogen interactions. Adv Microb Physiol. 2014; doi: 10.1016/bs.ampbs.2014.08.003.
51. Olsen KN, Larsen MH, Gahan CGM, Kallipolitis B, Wolf XA, Rea R, Hill C, Ingmer H. The Dps-like protein Fri of Listeria monocytogenes promotes stress tolerance and intracellular multiplication in macrophage-like cells. Microbiology (Reading). 2005; doi: 10.1099/mic.0.27552-0.
52. Henle ES, Linn S. Formation, prevention, and repair of DNA damage by iron/hydrogen peroxide. J Biol Chem. 1997; doi: 10.1074/jbc.272.31.19095.
53. Carvalho F, Atilano ML, Pombinho R, Covas G, Gallo RL, Filipe SR, Sousa S, Cabanes D. L-rhamnosylation of Listeria monocytogenes wall teichoic acids promotes resistance to antimicrobial peptides by delaying interaction with the membrane. PLoS Pathog. 2015; doi: 10.1371/journal.ppat.1004919.
54. Chmielowska C, Korsak D, Chapkauskaitse E, Decewicz P, Lasek R, Szuplewska M, Bartosik D. Plasmidome of Listeria spp.-The repA-family business. Int J Mol Sci. 2021; doi: 10.3390/ijms221910320.
55. Gonzalez-Escalona N, Kastanis GJ, Timme R, Roberson D, Balkey M, Tallent SM. Closed genome sequences of 28 foodborne pathogens from the CFSAN verification set, determined by a combination of long and short reads. Microbiol Resour Announc. 2020; doi:10.1128/MRA.00152-20.
56. Portmann AC, Fournier C, Gimonet J, Ngom-Bru C, Barretto C, Baert L. A validation approach of an end-to-end whole genome sequencing workflow for source tracking of Listeria monocytogenes and Salmonella enterica. Front Microbiol. 2018; doi: 10.3389/fmicb.2018.00446.
57. Chen P, Kong N, Huang B, Thao K, Ng W, Storey DB, Arabyan N, Foutouhi A, Foutouhi S, Weimer BC. 100K pathogen genome project: 306 Listeria draft genome sequences for food safety and public health. Genome Announc. 2017; doi: 10.1128/genomeA.00967-16.
58. Kuenne C, Voget S, Pischimarov J, Oehm S, Goesmann A, et al. Comparative analysis of plasmids in the genus Listeria. PLoS ONE. 2010; doi:10.1371/journal.pone.0012511.
59. Orsini M, Cornacchia A, Patavino C, Torresi M, Centorame P, Acciari VA, Ruolo A, Marcacci M, Ancora M, Di Domenico M, et al. Whole-genome sequences of two Listeria monocytogenes serovar 1/2a strains responsible for a severe listeriosis outbreak in central Italy. Genome Announc. 2018;6: e00236-18.
60. Cortes BW, Naditz AL, Anast JM, Schmitz-Esser S. Transcriptome sequencing of Listeria monocytogenes reveals major gene expression changes in response to lactic acid stress exposure but a less pronounced response to oxidative stress. Front Microbiol. 2020; doi: 10.3389/fmicb.2019.03110.
61. Galperin MY, Makarova KS, Wolf YI, Koonin EV. Expanded microbial genome coverage and improved protein family annotation in the COG database. Nucleic Acids Res. 2015; doi: 10.1093/nar/gku1223.
62. Elbourne LD, Tetu SG, Hassan KA, Paulsen IT. TransportDB 2.0: a database for exploring membrane transporters in sequenced genomes from all domains of life. Nucleic Acids Res. 2017; doi: 10.1093/nar/gkw1068.

63. Bosshart PD, Fotiadis D. Secondary active transporters. In Bacterial Cell Walls and Membranes, Subcellular Biochemistry 92; Kuhn A., Ed.; Springer Nature, Switzerland AG, 2019; doi: 10.1007/978-3-030-18768-2_9.
64. Zhou Q, Zhang Q, Qu H, Li W, Feng F, Luo Q. Comparative proteomic analysis of Listeria monocytogenes tolerance to bile stress. Ann Microbiol. 2013; https://doi.org/10.1007/s13213-012-0452-5.
65. Mosyak L, Reshetnikova L, Goldgur Y, Delarue M, Safro MG. Structure of phenylalanyl-tRNA synthetase from Thermus the rmophilus. Nat Struct Biol. 1995; doi: 10.1038/nsb0795-537.
66. Swayze EE, Griffey RH, Bennett CF. Chapter 2.26 - Nucleic Acids (Deoxyribonucleic Acid and Ribonucleic Acid). In Comprehensive Medicinal Chemistry II; Taylor J.B., Triggle D.J., Eds.; Elsevier, Amsterdam, London, 2007; doi: 10.1016/B0-08-045044-X/00065-1.
67. Leu FP, Hingorani MM, Turner J, O'Donnell M. The delta subunit of DNA polymerase III holoenzyme serves as a sliding clamp unloader in Escherichia coli. J Biol Chem. 2000; doi: 10.1074/jbc.M005495200.
68. Darmon E, Lopez-Vernaza MA, Helness AC, Borking A, Wilson E, Thacker Z, Wardrope L, Leach DR. SbcCD reg-ulation and localization in Escherichia coli. J Bacteriol. 2007; doi: 10.1128/JB.00489-07.
69. Schrecke K, Jordan S, Mascher T. Stoichiometry and perturbation studies of the LiaFSR system of Bacillus subtilis. Mol Mi-crobiol. 2013; doi: 10.1111/mmi.12130.
70. Huang B, Zhao Z, Zhao Y, Huang S. Protein arginine phosphorylation in organisms. Int J Biol Macromol. 2021; doi: 10.1016/j.ijbiomac.2021.01.015.
71. Chomvong K, Kordić V, Li X, Bauer S, Gillespie AE, Ha SJ, Oh EJ, Galazka JM, Jin YS, Cate JH. Overcoming inefficient cellobiose fermentation by cellobiose phosphorylase in the presence of xylose. Biotechnology Biofuels. 2014; doi: 10.1186/1754-6834-7-85.
72. Bréchemier-Baey D, Domínguez-Ramírez L, Oberto J, Plumbridge J. Operator recognition by the ROK transcription factor family members, NagC and Mlc. Nucleic Acids Res. 2015; doi: 10.1093/nar/gku1265.
73. Sencio V, Machado MG, Trottein F. The lung-gut axis during viral respiratory infections: the impact of gut dysbiosis on secondary disease outcomes. Mucosal Immunol. 2021; doi: 10.1038/s41385-020-00361-8.
74. Šteingolde Ž, Meistere I, Avsejenko J, Ķibilds J, Bergšpica I, Streikiša M, Gradovska S, Alksne L, Roussel S, Ter-entjeva M, Bērziņš A. Characterization and genetic diversity of Listeria monocytogenes isolated from cattle abortions in Latvia, 2013-2018. Vet Sci. 2021; doi: 10.3390/vetsci8090195.
75. Kubicová Z, Roussel S, Félix B, Cabanová L. Genomic diversity of Listeria monocytogenes isolates from Slovakia (2010 to 2020). Front Microbiol. 2021; doi: 10.3389/fmicb.2021.729050.
76. Hluchanova L, Korena K, Juricova H. Vacuum-packed steak tartare: prevalence of Listeria monocytogenes and evaluation of efficacy of Listex TM P100. Foods 2022; https://doi.org/10.3390/foods11040533.
77. Cabal A, Pietzka A, Huhulescu S, Allerberger F, Ruppitsch W, Schmid D. Isolate-based surveillance of Listeria monocytogenes by whole genome sequencing in Austria. Front. Microbiol. 2019; doi: 10.3389/fmicb.2019.02282.
78. Russini V, Spaziante M, Zottola T, Fermani AG, Di Giampietro G, Blanco G, Fabietti P, Marrone R, Parisella R, Parrocchia S, Bossù T, Bilei S, De Marchis ML. A nosocomial outbreak of invasive listeriosis in an Italian hospital: epidemiological and genomic features. Pathogens. 2021; doi: 10.3390/pathogens10050591.
79. Alvarez-Molina A, Cobo-Díaz JF, López M, Prieto M, de Toro M, Alvarez-Ordóñez A. Unraveling the emergence and population diversity of Listeria monocytogenes in a newly built meat facility through whole genome sequencing. Int J Food Microbiol. 2021; doi: 10.1016/j.ijfoodmicro.2021.

80. Maury MM, Bracq-Dieye H, Huang L, Vales G, Lavina M, Thouvenot P, Disson O, Leclercq A, Brisse S, Lecuit M. Hypervirulent Listeria monocytogenes clones' adaption to mammalian gut accounts for their association with dairy products. Nat Commun. 2019; doi: 10.1038/s41467-019-10380-0.
81. Charlier C, Disson O, Lecuit M. Maternal-neonatal listeriosis. Virulence. 2020; doi: 10.1080/21505594.2020.1759287.
82. Kremer PH, Lees JA, Koopmans MM, Ferwerda B, Arends AW, Feller MM, Schipper K, Valls SM, van der Ende A, Brouwer MC, van de Beek D, Bentley SD. Benzalkonium tolerance genes and outcome in Listeria monocytogenes meningitis. Clin Microbiol Infect. 2017; doi: 10.1016/j.cmi.2016.12.008.
83. Salcedo C, Arreaza L, Alcala B, de la Fuente L, Vázquez JA. Development of a multilocus sequence typing method for analysis of Listeria monocytogenes clones. J Clin Microbiol. 2003; doi: 10.1128/jcm.41.2.757-762.2003
84. Ragon M, Wirth T, Hollandt F, Lavenir R, Lecuit M, Le Monnier A, Brisse S. A new perspective on Listeria monocytogenes evolution. PLoS Pathog. 2008; doi: 10.1371/journal. ppat.1000146.
85. Psareva EK, Liskova EA, Razheva IV, Yushina YK, Grudistova MA, Gladkova NA, Potemkin EA, Zhurilov PA, Sokolova EV, Andriyanov PA, Voronina OL, Kolbasov DV, Ermolaeva SA. Diversity of Listeria monocytogenes strains isolated from food products in the Central European part of Russia in 2000-2005 and 2019-2020. Foods (Basel, Switzerland). 2021; https://doi.org/10.3390/foods10112790.
86. Voronina OL, Ryzhova NN, Kunda MS, Kurnaeva MA, Semenov AN, Aksenova EI, et al. Diversity and pathogenic potential of Listeria monocytogenes isolated from environmental sources in the Russian Federation. IJMER. 2015;5(3): 515.
87. Grant JR., Stothard P. The CGView Server: A comparative genomics tool for circular genomes. Nucleic Acids Res. 2008; doi:10.1093/nar/gkn179.
88. Aziz RK, Bartels D, Best AA, DeJongh M, Disz T, Edwards RA, Formsma K, Gerdes S, Glass EM, Kubal M., et al. The RAST Server: Rapid annotations using subsystems technology. BMC Genom. 2008; doi:10.1186/1471-2164-9-75.
89. Overbeek R, Begley T, Butler RM, Choudhuri JV, Chuang H-Y, Cohoon M, de Crécy-Lagard V, Diaz N, Disz T, Edwards R, et al. The subsystems approach to genome annotation and its use in the project to annotate 1000 genomes. Nucleic Acids Res. 2005; doi:10.1093/nar/gki866.
90. Arndt D, Grant JR, Marcu A, Sajed T, Pon A, Liang Y, Wishart DS. PHASTER: A better, faster version of the PHAST phage search tool. Nucleic Acids Res. 2016; doi:10.1093/nar/gkw387
91. Moura A, Criscuolo A, Pouseele H, Maury MM, Leclercq A, Tarr C, Björkman JT, Dallman T, Reimer A, Enouf V, Larsonneur E, Carleton H, Bracq-Dieye H, Katz LS, Jones L, Touchon M, Tourdjman M, Walker M, Stroika S, Cantinelli T, Chenal-Francisque V, Kucerova Z, Rocha EP, Nadon C, Grant K, Nielsen EM, Pot B, Gerner-Smidt P, Lecuit M, Brisse S. Whole genome-based population biology and epidemiological surveillance of Listeria monocytogenes. Nat. Microbiol. 2016; https://doi.org/10.1038/nmicrobiol.2016.185.
92. Alikhan NF, Petty NK, Ben Zakour NL, Beatson SA. BLAST Ring Image Generator (BRIG): simple prokaryote genome comparisons. BMC Genomics 2011; doi: 10.1186/1471-2164-12-402.

This page is intentionally left blank

Effect of Methanolic Extract of *Mucuna Pruriens* on Hormonal Modulation and Sperm Parameters in Male Rat

Chitra Kalyanaraman & PD Gupta

ABSTRACT

Objective: Studies on hormonal changes is an effective method for assessing infertility conditions. A widely used pesticide 1, 2 Dibromo 3 Chloropropane (DBCP) causes infertility by damaging testis in humans. This in turn disturbs Follicle Stimulating Hormone (FSH) and Luteinizing Hormone (LH), sex steroid hormone levels. The seed extract of Mucuna pruriens (M. pruriens) is well known antioxidant and is expected to improve the sperm quality after exposure to DBCP. Method: Male Sprague-Dawley rats were divided into four Groups. Group I – Control received 0.9% saline, Group II – single dose of 50mg/kg 1, 2-Dibromo 3 Chloro Propane (DBCP) dissolved in Dimethyl sulphoxide (DMSO) (1ml) was administered for 30 days, Group III – Methanolic extract of Mucuna pruriens (200mg/kg body weight) was administered for 45 days after 50mg/kg of 1,2 dibromo 3 chloropropane (DBCP) treatment (30 days). Group IV – 200mg/kg/day BW methanolic extract of M. pruriens for 45 days. Results: The body, testis, and epididymis weights of all the rats were taken. DBCP induced group II toxicity bearing animals were significantly decreased when compared to group I control animals. In group II DBCP-induced toxicity rats, there was a reduction in sperm morphology, concentration, and motility as well as follicle stimulating hormone (FSH), testosterone, and luteinizing hormone (LH) levels.

Keywords: methanolic seed extract, sperm motility, sperm count, luteinizing hormone, follicle stimulating hormone, testosterone.

Classification: UDC: 613.95

Language: English

London Journals Press

LJP Copyright ID: 925642
Print ISSN: 2631-8490
Online ISSN: 2631-8504

London Journal of Research in Science: Natural and Formal

Volume 23 | Issue 5 | Compilation 1.0

Effect of Methanolic Extract of *Mucuna Pruriens* on Hormonal Modulation and Sperm Parameters in Male Rats

Chitra Kalyanaraman[α] & PD Gupta[σ]

ABSTRACT

Objective: Studies on hormonal changes is an effective method for assessing infertility conditions. A widely used pesticide 1, 2 Dibromo 3 Chloropropane (DBCP) causes infertility by damaging testis in humans. This in turn disturbs Follicle Stimulating Hormone (FSH) and Luteinizing Hormone (LH), sex steroid hormone levels. The seed extract of Mucuna pruriens (M. pruriens) is well known antioxidant and is expected to improve the sperm quality after exposure to DBCP. Method: Male Sprague-Dawley rats were divided into four Groups. Group I – Control received 0.9% saline, Group II – single dose of 50mg/kg 1, 2-Dibromo 3 Chloro Propane (DBCP) dissolved in Dimethyl sulphoxide (DMSO) (1ml) was administered for 30 days, Group III – Methanolic extract of Mucuna pruriens (200mg/kg body weight) was administered for 45 days after 50mg/kg of 1,2 dibromo 3 chloropropane (DBCP) treatment (30 days). Group IV – 200mg/kg/day BW methanolic extract of M. pruriens for 45 days. Results: The body, testis, and epididymis weights of all the rats were taken. DBCP induced group II toxicity bearing animals were significantly decreased when compared to group I control animals. In group II DBCP-induced toxicity rats, there was a reduction in sperm morphology, concentration, and motility as well as follicle stimulating hormone (FSH), testosterone, and luteinizing hormone (LH) levels. DBCP-induced group II toxicity-bearing animals' above-mentioned parameters improved after treatment with Mucuna pruriens seed extract. Conclusion: The administration of M. pruriens seed extract improves sperm quality and Hormone levels in the DBCP exposed group III rats.

Keywords: methanolic seed extract, sperm motility, sperm count, luteinizing hormone, follicle stimulating hormone, testosterone.

Author α: Dr. ALM Post Graduate Institute of Basic Medical Sciences, Taramani, Chennai, TamilNadu, India.
σ: Former Director grade Scientists, Centre for Cellular and Molecular biology, Hyderabad, India.

I. INTRODUCTION

Infertility is an International problem that involves young couples having unprotected intercourse. According to global evidence, infertility in male ranges from 20-70% (1). Declining male reproductive health is a major concern among the population of reproductive age. Various environmental factors causing male infertility are described in the scientific and medical literature (2). Numerous external and internal factors can increase the production of reactive oxygen species (ROS) above and beyond the capacity of cellular antioxidants, leading to oxidative stress. Exposure to Endocrine - Disrupting Chemicals (EDCs) is ubiquitous in our everyday lives and may result in oxidative stress, which can have an impact on human reproduction and development (3). Pesticides such as Pyrethroids, Organophosphates, Peroxyacetic acids, Carbamates and Organochlorines have been investigated in the study of male fertility (4). Mankind that promoted a negative effect on the environment due to the increase of its own requirements and technology producing unfavorable consequences on the surroundings.

1, 2 Dibromo 3 chloropropane (DBCP), is one such organochlorine pesticide that was used widely for the control of Agricultural and Domestic pests. Twenty years after it was banned, it is still found in the environment, because it takes 140 years to degrade completely (5). Pesticides' effects on sperm parameters have been related in numerous studies (6). Teitelbaum (1999) established that DBCP causes a significant reduction in spermatogenesis among pesticide manufacturing workers. Also, hormones play role in the fertility and infertility conditions. Thus, investigations on hormonal changes may be useful tool in the assessment of both fertility and infertility conditions. Whorton *et al.*, 1977, Kelce *et al.*, 1995, Bernard *et al.*, 2007 (8-10) also verified that DBCP also have estrogenic effects in males by blocking androgen receptors. It is well established that the acute stress that produces excess cortisol decreases the Testosterone production and suppress male sex hormones such as Luteinizing hormone (LH), Follicular-Stimulating Hormone (FSH) (11-13).

Mucuna pruriens (*M. pruriens*) belongs to the family Fabaceae, native to tropical countries from Africa and Asia, including India, Bangladesh, Srilanka & China (14). The seeds have been considered as magic velvet bean in several published reviews (15,16). It has a long history in Indian Ayurvedic medicine, where it is used to treat for Diarrhea, Sexual Debility, Tuberculosis, Impotence, Rheumatic disorders (17,18). Suresh *et al.*, (2009) (19) reported that *M. pruriens* helps in increasing the semen quality and it acts as aphrodisiac. *M. pruriens* seed is economically available all year and it contains phytochemicals such as alkaloids, glycosides, saponins (20). Due to its richness in various biological activities, it has been characterized by in vitro antioxidant activity, anti-microbial agents, and natural antioxidants (21). *M. pruriens* is not only a reproductive enhancer, but also an important natural material for the treatment of male infertility (22). Thus, there is a great possibility that this plant may act through the mechanism of free radical removal in the management of reproductive toxicity.

II. MATERIALS AND METHODS

2.1 Animals

Healthy adult male Sprague- Dawley rats (8 weeks old), weighing between 160-220g were used in the present study. All rats were kept in plastic cages under the experiment room condition at Laboratory Animal Unit PGIBMS, University of Madras, India. The rats were housed under conditions of controlled temperature (26±2°C) with 12 h light and 12 h dark exposure. The rats received a standard rat pellet diet and water *ad libitum*.

2.2 Animal Ethics

The 24 Sprague- Dawley Male Rats were obtained from the Central Animal House facility, Dr. ALM Post Graduate Institute of Basic Medical Sciences, University of Madras, Taramani, Chennai, Tamilnadu, India. Rats were used as per the guidelines from the Institutional Animal Ethics Committee (07/021/08).

2.3 Experimental design

The rats were divided into four groups of six animals each in this experiment. Group I - Animals were treated as control (0.9% saline). Group II - To induce reproductive dysfunction, a single dose of 50mg/kg body weight of 1,2 Dibromo 3 chloropropane (DBCP) dissolved in Dimethyl sulphoxide (DMSO) (1ml) was administered intragastrical for 30 days. Group III - After 1,2 dibromo 3 chloropropane (DBCP) treatment, a methanolic extract of *M. pruriens* (200mg/kg/day body weight) was administered intragastrical for 45 days. For 45 days, Group IV received a 200mg/kg/day body weight methanolic extract of *M. pruriens*. Dosage of *M. pruriens* was selected according to Suresh *et al.* (2009) (19) with ±200 mg to confirm effective concentration.

2.4 Collection of samples

At the end of the experiment, the animals were anesthetized by mild ether and euthanized by cervical dislocation. Blood was collected and was centrifuged at 4 ℃, 13,000 rpm for 15 min to separate the serum from the blood cells. After that, the testosterone and cortisol hormone levels were analyzed from the blood serum. The abdominal region was wiped with normal saline and the scrotum was dissected out. The testes, epididymis plus vas deferens were rapidly collected and their fat pads surrounding tissues were removed before weighed and recorded. Then the right testis and right epididymis plus vas deferens were fixed in Bouin's fixative (85 ml of saturated picric acid added to 10 ml of 40% formaldehyde and made up to 100 ml with glacial acetic acid) for histological examinations.

2.5 Preparation of Methanolic M. Pruriens Seed Extract

The seeds of *Mucuna pruriens* were purchased from a local country drug shop, Chennai Tamilnadu, India. The seeds of *M. pruriens* were shade dried and then coarsely powdered. A known weight of the seed powder was soaked in 100% methanol and kept at room temperature (22 ± *°C*) for 96 h. Then it was filtered, and the process was repeated three times. The extract was concentrated to obtain a semisolid viscous brown mass, which is “crude extract” by using a water bath. This crude extract is then resuspended in water and injected to rats for the experimental studies.

III. SPERM ANALYSIS

3.1 Sperm morphology

Sperm morphology was evaluated by determining the percentage of normal and abnormal forms by Diff-Quick staining method (23). To assess the percentage of morphologically abnormal sperm, the cauda of epididymis was rinsed with 0.5 mL of physiological saline (0.9% NaCl) to obtain a sperm suspension. Aliquots of sperm suspension were stained with 2% eosin. Hundred spermatozoa per animal were analyzed microscopically at 400× magnification and counted spermatozoa with abnormal traits as follows: twisted body, detached head, round tails, and abnormal neck.

3.2 Epididymal Sperm Count

Epididymal sperm count of the control and treated animals was determined by the method as described by Latchoumycandane and Mathur, (2002) (24). An incision was made through the cauda of epididymis, light pressure was applied to this region, and sperm was extruded. 5µl aliquot of epididymal sperm was diluted with 95 µl diluent (5% sodium bicarbonate, 10ml 0.35 % formalin and 0.25 g trypan blue) and approximately 10 µl of this diluted sperm was allowed to stand for 5 min in a humit chamber to prevent drying. The sedimented sperms were counted under the light microscope at 400x magnifications. The measured sperm number was multiplied by the dilution factor to yield the total sperm count.

3.3 Sperm concentration and motility

Epididymal sperms were counted with a hemocytometer using a method described by Yokoi *et al.*, (2003) (25). 5 µl of sperm suspension was diluted with 95 µl of phosphate-buffered saline (PBS, pH 7.4) solution. Approximately 10 µl of the diluted sperm suspension was transferred to each counting chamber of the hemocytometer and was allowed to stand for 5 minutes. The settled sperms were counted with the help of a light microscope at 400x magnifications. Under light microscope, the sperm were counted within two upper and lower counting chambers in triplicate examinations and calculated to be sperm concentration (million cells/mL).

The percentage of motile sperm was evaluated microscopically in each sample by viewing a drop of sperm suspension obtained from left cauda epididymis diluted with Tris buffer solution (3.63 g of Tris-hydroxymethyl aminomethane, 0.50 g of glucose, 1.99 g of citric acid and 100 ml of distilled water) on a prewarmed (37°C) slide and cover slip and observed under light microscopy at 400x magnification. Motility estimations were performed from four different fields in each sample. The mean of the four estimations were used as the final motility score (Sonmez *et al.,* 2005) (26).

3.4 Dead and abnormal sperms

20 µl of sperm suspension was mixed with an equal volume of 0.05% eosin-Y (Sigma Chemicals). After 2 min of incubation at room temperature, slides were viewed under microscope at 400x magnification. Dead sperms appeared pink and live sperms were not stained. Two hundred sperms were counted for each sample and viability percentage was calculated. For the analysis of morphological abnormalities, sperm smears were drawn on clean slides, and allowed to dry in air overnight. The slides were stained with 1% eosin-Y and 15% nigrosin. This was examined at 400x magnifications for morphological abnormalities such as amorphous, head less, bicephalic, coiled or abnormal tails (Wyrobek *et al.,* 1983) (27).

3.5 Sperm Vitality tests

3.5.1 Hypo-osmotic swelling test (HOS)

The Hypo Osmotic Swelling (HOS) test was performed as described by Jeyendran *et al.,* (1984) (28). This is based on the semi permeability of the intact cell membrane, which causes spermatozoa to swell under hypo-osmotic conditions when an influx of water results in an expansion of cell volume. Through HOS test the ability of the plasma membrane to transport water by subjecting the spermatozoa to hypo-osmotic conditions can be measured.

3.5.2 Dye exclusion tests (Eosin and Nigrosin stain) Sperm vitality test

Eosin-nigrosin staining was used to assess the vitality of sperms. This test was studied according to the method of WHO (1999) (23). One drop of sperm suspension was mixed with two drops of 1 % eosin Y. After 30 seconds, three drops of 10 % nigrosin were added and mixed well. Thin smears were then prepared and observed under the light microscope at 400X magnification. Viable sperms remained colorless while non-viable sperms-stained red.

3.6 Hormonal Assays

Blood samples were separated by centrifugation at 10000 rpm for 15 minutes to determine the testosterone (T), follicular stimulating hormone (FSH), and luteinizing hormones (LH) levels (29). Serum FSH was assayed by solid phase tube method by making use of a commercial kit obtained from Diagnostic Products Corporation (DPC), USA. Serum LH was assayed by solid phase coated tube methodology by making use of a commercial kit obtained from Diagnostic Products Corporation (DPC), USA. Serum testosterone was assayed by solid phase coated tube methodology by making use of a commercial kit obtained from Diagnostic Products Corporation (DPC), USA.

3.7 Statistical analysis

Data were presented as Mean ± Standard Deviation (SD). One way analysis of variance (ANOVA) followed by Tukey's multiple comparison method was used to compare the means of different groups by using SPSS.7.5 students version.

IV. RESULTS

4.1 Bodyweight and Organ weight

In this present investigation, the administration of DBCP has caused significant reduction in the weight of testis and accessory sex organs in group II with respect to its controls. On *M. pruriens* supplementation the weight of testis and accessory sex organs recovered remarkably ($p \leq 0.05$), from the DBCP toxicity (Table 1). The body weight of group III male rats shows significant improvement after treated with *M. pruriens* seeds.

Table 1: Body and Organ weight of Experimental animals

Parameters	Group I (Control)	Group II (DBCP)	Group III (DBCP + *M. pruriens*)	Group IV (*M. pruriens*)
Body weight(g)	160.33±4.33	132.30±4.43a*	146.06± 2.51a* b*	157.49±3.19a^{NS}
Testicular weight (g)	2.67±0.16	1.61±0.09a*	2.38±0.16a* b*	2.69±0.10 a ^{NS}
Testis weight relative (g)	1.76± 0.04	1.14 ±0.09 a*	1.63± 0.11 a$^{@}$ b*	1.79 ±0.05 a ^{NS}
Epididymis weight (g)	0.379± 0.01	0.28 ±0.02 a*	0.320±0.02 a$^{\#}$ b*	0.359±0.01 a ^{NS}

Values are expressed as mean ± SD for six animals in each group, a – Group II, III, IV compared with Group I, b – Group III compared with Group II. The significance level of $p<0.05$.

4.2 Sperm Count

The results demonstrated the decrease in sperm count of rats under stress. Fig 1 shows the sperm count of experimental animals, and it is inferred that the sperm count was drastically reduced in group II DBCP treated animals when compared to group I control animals. Conversely upon treatment with *M. pruriens*, the sperm count was significantly increased in group III *M. pruriens* treated animals and were comparable to that of group II toxicity bearing animals.

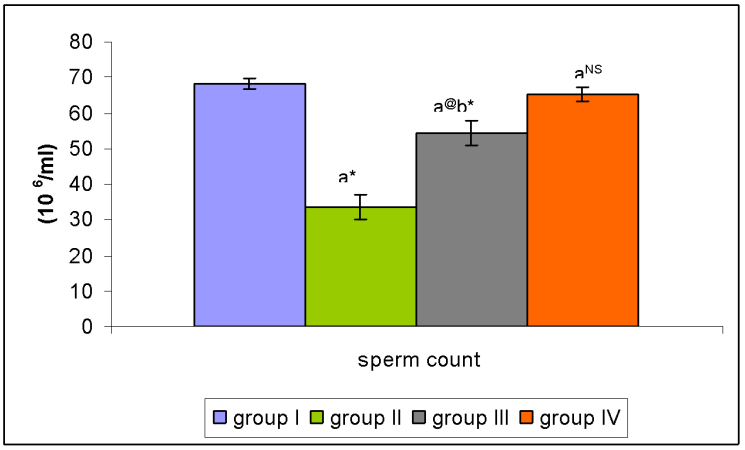

Each value represents mean ± SD, a – Group II, III, IV compared with Group I, b – Group III compared with Group II $^{*}p<0.001$; $^{\#}p<0.01$; $^{@}p<0.05$; ^{NS} – Not significant

Fig 1: Sperm Count in Experimental animal

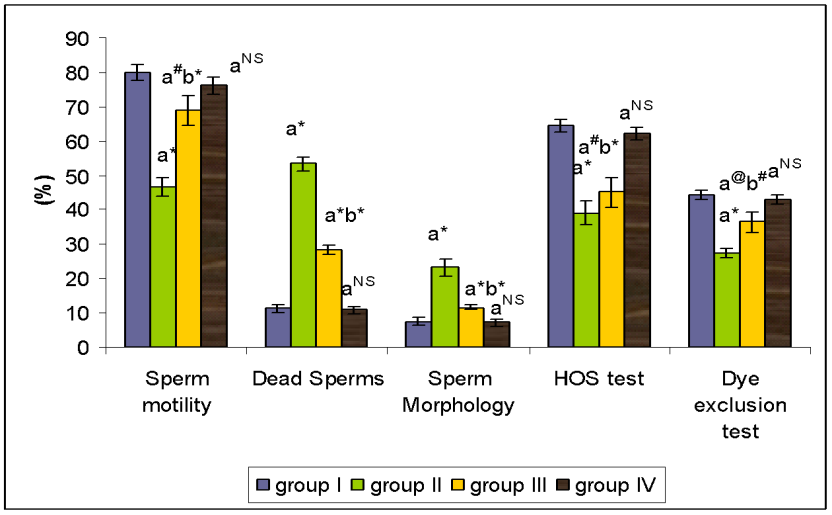

Each value represents mean ± SD, a – Group II, III, IV compared with Group I, b – Group III compared with Group II $^{*}p<0.001$; $^{\#}p<0.01$; $^{@}p<0.05$; ^{NS} – Not significant

Fig 2: Sperm motility, Morphology and Vitality of Control and Experimental animals

Fig 2 demonstrates Sperm motility, morphology, viability by HOS and Dye exclusion test. The negative impact of DBCP on spermatozoa was confirmed by an increased abnormality in the sperm head. Also, abnormal spermatozoa with twisted bodies, detached heads, abnormal necks, and round tails were predominantly noticed. On DBCP exposure, the proportion of sperm with progressive movement was significantly ($p<0.05$) decreased. Whereas the treatment with methanolic extract of *M. pruriens*, the percentage of abnormal sperms significantly decreased ($p<0.05$), and movement was significantly improved. In contrast to this, the sperm Motility, Viability and Dye exclusion test shows Decrease level in group II DBCP exposed rats (Fig 2) and was significantly reverted to near normal in *M. pruriens* extract treated group III animals. Not much changes observed in group IV *M. pruriens* alone treated animals when compared to group I control animals.

4.3 Hormonal Parameters

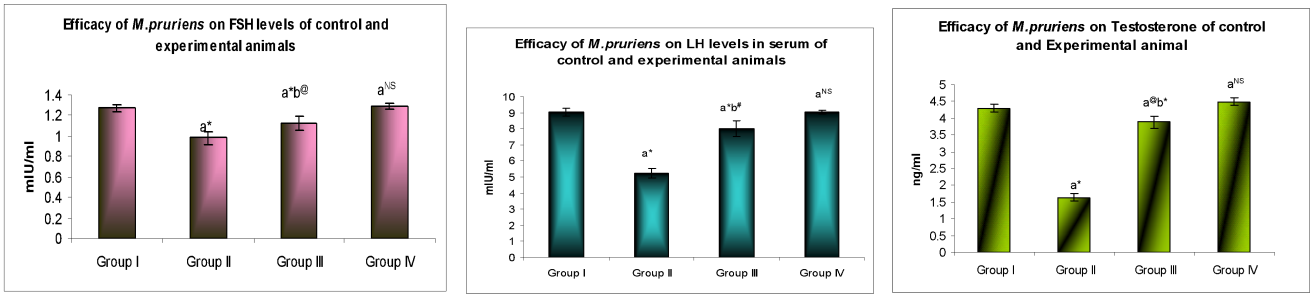

Each value represents mean ± SD, a – Group II, III, IV compared with Group I, b – Group III compared with Group II $^{*}p<0.001$; $^{\#}p<0.01$; $^{@}p<0.05$; ^{NS} – Not significant

Fig 3a, 3b, 3c: FSH, LH & Testosterone level of Control and Experimental animals

Testosterone, luteinizing hormone and follicle stimulating hormone levels in the male experimental rats were observed (Fig. 3a,3b &3c). The level of these hormones in the experimental rats followed similar trend. They were significantly less in group II rats which received 50mg/kg of DBCP. Contrarily, upon administration of *M. pruriens* extract these hormone levels were significantly increased in group III comparable to that of group II toxicity bearing rats. There was however no significant difference ($p > 0.05$) in the level of these hormones recorded in group 4 rats compared to control group.

V. DISCUSSION

In recent years, the major health concern is toxic effects of drug and environmental chemicals on Human reproductive system. Reproductive toxicity can be defined as adverse effect of chemical substance on sexual function and fertility effects on male and females or dysfunction of the reproductive system. The oxidative stress that causes dysfunction of male reproductive hormone, which could eventually lead to male infertility. According to global evidence, infertility is a common and severe health problem affecting 20-70% of male population (1). Most of those patients were most likely exposed to toxicants, which may have contributed to their infertility (30).

In the present investigation, DBCP treated rats showed a significant decrease in body weight and testicular weight when compared to the control. This may be due to the disturbance in the general metabolic functions of the rats exposed to toxicant. It is reported that in toxicity conditions, the body weight of Experimental Animal is significantly reduced (31). In addition to these, hormonal changes may also be one of the reasons for weight loss (32). Also, the loss of testicular and epididymal weight may be due to reduced bioavailability of sex hormones (33). Additionally, it is suggested that the decrease in body weight may be for increased degeneration of lipids and proteins because of the direct effects of reproductive toxicant (34). Treatment with *M. pruriens* in Group III animal shows significant increase in the body and testicular weight. This may be due to the cytoprotective property of the seed extract (31).

The sperm count in the epididymis is one of the most sensitive tests for evaluating spermatogenesis (35). In the current study, administration of DBCP to group II animals caused the epididymal epithelium to degenerate, which resulted in a significant decrease in sperm count compared to group I control animals. Upon treatment with *M. pruriens* increase the sperm count due to the huge amounts of phenolic constituents that are characterized by free radical scavenging and high antioxidant activities which suppress the free radical mediated disturbances in sperm. This is in well accordance with Suresh *et al.*, (2009) and Chitra (2022) (19,22) revealed an increase in sperm count and motility by the seed extracts of *M. pruriens*.

Sperm motility is often used as a marker of chemically induced testicular toxicity. Sperm movement is important for sperm functional capacity and the assessment of sperm movement is useful for detection or evaluation of male reproductive toxicity (36). It is reported that the increase in the Oxidative stress leads to a decreased sperm motility, damage to the acrosome membranes and inability of the sperm to fertilize (37). In the present study, DBCP leads to diverse cells and oxidative damage to sperms can lead to DNA damage, alter membrane functions, impair motility.

Decrease in sperm motility and abnormal morphology of sperm was noticed in DBCP treated rats when compared to control rats. On the contrary, treatment with seed extract of *M. pruriens*, significantly increased the sperm motility and in contrast reduced the abnormal sperm morphology. This may be due to the protective and restorative effect rendered by the methanolic seed extract of *M. pruriens*. In view of this, Shami *et al.*, (2009) (38) have also reported that antioxidants play a major role in improving sperm morphology and sperm count.

The hypo-osmotic swelling (HOS) test was used for evaluating the functional integrity of human spermatozoa membranes, by evaluating its reaction under hypoosmotic conditions. In the present investigation exposure to DBCP caused severe plasma membrane damage in the sperm due to the generation of free radicals. The administration of *M. pruriens* stabilized and restored the normal membrane potential due to the presence of glycoside, saponins and sterols present in the seed extract. In this view Yousef *et al.*, (2005) (39) also reported that the active compounds such as glycosides and

Lafuente *et al.*, (2000) (40) reported that Leutinizing hormone (LH), Follicle stimulating hormone (FSH) and Testosterone are required for normal spermatogenesis. Elevated levels of FSH and LH are as deleterious as sub-normal levels (41). Previous studies have shown that decreases in serum testosterone, testicular LH receptors, and Leydig cell damage might be adversely affected by the toxicant (42-44). Testosterone is the main male gonadal hormone produced by the interstitial cells of the Leydig cells in the testis. The role of testosterone and gonadotrophin has been studied extensively in androgen- deficient rats using different models and in prevention of degeneration of spermatogenic cells (45). A reduction in testosterone level could be the primary cause of induction of infertility induced by the compound. Testosterone is one of the major indexes of androgenicity (46,35). In the present study, there is a decline in testosterone levels in the DBCP treated group II rats. The reduced serum testosterone levels support the possibility of reproductive tract alterations due to androgen deficiency.

The morphological changes of the seminiferous tubule including Leydig and Sertoli cells would indicate damage to the reproductive system. In the present study the administration of DBCP decreases the FSH and LH levels, due to the toxic action of DBCP. This is in consistence with the finding of Pease *et al.*, (1991) (47) that chemical toxicant causes persistent dysfunction of Leydig cells which disturb normal testosterone levels. In this connection, Fiorini *et al.*, 2004 (48) have also reported that LH concentration was rise and Testosterone levels were decreased during the complete failure of Leydig cells. However, hormonal production may be reduced in rats due to the seminiferous tubular damage (49). On the contrary , treatment with *M. pruriens in* group III significantly decreases the toxic effects of DBCP and the level of FSH, LH and testosterone were increased. This might be due to the presence of the active constituents such as flavonoids and saponins which directly or indirectly scavenge the oxidative damage to different cells and organs while normalizing their function. In this regard, Doshi *et al.,* (2003) (50) have reported that flavonoids and antioxidants remarkably reduce oxidative damages in the cells. Based on the results of this study, future research could investigate male rat sterility using a fertility test. In addition, sire litters can be examined after mating.

VI. CONCLUSION

In conclusion, the current study supports the methanolic extract of *M. pruriens* has a remarkable fertility effect in male rats. These results conclude that the seed extract of *M. pruriens* significantly increase sperm quality by elevating antioxidant enzyme activity and improve Hormone levels. Because of its efficacy, it can be considered as potential seed extract for further pharmaceutical development in the treatment of infertility.

ACKNOWLEDGEMENT

I would like to express deep and Sincere gratitude to my Research Supervisor Late Dr. M.P. Balasubramanian, Professor, Dr. ALM PGIBMS, Taramani, Chennai-113. for giving me the opportunity to do research and invaluable guidance throughout my Research work. My Sincere Thanks goes to Dr. K. Pushkala, SDNB Vaishnav college for women for the continuous support and encouragement throughout the paperwork.

REFERENCES

1. Agarwal A, Parekh N, Panner Selvam M.K. Male Oxidative Stress Infertility (MOSI): Proposed Terminology and Clinical Practice Guidelines for Management of Idiopathic Male Infertility. World J Mens Health, 37(3): 296–312 (2019).
2. Nykolaichuk P. Roksolana, Oleksandr S, Fedoruk, Volodymyr V. Vizniuk. Impact of Environmental Factors on Male Reproductive Health Wiad Lek. 73(5):1011-1015 (2020).
3. Irma Virant-Klun, Senka Imamovic-Kumalic and Bojana Pinter. Endocrine-Disrupting Chemicals (Bisphenols, Phthalates, and Parabens) with Human Semen Quality *Antioxidants*, *11*(8): 1617 (2022).
4. Perry MJ. Effects of environmental and occupational pesticide exposure on human sperm: a systematic review. Hum Reprod ,14: 233-42 (2008).
5. Reed J, Kinzel V, Cheng HC, Walsh DA. Circular dichroic investigations of secondary structure in synthetic peptide inhibitors of cAMP-dependent protein kinase: a model for inhibitory potential. *Biochemistry*, 1;26(24) :7641-7 (1987).
6. Krzastek Sarah C, Jack Farhi, Marisa Gray and Ryan P. Smith. Impact of environmental toxin exposure on male fertility potential**.** Transl Androl Urol., 9(6): 2797–2813 (2020).
7. Teitelbaum DT. The toxicology of 1,2-dibromo-3- chloropropane (DBCP): a brief review. Int J Occup Environ Health, 5:122-6 (1999).
8. Whorton D, Krauss R.M, Marshall S, Milby T.H. and Stubbs. Function in DBCP exposed pesticide workers. *Lancet,* ii, 161-167 (1977).
9. Kelce WR, Stone CR, Laws SC. Persistent DDT metabolite p,p'-DDE is a potent androgen receptor antagonist. Nature; 375:581-5 (1995).
10. Bernard L, Martinat N, Lécureuil C. Dichlorodiphenyltrichloroethane impairs follicle stimulating hormone receptor-mediated signaling in rat Sertoli cells. Reprod Toxicol; 23:158-64 (2007).
11. Herman JP. Neural control of chronic stress adaptation. Front Behav Neurosci. 7:61 (2013).
12. LinH, YuanK, ZhouH-y ,BuT, SuH, LiuS, ZhuQ, WangY, HuY, ShanY. Time-course changes of steroidogenic gene expression and steroidogenesis of rat Leydig cells after acute immobilization stress. Int J Mol Sci. 15(11): 21028–21044 (2014).
13. Mohamadpour M, Noorafshan A, Karbalay S, Talaei T, Aliabadi E. Protective effects of curcumin co-treatment in rats with establishing chronic variable stress on testis and reproductive hormones. Int J Reprod Biomed. 15(7):447–452 (2017).
14. Fung SY, Tan NH, Sim SM, Marinello E, Guerranti R, Aguiyi JC. *Mucuna pruriens* Linn. seed extract pretreatment protects against cardiorespiratory and neuromuscular depressant effects of *Naja sputatrix* (Javan spitting cobra) venom in rats. Indian Journal of Experimental Biology. 49(4):254-259 (2011).
15. Lampariello LR, Cortelazzo A, Guerranti R, Sticozzi C, Valacchi G. The magic velvet bean of *Mucuna pruriens*. Journal of traditional and complementary medicine. 2(4):331-339 (2012).
16. Kavitha, Thangamani C. Amazing bean *Mucuna pruriens*: A comprehensive review. Journal of Medicinal Plants Research. 8:138-143 (2014).
17. Suryawanshi, Prajakta P Kamble, Vishwas A Bapat, Jyoti P Jadhav. Bioactive Components of Magical Velvet Beans, Legume Crops - Prospects, Production, and Uses. Intech Open. 92124/chapters/72106 (2020).
18. Natarajan K, Narayanan N, Ravichandran N. Review on "Mucuna"-The wonder plant. International Journal of Pharmaceutical Science Rev Res. 17(1):86-93 (2012).
19. Suresh S, Elumalai Prithiviraj and Seppan Prakash. Effect of *Mucuna pruriens* on oxidative stress mediated damage in aged rat sperm. Volume 33 Issue 1: Pages 22 – 32 (2009).
20. Pathania R, Chawla P, Khan H, Kaushik R, Khan M A. An assessment of potential nutritive and medicinal properties of *Mucuna pruriens*: a natural food legume. 3 Biotech 10 :261 (2020).

21. Rajeshwar Y, Gupta M, Mazumder UK. Antitumor and in vivo antioxidant status of *Mucuna pruriens* (Fabaceae) seeds against Ehrlich ascites carcinoma in Swiss albino mice. *Iranian J Pharm Ther*. 4: 46-53 (2005).
22. Chitra Kalyanaraman. Infertility Treatment in male rats by methanol extract of Mucuna pruriens. Journal of Cell and Tissue Research Vol. 22(2): 7255-7261 (2022).
23. World Health Organization. Laboratory manual for the examination of human semen and sperm cervical mucus interaction 4th. New York: Cambridge University Press (1999).
24. Latchoumycandane C, Mathur PP. Effects of vitamin E on reactive oxygen species-mediated 2,3,7,8-tetrachlorodi-benzo-p-dioxin toxicity in rat testis. *J Appl Toxicol*.22(5):345-51 (2002).
25. Yokoi K, Imai T, Shibata A, Hibi Y, Kikumori T, Funahashi H, Nakao A. Mild persistent hypercalcitoninemia after total thyroidectomy in patients with papillary thyroid carcinoma. *J. Ethnopharmacol*. 62: 183-193 (2003).
26. Sonmez S, Kirilmaz L, Yucesoy M, Yücel B, Yilmaz B. The effect of bee propolis on oral pathogens and human gingival fibroblasts. *J Ethnopharmacol*. Dec 1;102(3):371-6 (2005).
27. Wyrobek AJ, Gordon LA, Burkhart JG, Francis MW, Kapp RW Jr, Letz G, Malling HV, Topham JC, Whorton MD. An evaluation of human sperm as indicators of chemically induced alterations of spermatogenic function. A report of the U.S. Environmental Protection Agency Gene-Tox Program. *Mutat Res* 115(1):73-148 (1983).
28. Jeyendran RS, Van der Ven HH, Perez-Pelaez M, Crabo BG, Zaneveld L J. Development of an assay to assess the functional integrity of the human sperm membrane and its relationship to other semen characteristics. *J Reprod Fertil*.70(1):219-28 (1984).
29. Yamamoto M, Takeuchi N, Kotani S, Kumagai A. Effects of glycyrrhizin and cortisone on cholesterol metabolism in the rat. *Endocrinol Jpn*.;17(5):339-48 (1970).
30. Filho DW, Torres MA, Bordin AL B. Spermatic cord torsion, reactive oxygen and nitrogen species and ischemia-reperfusion injury. *Mol Aspects Med*. 25(1-2):199-210 (2004).
31. Amin KMY, Khan MN, Rahman SZ, Khan NA. Sexual function improving effect of *Mucuna pruriens* in sexually normal male rats. *Fitoterapia*. 67: 53-8 (1996).
32. Rajesh Kumar T and Muralidhara. Oxidative stress response of rat testis to model prooxidants in vitro and its modulation. Toxicology in Vitro. Volume 16, Issue 6: 675-682 (2002).
33. Schrade, S M. Man and the workplace; Assessing his reproductive health. Chemical Health and Safety 2013, 11-16 (2003).
34. Takahashi and Oishi. Testicular toxicity of dietary 2,2-bis(4-hydroxyphenyl) propane (bisphenol A) in F344 rats. *Archives of Toxicology* . volume 75: pages42–51 (2001).
35. Meistrich ML, Wilson G, Huhtaniemi I. Hormonal treatment after cytotoxic therapy stimulates recovery of spermatogenesis. *J. Am. Coll. Toxicol*. 8: 551–567 (1989).
36. Perreault SD. The mature spermatozoa as a target for reproductive toxicants. In: Boekelheide K, Chapin RE, Hoyer PB, Harris C, eds. Comprehensive toxicology, vol. 10. *Reproductive and Endocrine Toxicology*:165–79 (1997).
37. Aitkin R J, Clarkson J S, Fishel S. Generation of reactive oxygen species, lipid peroxidation and human sperm function. *Biol. Reprod* .41 :183-187 (1989).
38. Shami PJ, Maciag AE, Eddington JK, Udupi V, Kosak KM, Saavedra JE, Keefer LK. JS-K, an arylating nitric oxide (NO) donor, has synergistic anti-leukemic activity with cytarabine (ARA-C). *Leuk Res* 33(11):1525-9 (2009).
39. Yousef MI, El-Morsy AM, Hassan MS. Aluminium -induced deterioration in reproductive performance and seminal plasma biochemistry of male rabbits: protective role of ascorbic acid. *Toxicology*. 5;215(1-2):97-107 (2005).
40. Lafuente A, Marquez N, Pousada Y, Pazo Dm Esquifino AL. Possible estrogenic and or antiandrognic effects of methoxychlor on prolactin release in male rats. Arch Toxicol .74 (4-5):270-275 (2000).

41. Zhai J, Lanclos K D, Abney TO. Estrogen receptor messenger ribonucleic acid changes during Leydig cell development. *Biol Reprod*. 55(4):782-8 (1996).
42. Warren DW, Wisner Jr JR, Ahmad N. Effects of 1,2-dibromo-3- chloropropane on male reproductive function in the rat. *Biol Reprod*; 31:454–63 (1984).
43. Ahmad N, Wisner JR, Warren DW. Morphological and biochemical changes in the adult male rat reproductive system following long-term treatment with 1,2-dibromo-3-chloropropane. *Anat Rec*, 222: 340–9 (1988).
44. Yoshida S, Yamada H, Sugawara I, Takeda K. Effect of dibromochloropropane(DBCP) on the hormone receptors of the male rat reproductive system. *Biosci Biotechnol Biochem*; 62:479–83 (1998).
45. Mantovani A. Hazard identification and risk assessment of endocrine disrupting chemicals with regard to developmental effects. Toxicology. 181-182:367-370 (2002).
46. Walton S, Cunliffe W J, Keczkes K, Early A S, Mcgarrigle H H G, Katz M, Reese R. A Clinical, ultrasound and hormonal markers of androgenicity in acne vulgaris. BJD Volume133, Issue2 August Pages 249-253 (1995).
47. Pease W, Vandenberg J, Hooper K. Comparing alternative approaches to establishing regulatory levels for reproductive toxicants: DBCP as a case study. *Environ Health Perspect*. Feb; 91:141-55 (1991).
48. Fiorini C, Tilloy-Ellul A, Chevalier S, Charuel C, Pointis G. Sertoli cell junctional proteins as early targets for different classes of reproductive toxicants. *Reprod Toxicol*. 18:413–21 (2004).
49. Pectasides D, Pectasides M, Farmakis D, Nikolaou M, Koumpou M, Kostopoulou V, Mylonakis N. Testicular Function in Patients with Testicular Cancer Treated with Blieomycin- Etoposide – Carboplatin (BEC 90) combination chemotherapy. European Urology. Volume 45, Issue 2, Pages 187-193 (2004).
50. Doshi PK, Chhaya NA, Bhatt MA. Bilateral subthalamic nucleus stimulation for Parkinson's disease. *Neurol* India. 51(1):43-8 (2003).

London Journal Press Membership

For Authors, subscribers, Boards and organizations

London Journals Press membership is an elite community of scholars, researchers, scientists, professionals and institutions associated with all the major disciplines. London Journals Press memberships are for individuals, research institutions, and universities. Authors, subscribers, Editorial Board members, Advisory Board members, and organizations are all part of member network.

Read more and apply for membership here:
https://journalspress.com/journals/membership

For Authors

Author Membership provide access to scientific innovation, next generation tools, access to conferences/seminars /symposiums/webinars, networking opportunities, and privileged benefits.
Authors may submit research manuscript or paper without being an existing member of LJP. Once a non-member author submits a research paper he/she becomes a part of "Provisional Author Membership".

For Institutions

Society flourish when two institutions come together." Organizations, research institutes, and universities can join LJP Subscription membership or privileged "Fellow Membership" membership facilitating researchers to publish their work with us, become peer reviewers and join us on Advisory Board.

For Subscribers

Subscribe to distinguished STM (scientific, technical, and medical) publisher. Subscription membership is available for individuals universities and institutions (print & online). Subscribers can access journals from our libraries, published in different formats like Printed Hardcopy, Interactive PDFs, EPUBs, eBooks, indexable documents and the author managed dynamic live web page articles, LaTeX, PDFs etc.

GO GREEN AND HELP
SAVE THE ENVIRONMENT

JOURNAL AVAILABLE IN

PRINTED VERSION, INTERACTIVE PDFS, EPUBS, EBOOKS, INDEXABLE DOCUMENTS AND THE AUTHOR MANAGED DYNAMIC LIVE WEB PAGE ARTICLES, LATEX, PDFS, RESTRUCTURED TEXT, TEXTILE, HTML, DOCBOOK, MEDIAWIKI MARKUP, TWIKI MARKUP, OPML, EMACS ORG-MODE & OTHER

SCAN TO KNOW MORE

support@journalspress.com
www.journalspress.com

*THIS JOURNAL SUPPORT AUGMENTED REALITY APPS AND SOFTWARES